RESIDUAL STRESSES IN MACHINED TITANIUM (Ti-6Al-4V) ALLOYS

by

Avadhoot Paranjpe

A thesis submitted to the faculty of
The University of Utah
in partial fulfillment of the requirements for the degree of

Master of Science

Department of Mechanical Engineering

The University of Utah

May 2014

Copyright © Avadhoot Paranjpe 2014

All Rights Reserved

The University of Utah Graduate School

STATEMENT OF THESIS APPROVAL

The thesis of **Avadhoot Paranjpe**

has been approved by the following supervisory committee members:

A. K. Balaji	, Chair	**02/24/2014** Date Approved
K. L. DeVries	, Member	**02/27/2014** Date Approved
David Hoeppner	, Member	**02/28/2014** Date Approved

and by **Tim Ameel** , Chair/Dean of

the Department/College/School of **Mechanical Engineering**

and by David B. Kieda, Dean of The Graduate School.

ABSTRACT

Surface integrity plays a very important role in the life and functionality of machined surfaces used in a variety of engineering applications. Manufacturing processes and their sequence, along with the selection of cutting conditions and cutting tools, eventually dictate the type of surface that is being produced. Surface integrity is subdivided into several components, of which, some important components are surface roughness, residual stresses and subsurface microstructures. Enhanced understanding of all these factors and their interactions will potentially lead to advanced knowledge driven machining process planning.

This thesis focuses on an experimental investigation of the effects of cutting tool coatings and cutting fluid application on surface integrity (residual stress, surface roughness and subsurface microstructure) in machined Ti6Al4V titanium alloy. For measuring residual stresses, the hole drilling method was used in this thesis research. The tools selected for the machining were uncoated flat-faced, uncoated grooved, multilayered ($TiCN/Al_2O_3/TiN$) CVD coated grooved, and single-layered (TiAlN) PVD coated grooved tools with tungsten carbide substrates. Three different cutting fluid application conditions were used namely: dry, minimal quantity lubrication (MQL) and flood.

To illustrate the significance of this thesis, it was observed that a grooved multilayered CVD coated cutting tool under the influence of MQL condition, induced the

highest near-surface residual stresses; on the other hand, the same tool, when machined under dry condition, produced the lowest residual stresses. Thus, it can be seen that a specific cutting tool material and/or geometry produce significantly different surface integrity when it is combined with different cutting fluid application conditions. Moreover, the microstructural analysis performed on these machined workpieces revealed significant changes in the subsurface microstructure with respect to the type of cutting tool-cutting fluid application combination used and correlated strongly with the measured residual stress profiles.

The combined effect of the type of cutting tool along with the type of cutting fluid application condition on surface integrity is extremely significant. The results and findings of this thesis have the potential to aid in choosing the combination of the cutting tool and the cutting fluid application that are best suited for machining. Apart from that, this thesis also provides several recommendations for future research on the fundamentals of the interactions between machining parameters such as tool coatings, tool geometry and cutting fluid applications and their significant effects on the generated surface integrity and the life of the component there after.

TABLE OF CONTENTS

LIST OF TABLES

CHAPTER 1

INTRODUCTION

The main objective of this thesis is to understand the individual and combined effects of tool coatings and cutting fluid application on the surface integrity of machined Ti-6Al-4V titanium alloy. Cutting tool coatings play a very important role in the longevity and performance of the cutting tool and also in the production of the machined surface. Hence, proper selection of the tool is of prime importance. Coatings are applied on the tool to obtain different advantages. For example, some coatings increase the life of the cutting tool; some coatings are responsible for producing better surface finish, etc. Similarly, cutting fluid application also plays an important role in manufacturing applications. The two main functions of cutting fluid application are lubrication at relatively low cutting speed and cooling at relatively higher cutting speed [1]. In this thesis, the effects of tool coatings and cutting fluid application on surface integrity of machined titanium alloy are investigated. Three specific factors, namely: residual stresses, surface roughness, and microstructural analysis comprise the primary means of assessing surface integrity in these machined titanium alloy surfaces.

Machining is the process of achieving the final shape and dimensions of a work-piece by removing unwanted material with the help of cutting tools so as to obtain a final mechanical component. All manufactured mechanical components possess some level of surface integrity. "Surface integrity" is defined as the state and attributes of a

manufactured surface that influence the performance of a product or component [2]. The fundamental theories of machining and surface integrity are discussed in detail in Chapter 2 of this thesis. The variables affecting the surface integrity (residual stresses, surface roughness, etc.) studied in this thesis are: i) the tool material; ii) the type of coating deposited on the tool material, and iii) the type of cutting fluid application. This chapter describes the main motivation behind the study and also provides an introduction to the selection of the machining parameters.

1.1 Motivation

Technologically, manufacturing is the application of physical and chemical processes to alter the geometry, properties, and/or appearance of a given starting material to create final parts or products. It is an important means by which a nation creates material wealth. "In the United States, manufacturing industries account for about 20% of gross national products (GNP) [3]". Surface integrity plays an important role in the life of the component. Surface integrity can be further subdivided into several categories such as surface finish, chemistry, topography, metallurgy, thermal damage (burn, transformation and over-tempering), and residual stresses, of which, two important components are surface roughness and residual stresses [2].

Traditional manufacturing process planning is based on old empirical methods for choosing the appropriate manufacturing process and other conditions for manufacturing a component. Process planning is initiated with the building of a CAD drawing/model of the required component. The next step is to separate the drawing into parts. The required operations for each part are then identified, listed and sequenced. Equipment and tooling are assigned to the sequenced parts. Then the cost, productivity and throughput of the

designed component are calculated for manufacturing. Due to minimal understanding of the causes that affect surface integrity, typically at no point in the process planning stage is the desired optimum surface integrity considered as an input parameter in the planning process. Hence, this makes the end product suboptimal with unknown or undesired surface integrity. Expensive and time-consuming postprocessing techniques such as shot peening, low plasticity burnishing (LPB), laser shock processing (LSP), etc., are then used to achieve the desired surface integrity of the product. This increases the cost, infrastructure needed, labor and the valuable time that are involved in manufacturing the part. Moreover, there is no immediate and active feedback on how to correct the manufacturing process so as to achieve the desired surface integrity in the manufactured component.

In order to remove this loop-hole from the design and manufacturing system, the aim of the Sustainable Manufacturing Research laboratory, where the author of this thesis conducted this work, is that the desired surface integrity should be considered as a design input or requirement to the process planning methodology rather than using traditional empirical based process planning methods. The rest of the parameters should be selected based on this process model in order to reduce the tremendous cost of postprocessing techniques. The only challenge is that, right now the knowledge of predicting and understanding surface integrity in machined components is limited and not up to date to implement it as an input parameter to the process model. Hence, the study of surface integrity in machined components is of prime importance in manufacturing. This approach will also help in achieving better process control. The flow diagram that is shown in Figure 1.1 gives a schematic of the necessary improvements, involving active

presence of surface integrity, to be made in manufacturing process planning. The surface integrity aspects are described in detail in Chapter 2 of this thesis.

1.2 Surface Integrity

Surface integrity may be defined as the state and attributes of a manufactured surface that influence performance of a product or component [2]. In manufacturing, surface integrity plays a very important role in the life and functionality of the machined surface. The type and sequence of manufacturing processes selected at the beginning along with the selection of cutting conditions and tools, decide the type of surface that will be produced.

One of the main aims towards enhancing surface integrity is to increase the life of the component by adjusting the other factors to an optimum level. Surface integrity is subdivided into several components such as surface finish, chemistry, topography, metallurgy, thermal damage (burn, transformation and over-tempering), and residual stresses, of which, two potentially important components are surface roughness and residual stresses. Proper understanding of all these factors and their correlation will lead to advanced knowledge driven machining process planning.

Residual stresses are those stresses that remain in the material body even after all the external loads such as forces, couples and applied stresses, acceleration and gravitation are removed [5]. Residual stresses are present in almost all the machined materials and product forms. They may also be created during the life of the component. If not recognized and accounted for in the design process, they can be a major factor for the failure of the component, particularly those subjected to alternating service loads or corrosive environments. They often are a cause of premature failure of some critical

mechanical components. Surface residual stresses are either tensile or compressive in nature. Tensile residual stresses are generally harmful or undesirable, especially for parts that are under cyclic loading. The growth of fatigue cracks is usually aggravated when encountered with tensile residual stress areas as compared to a compressive residual stress area. The basic aim of designers is to reduce the tensile residual stresses as much as possible or to convert them all into compressive residual stresses. Even though residual stresses are undesirable, certain applications such as toughened glass and prestressed concrete benefit with the presence of compressive residual stresses within the body [5]. Residual stresses are a very important parameter in all manufacturing industries, especially in aerospace applications, since the demands on functional performance required in the manufacturing of aerospace components is much higher. To attain high degrees of functional performance in the manufacturing of aerospace components, optimal manufacturing process parameters are essential. At this point of time, most of manufacturing process parameters are yet to be established with great a degree of confidence.

1.3 Work Material

Titanium alloys are among the most commonly used material in the manufacturing industry, especially in aerospace industries. Hence, Ti-6Al-4V titanium alloy is selected as the work material for this research. Ti-6Al-4V titanium alloy is known as the "work-horse" of the titanium industry because it is by far the most common Ti alloy, accounting for more than 50% of total titanium usage [6].

Titanium and its alloys are industrially of great importance due to their excellent properties such as high strength, hot workability, corrosion resistance, strength-to-weight

ratio, toughness, etc. in some of the high performance applications such as aerospace, automobile, biomedical, etc. The biocompatibility of the metal is greatly appreciated for medical use, in that worn out or broken body parts can be replaced with new artificial titanium made components, such as artificial knees, hip-joints, teeth, etc. Consumer goods such as cameras, wrist watches, etc. are a more recent area of application. However, the biggest application of titanium alloys is still in the aerospace industry, where these alloys are used in compressor discs and blades in jet engines and airframe components and structures in aircraft, space rockets and satellites [6]. The main reason for the large use of titanium alloys in the aerospace industry is their high specific strength ratio or higher strength to weight ratio and the fact that they can be used at high temperatures than many other light alloys. Only composites have a better ratio than titanium. However, due to their relatively poor toughness, poor ductility and most importantly, limited temperature capability, composites still have their challenges.

For such demanding applications, functionality and reliability of components are of prime importance. Hence, research aimed towards better knowledge and understanding of all processes in the manufacture of titanium components from mineral ore to final finished products is of great importance, not only for the purpose of developing new stronger materials but also for the optimization of already existing processes [6]. More information on the titanium alloys along with the classification is described in Chapter 2 of this thesis.

1.4 Ti-6Al-4V

Ti-6Al-4V was selected as the work material in this thesis. It is a type of alpha-beta titanium alloy containing around 6% aluminum and 4% vanadium. In the United

States, 70 to 80% of the demand for titanium is from the aerospace industry, and the remaining is from other industrial applications [6]. It is the most common and widely used titanium alloy which accounts for about 50% of the total weight of all titanium alloys shipped [7]. It has an excellent combination of high strength, toughness and corrosion resistance. Some of the important applications are in rocket motor cases, blades, discs and rings for aircraft turbines, compressors, structural forgings, fasteners, pressure vessels, chemical pumps, cryogenic parts, ordnance equipment, marine components, steam turbine blades, space capsule components, helicopter rotor hubs, critical forgings requiring high strength to weight ratios, down-hole explorations, logging equipments, springs and hubs, human implants, etc. This alloy may be used over a broad range of temperatures from cryogenic to about 427 °C (800 °F) for long term applications [7]. This alloy has the perfect balance of the properties of alpha alloys and beta alloys due to the presence of both alpha and beta stabilizers.

1.5 Cutting Tool Materials

The tool material plays a very important role in the life of the cutting tool and also in the production of the machined surface. Hence, proper selection of the tool is of prime importance. Cutting tools are selected based upon the industrial requirement and the type of work material to be machined. Cutting tools are grouped depending on the tool geometry or depending on the type of coatings applied on the cutting tool substrate. A detailed description on the types of cutting tools is given in Chapter 2 of this thesis. There are four different tools used in this present thesis; namely: uncoated flat-faced carbide, uncoated grooved carbide, multilayered ($TiCN/Al_2O_3/TiN$) CVD coated grooved carbide, and single-layered (TiAlN) PVD coated grooved carbide cutting tool. All the tools were

selected in accordance with common industrial recommendations.

1.6 Cutting Fluid Applications

Cutting fluids in general are the various fluids that are used in machining operations to cool and/or lubricate the cutting tool. The two main functions of cutting fluid application are lubrication at relatively low cutting speeds and cooling at relatively higher cutting speeds [1]. There are various kinds of cutting fluids available in the market that include oil, oil-water emulsions, paste, gels and mist. Evaluating the effects of different cutting fluid application on the surface integrity of the work-piece is also a part of this thesis. Three different cutting fluid conditions were selected as a part of this thesis; namely: dry, minimal quantity lubrication (MQL), and flood. The detailed description on the type of cutting fluids is given in Chapter 2 of this thesis.

1.7 Thesis Outline

This section provides information about the outline and contents of this thesis.

Chapter 1 provides information about the motivation behind this research, the work materials and cutting tools used in this thesis.

Chapter 2 gives a background of the machining process, various types of residual stress measurement methods, and previous research that has been performed in the area of residual stresses related to machining aspects.

Chapter 3 explains the experimental setup for machining and residual stress measurement, various materials and cutting conditions used, and a description of the residual stress calculation methods.

Chapter 4 provides the results of the experiments that were conducted as a part of

this thesis and discusses in detail, the effect of cutting tool coatings, cutting fluid application conditions, and chip-breaker geometry effects on the residual stress distribution in the Ti-6Al-4V titanium alloy. This chapter also discusses the microstructural analysis of the machined work-piece with reference to the above machining conditions.

Chapter 5 summarizes the current research presented in this thesis and lists the future directions that may be pursued from this thesis.

All the referenced citations are provided at the end after Chapter 5.

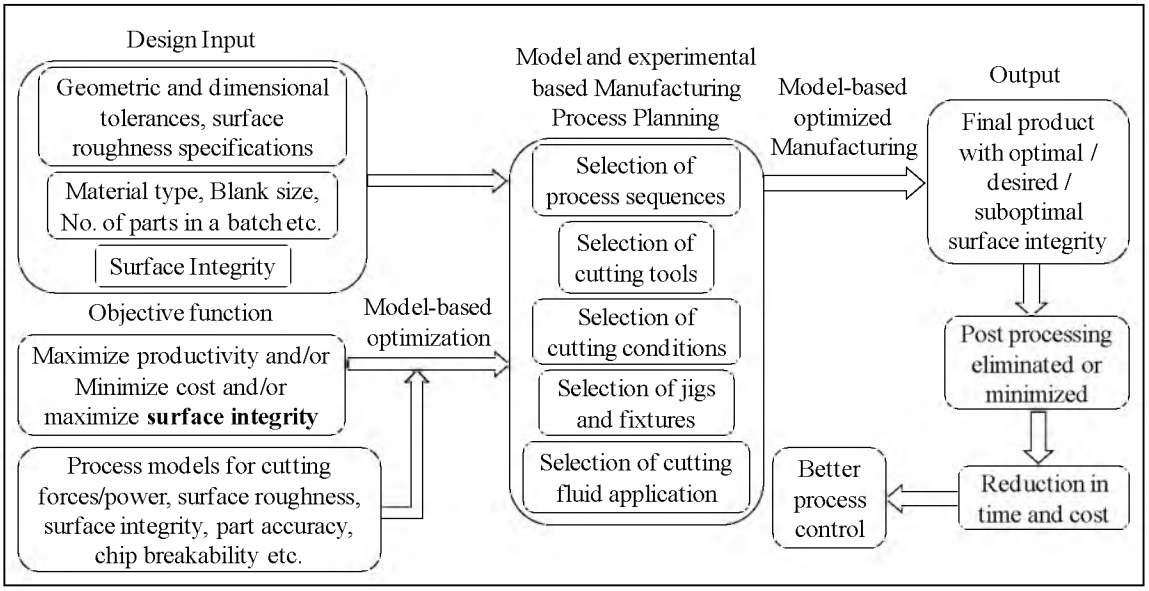

Figure 1.1: Schematic diagram of a manufacturing process plan with active control of surface integrity. (Adapted from [4])

CHAPTER 2

BACKGROUND

This chapter provides detailed information about the general background to the work performed as a part of this thesis.

2.1 Work Material

As mentioned in the previous chapter, Ti6Al4V alloy was selected as the work material for this thesis. Ti6Al4V is grouped under the alpha-beta titanium alloy category. Basically, titanium exists in two crystallographic forms. At room temperature, commercially pure unalloyed titanium has a hexagonal close packed (HCP) crystal structure called "alpha (α) phase." At 1621° F (883° C), this structure transforms to body centered cubic (BCC) structure called "beta (β) phase" [7]. By controlling these crystallographic variations with the help of varying alloying additions and using different thermo-mechanical processing techniques, a wide range of titanium alloys can be developed. Titanium can be grouped into different types as follows.

2.1.1 Unalloyed Titanium

There are several grades of unalloyed titanium. The primary difference between them is the oxygen and iron content present in them. The addition of such contents improves the strength, hardness and transformation temperatures [7]. These groups are usually selected because of their excellent corrosion resistance, especially in applications

where very high strength is not required.

2.1.2 Alpha (or Near Alpha) Alloys

This group contains elements such as aluminum, tin and/or zirconium. These elements are called as α-stabilizing elements. These α-stabilizing elements work by either preventing change in the phase transformation temperature or by causing it to increase [7]. These alloys are generally more resistant to creep at high temperature as compared to alpha-beta or beta alloys and are therefore preferred for high temperature applications. They most often are used in the annealed or recrystallized condition to eliminate residual stresses caused by working [7]. Examples of this group of alloys are Ti-5Al-2.5Sn-ELI, Ti-8Al-1Mo-1V, etc. [7].

2.1.3 Alpha-Beta Alloys

This group has a composition that contains both α and β stabilizers. They can be strengthened by solution treating and aging. Solution treating and aging can increase the strength of alpha-beta alloy from 30% to 50% or more, over the annealed or over-aged condition [6]. The properties of these alloys can be controlled through heat treatment, which is used to adjust the amounts and types of β phase present in the alloy. Examples of this group of alloys are Ti-6Al-4V, Ti-5Al-2Sn-2Zr-4Mo-4Cr, etc. [7].

2.1.4 Beta (or Near Beta) Alloys

This group of alloys is richer in beta stabilizers and leaner in alpha stabilizers as compared to alpha-beta alloys. The types of beta stabilizers are vanadium, niobium and molybdenum. These stabilizers tend to decrease the temperature of α to β phase transition and thus promote development of the BCC (body centered cubic) β phase [7]. They have

excellent forgeability over a wide range of forging temperatures. An example of this group is Ti-10V-2Fe-3Al [7].

2.2 Machining

Machining is a group of processes which use a relatively sharp cutting tool to remove excess or unwanted material from the surface of a work-piece in the form of chips to obtain desired shapes, specifications, or dimensions of the end product. The principal cutting action in machining involves shear deformation of the work material to form a chip. As soon as the chip is removed, a new "machined surface" is generated on the work material. A relative motion between the tool and the work-piece is required to perform the operation of machining. There are two types of relative motions associated with machining. The primary relative motion is called as the "speed" while the secondary relative motion is called as the "feed" [3]. The geometry and shape of the tool and its contact with the work surface, combined with these motions, produces the desired shape of the work-piece. This desired shape is obtained by changing the geometry of the work-piece. Generally, this change of geometry to produce a desired shape is performed by either adding material, removing material or moving material [1]. Examples of adding material are welding, soldering, etc. Examples of moving material are drawing, extrusion, etc. Examples of removing material are machining, punching, etc. The present study is based on a material removal process such as a facing operation.

There are one or more relatively sharp cutting edges present on a cutting tool. While machining, when this sharp cutting edge comes in contact with work material under the used cutting conditions, a chip is separated from the work material and a new "machined surface" is generated on the work material. There are two faces on the cutting

edge; namely: the rake face and the flank face [3]. The rake face is oriented at an angle called the rake angle (shown in Figure 2.1) with respect to the plane perpendicular to the work surface, and it is responsible for directing the flow of the chip. The rake angle may be positive or negative depending on the user requirement. The flank face protects the newly generated surface from abrasion by providing a clearance between the tool and the newly generated surface [3]. The flank face is oriented at an angle called the clearance angle as shown in Figure 2.1.

A schematic diagram of a two-dimensional machining process showing the basic terminology is given in Figure 2.1.

2.3 Surface Integrity

As discussed in the previous chapter, surface integrity may be defined as the state and attributes of a manufactured surface that influence performance of a product or component [2]. Field and Kahles [8-10] were the first to introduce the concept of surface integrity by means of defining the enhanced condition of a surface produced in machining or other surface generation operation. In manufacturing processes, surface integrity plays a very important role in the life and functionality of the machined surface. The type and sequence of manufacturing processes selected at the beginning, along with the selection of cutting conditions and tools, dictates the type of surface that is being produced. One of the main aims towards enhancing surface integrity is to increase the life of the component by adjusting other factors to an optimum level. Surface integrity is subdivided into several components such as surface finish, chemistry, topography, metallurgy, thermal damage (burn, transformation and over-tempering), microstructural changes and residual stresses.

2.4 Residual Stresses

As discussed in the previous chapter, residual stresses are those stresses that remain in the material body even after all the external loads such as forces, couples and applied stresses, acceleration and gravitation are removed [5]. Residual stresses are present in almost all machined materials and product forms. They may be created during the life of the component. If not recognized and accounted for in the design process, they can be a major factor for the failure of the component, particularly those subjected to alternating service loads or corrosive environments. They often are a cause of premature failure of some critical mechanical components. Surface residual stresses are either tensile or compressive in nature. Tensile residual stresses are generally harmful or undesirable, especially for parts that are under cyclic loading [11]. The growth of fatigue cracks is usually aggravated when coupled with tensile residual stress areas as compared to a compressive residual stress area. One of the basic desires of design engineers is to reduce the tensile residual stresses as much as possible or to convert them all into compressive residual stresses. Even though residual stresses are undesirable, certain applications such as toughened glass and prestressed concrete benefit from the presence of compressive residual stress. Residual stresses are very important parameter in all manufacturing industries, especially in aerospace applications, since the demands on functional performance required in the manufacturing of aerospace components is higher [2]. To attain high degree of functional performance in the manufacturing of aerospace components, optimal manufacturing process parameters are essential. At this point of time, several manufacturing process parameters are yet to be established with a great degree of confidence.

Residual stresses can be divided into three types of stresses: namely, Type – I, Type – II and Type – III residual stresses [12]. Type – I residual stresses are also referred to as "macroresidual stresses" [12], since these types of stresses develop in body of the component over a range much larger than the material grain size. Type – II and Type – III residual stresses are microlevel residual stresses and are also referred to as "microresidual stresses" [12], since these types of stresses result from the differences within the microstructure of a material. Type – II residual stresses are a type of microresidual stresses that operate at the individual grain-size level, while Type – III residual stresses are generated at the atomic level due to the presence of defects and dislocations [12]. Figure 2.2 describes the classification of stresses on the basis of the discussion in this section.

Residual stresses in a given component are the cumulative effect of stresses generated due to mechanical effects, thermal effects, and chemical effects [12]. Mechanically generated residual stresses are due to the result of different manufacturing processes. All mechanical-based manufacturing processes induce mechanically generated residual stresses in the component. Thermal residual stresses are mostly a result of non-uniform heating or cooling cycles (for example – quenching). Chemical residual stresses are generated due to chemical reactions, precipitations, or phase transformations taking place in the material [12]. It is very difficult to find out the exact residual stress due to any one of the above-mentioned effects. In this thesis, residual stresses refer to the cumulative effects of the above-mentioned effects. This thesis specifically concentrates on machining induced residual stresses in Ti6Al4V alloy.

2.5 Cutting Tool Material and Coatings

The choice of tool material plays a very important role in the life of the cutting tool and also in the production of the machined surface. Hence, proper selection of the tool is of prime importance. Nowadays, coatings are applied on the tool to obtain different advantages. For example, some coatings increase the life of the cutting tool; some coatings are responsible for producing better surface finish, etc. Different companies manufacture different coatings depending on user requirements. Moreover some coatings are single layered; some are multilayered. Some coatings are applied using physical vapor deposition (PVD) process; some are applied using chemical vapor deposition (CVD) process. The tool substrate also plays a major role in the integrity of the cutting tool.

2.5.1 Tool Substrate

In this thesis, a base tungsten carbide (WC) substrate is selected for all the tools. Tungsten carbide is around three times stiffer than the steel used in high speed steel cutting tools [3]. Tungsten carbide tools generally produce a better finish on the work-piece and also allow operation at faster machining speeds. Moreover, carbide tools can also withstand higher temperatures than standard high speed steel tools. There are four different tools used in this study: an uncoated flat-faced carbide, uncoated grooved (or with chip-breaker geometry) carbide, multilayered ($TiCN/Al_2O_3/TiN$) CVD coated grooved carbide, and single-layered (TiAlN) PVD coated grooved carbide. All the tools were selected in accordance with common industrial recommendations.

2.5.2 Tool Geometry

The production of continuous chips during machining might damage the newly machined surface or the cutting tool coating because of rubbing and friction. Therefore, in order to avoid the production of continuous chips, chip-breaker geometry (or a chip groove) is manufactured on the cutting tool rake surface which obstructs the flow of continuous chips by breaking them into pieces. These tools with chip-breaker geometry are sometimes referred to as grooved tools in this thesis and the tools without the chip-breaker geometry are referred to as flat-faced cutting tools. Cutting tools with flat-faced and grooved geometry are shown in Figures 2.3 and 2.4.

2.5.3 Tool Coatings

Tool coatings are mainly used to resist wear mechanisms and increase tool life significantly. They have been used successfully in the last 30 years. More than 70% of the cemented carbide cutting inserts in use today are coated cutting inserts [1].

Chemical vapor deposition (CVD) is a chemical process used to produce high purity, high-performance solid materials or coatings. In a typical CVD process, the substrate is exposed to one or more precursors, which react and/or decompose on the substrate surface to produce the desired deposit.

In this research, multilayered CVD ($TiCN/Al_2O_3/TiN$) coatings are applied on the tungsten carbide substrate. The main advantage of using a multilayer coating is that the total performance of the multilayer will (ideally) be the sum of the contributions of the individual layers [13]. The first coating on the selected tool is the TiN coating. It has a gold like appearance. These coatings have a very good welding resistance. A well-known use for TiN coating is for edge retention and also for enhancing corrosion resistance in

cutting tools. The second coating is an Al_2O_3 coating. These coatings are used for their high temperature stability and crater wear resistance. The final coating is the TiCN coating. TiCN coating is a well known coating responsible for improved fracture and wear resistance.

Physical vapor deposition (PVD) is a type of vacuum deposition-based technique and is a general term used to describe any of a variety of methods to deposit thin films by condensation of a vaporized form of the material on various surfaces [14]. The coating method involves physical processes such as high temperature vacuum evaporation or plasma sputter bombardment rather than involving a chemical reaction at the surface to be coated as in chemical vapor deposition [14]. They are mostly deposited using cathodic arc deposition or by magnetron sputtering. In this thesis, we use a single layered (TiAlN) PVD coating applied to the tungsten carbide substrate. These tools typically produce good, smooth surface finish on the machined component.

2.6 Cutting Fluid Application

Cutting fluids in general are the various fluids that are used in the machining operation to cool and lubricate the cutting tool. The two main functions of cutting fluid application are lubrication at relatively low cutting speed and cooling at relatively higher cutting speed [1]. There are various kinds of cutting fluids available in the market, which include oil, oil-water emulsions, paste, gels and mist. Evaluating the effects of different cutting fluid application on the surface integrity of the work-piece is also a part of this thesis. Three different cutting fluid conditions were selected as a part of this thesis; namely: dry, flood, and minimized quantity lubrication (MQL).

2.6.1 Dry Machining

Dry machining is a machining operation which is carried out without the presence of any type of cutting fluid. Dry machining is gaining popularity in recent years due to the increase in concerns regarding environmental pollution and concerns for worker health and safety [15]. Dry machining also reduces the overall cost of machining. Market research states that coolant usage and maintenance cost adds up to around 12-13% of the overall cost of the machining [15]. Moreover, after usage, the coolant needs to be disposed of at a safe location. Apart from these advantages, there are, however, some disadvantages to dry machining. Due to the absence of coolant, the temperature in the work-piece can increase, which may increase the thermal residual stresses and hence may prove harmful for the designed component. Tool life can also be reduced drastically due to wear driven by thermal activation.

2.6.2 Flood Cutting Fluid Application

Flood machining is a type of machining performed under the influence of the application of relatively high pressure coolant sprayed in the cutting zone. The coolant flow rate is around 9 liters per minute. Hence, this type of machining uses a bulk amount of the coolant. Some of the important advantages are that it helps to reduce temperature transferred to the work-piece during machining which in turn reduces the thermal residual stresses. It also improves the surface finish and also controls chip flow. Part distortion is also reduced with the help of flood machining [1]. One of the main disadvantages of using a flood machining is that coolant use is environmentally harmful due to the presence of hazardous chemicals added to the coolant. After using the coolant for a

period of time, it gets contaminated. Coolant recycling and disposal is also difficult and costly. Moreover, the overall cost of machining increases with the use of coolant.

2.6.3 MQL Cutting Fluid Application

While machining under minimal quantity lubrication (MQL), lubricant is sprayed on the rake face in the form of very fine mist. The lubricant flow rate can be changed depending on the requirement. This type of machining has both the advantages of dry and flood machining. Unlike dry machining, this type of machining has the potential to prevent large temperature rises in the work-piece and also lubricates the tool work-piece and tool-chip contact, thereby reducing friction between these surfaces while machining.

2.7 Residual Stress Measurement

Residual stresses are not measured directly. Strains are measured instead and then by using principles of solid mechanics, residual stresses are calculated. Residual stress measurement methods are basically categorized into three groups: destructive methods, semidestructive methods, and nondestructive methods. The various methods for residual stress measurements are described in detail in the following sections.

2.7.1 Brittle Lacquer Method

This is a semidestructive type of crude method for measuring the residual stresses in the component. In this method, the test specimen surface is coated with a brittle lacquer known as “stress coat.” Once it is thoroughly dried, a small hole is drilled at the location of interest. This relieves the stresses adjacent to the hole. As soon as this procedure is completed, cracks will appear on the coating in a direction normal to the principal tensile stress as it is relieved. The pattern and magnitude of the original residual

stresses can then be estimated from the direction and pattern of the cracks [5]. One main disadvantage of this method is that it imparts its own stresses due to the drilling of the small hole.

2.7.2 Dissection Method

This is a type of destructive method for measuring residual stresses which was reported by Heyn in 1914. "The process consists of removing successive layers of materials from the specimen and measuring the deformation of the remainder of the specimen after each layer is removed. From these measurements, the original residual stresses in the specimen can be calculated [5]." The main disadvantage of this method is that it is less accurate and it imparts its own stress. Moreover, it comes under the destructive method category.

2.7.3 Curvature Method

This is a type of destructive method. This method is frequently used to determine the residual stresses within coatings and layers. In the case of layers, the deposition of a layer can induce stresses, which causes the substrate to curve. This curvature can then be measured using contact methods or any other method (e.g., profilometry, strain gauges) [16].

2.7.4 Hole Drilling Method

Hole drilling is a type of semidestructive method for measuring the residual stresses. In this method, a small, shallow hole is drilled on the machined surface, thereby relieving the strains. These relieved strains are then measured by a specially configured three element strain gage rosette [17, 18]. The measured strain data set is then processed

with the help of the principles of solid mechanics to obtain relaxed residual stresses present in the machined component. The hole drilling method of residual stress measurement consists of the following steps: 1) Installation of a three radial grid strain gage rosette. 2) A through hole or blind hole of a precalculated depth and diameter is then drilled through the center of the rosette. 3) The relieved strains are then measured using a strain gage indicator. 4) The residual stresses are then calculated from the measured strain data set. This method is used for the residual stress measurement in this present thesis and is explained in greater detail in Section 2.8.

2.7.5 X-ray Diffraction Method

This is a type of nondestructive method that works on Bragg's principle [5]. When an x-ray beam is directed onto a crystalline material, the beam gets diffracted creating an observable peak. Directing an x-ray beam onto a crystalline material, whether it is metal, nonmetal or ceramic, causes the beam to be diffracted, creating an observable peak which can be measured using a detector. If the material is stress free, the peak occurs at a specific known angle depending on the combination of wavelength of the x-ray and the material being analyzed. If stresses are present in the material, the peak tends to shift its location at a certain angle depending on the intensity of the stresses present in the work-piece. The residual stresses can then be calculated using the degree and location of the shift and performing some fundamental physics calculations. Some of the allied methods such as synchrotron or hard x-ray methods work on the same principle. The only difference is that synchrotron X-rays are very strong as compared to the normal conventional X-rays. The increased penetration depth of this method helps in evaluating the stress profiles with high spatial resolution and also obtaining three-

dimensional strain maps [19]. One of the most important advantages is that it can also measure subsurface residual stresses.

2.7.6 Neutron Diffraction Method

This is also a type of nondestructive crystallographic method for the determination of the atomic and/or magnetic structure of a material [16]. The basic working principle is the same as x-ray diffraction, with the only difference being the use of neutron beams in place of an x-ray beam. As compared to the x-ray diffraction method, this method is much faster. One of the major disadvantages is that, this method is relatively costly and the overall operational procedure is also relatively complicated [19]. Also, there is a presence of a lot of noise in the data. The main advantage of the neutron diffraction method is its high penetration capacity for inspecting the materials to greater depth [20].

Table 2.1, based on Withers and Bhadeshia [19] - summarizes the different types of residual stress measurement techniques in terms of penetration, spatial resolution and accuracy of the measurement technique.

2.8 Hole Drilling Method

As mentioned in the previous section, the hole drilling strain gage method is a type of semidestructive method for measuring the residual stresses. The main concept behind this method is the fact that once a hole is drilled on the machined surface, the residual stresses present in the component are relaxed. These relaxed stresses are not measured directly; the relieved strains corresponding to these stresses are measured by installing the strain gage containing three radial grid rosettes and drilling a hole at the

centre of this strain gage array. The strain gage indicator attached to the strain gages then records the relieved strains. The strain gage indicator measures the change in resistance in the strain gage due to the drilled hole. The strain gage indicator works on the principle of Wheatstone's bridge [17]. The residual stresses are then calculated using fundamental solid mechanics principles as described in the ASTM standards [21]. This method was used to measure the residual stresses in the present thesis. ASTM standards were strictly followed during the experimentation. Once the strain data were collected, H-Drill software [22] was used to evaluate the machining induced residual stresses in the work material. A detailed explanation of the experimental methodology used is described in Chapter 3.

2.9 Research Background

This section gives a review of previous work which has been performed in machining induced residual stress measurement and related areas. This section is subdivided into several different areas depending upon the area of emphasis.

2.9.1 General Background on Surface Integrity

In 1951, Henriksen [23] was amongst the first to study and investigate the effects of residual stresses developed due to machining. He studied the stress inducing effect of single point cutting tools working on steels with varying carbon content and found that the stresses increase with the decreasing carbon content and also with decreasing speed. He also suggested that a bending action develops when materials deform over the cutting edge. Experimental methods for determining residual stresses were described by Colwell [24]. The pioneering work of Field and Kahles, through a series of publications, made a

significant contribution on the subject setting the stage for future work [25-27]. They were the first to introduce the concept of surface integrity (SI) by means of defining the enhanced condition of a surface produced in machining or other surface generation operation. They also documented the detailed description of the measuring methods for surface integrity inspection.

Matsumoto et al. [28], worked on the residual stresses in the machined surface of hardened steel (AISI 4340). They showed, when a sharp tool is used for machining, the phase transformations on the machined surface were not responsible for the creation of residual stresses. The phase transformation is present only if a chamfered tool is used in the machining. According to them, the thermal effects on the residual stresses formation were secondary as they are usually responsible for producing only tensile residual stresses. El-khabeery and Fattouh [11] showed in their research that the influence of residual stresses may be beneficial or detrimental depending on the magnitude and type of application. They also showed that compressive stresses are usually advantageous to fatigue and creep life, whereas tensile residual stresses are usually detrimental to the same.

Leskovar and Peklenik [29] found that by choosing the appropriate heat treatment, extremely high concentrations of residual stresses can be avoided. They also suggested, microhardness, residual stresses and metallographic analyses can be the most reliable factors in assessing surface integrity.

Sadat and Bailey [30], while working on AISI 4340 steel, concluded that the peak residual stresses and depth of the stressed region increases with an increase in feed rate and the depth of cut, but decreases with an increase in cutting speed. In 1988, Sadat [31]

worked on the effects of higher cutting speeds on the surface integrity of AISI 4340 and concluded that at higher speeds, the influence of feed rate on both the residual stress distribution and microhardness variation of the surface region was negligible.

Brief reviews of surface integrity in machined alloys can be found in references 32-37. From a detailed study of the above references, one can conclude that the effects of cutting fluid application and cutting tool coating on surface integrity as presented in this thesis were yet to be explored completely.

2.9.2 Effects of Cutting Tool Coatings and Geometry

Cutting tool coatings and cutting tool geometry plays very important role in the life of the cutting tool and also in the production of the machined surface. Hence, proper selection of the cutting tool is of prime importance. Coatings are applied on the tool to obtain different advantages. Very few people have worked on the effects of cutting tool coating and geometry on the surface integrity of the machined workpiece. Some of the research has been described in this section.

Liu and Barash [38, 39] studied the basic mechanism of surface and subsurface layer formation in machining with sharp and worn tools using experimental and analytical methods. They also found out that a linear correlation exists between the apparent strain energy density and the length of the shear plane.

Elkhabeery and Bailey [40, 41] showed that the depth of the affected zone, below the surface where the residual stress effects are observed, increases with both an increase in cutting speed and increase in chip-tool contact length, but appears to be unaffected by the method of tool preparation. Power consumption also increases with an increase in cutting speed and also with an increase in chip-tool contact length. They also worked on

the effect of lubrication conditions on surface integrity in the same year and concluded that at low cutting speeds, application of a lubricant produces a reduction in tool forces, power consumption, surface roughness, surface defects and subsurface deformation, whereas at high cutting speeds, application of a lubricant has little influence on the cutting process.

Okushima and Kakino [42] showed that the residual stresses in the subsurface layer of the machined surface are caused by the mechanical effect of the ploughing force and the thermal effect of the temperature distribution produced during metal cutting. Their investigation also showed that mild cutting conditions such as low cutting speed, low frictional force and low temperature are needed to reduce the tensile residual stresses.

Sadat and Bailey [43] studied the residual stress distribution in machining an annealed bearing bronze. They found that the residual stresses are tensile when machining is carried out at large depths of cut with worn tools and in the absence of a lubricant, but may be compressive when machining at small depth of cut with sharp tools and when using lubricants. Jeelani [44] worked on the effects of cutting speed and tool rake angle on the residual stress distribution in 2024 T351 aluminum alloy. His results concluded that the maximum residual stress and the depth of the severely stressed region increase with an increase in the cutting speed. According to him, there seems to be little change in the residual stress distribution due to a change in the rake angle. He also showed that the residual stresses in the surface regions of the machined work-pieces are produced principally by these factors: plastic deformation and volume of material associated with thermal gradients, and metallurgical alterations in the structure.

M'Saoubi et al. [45] worked on the residual stress analysis in orthogonal machining of AISI 316L steels. Their main focus was to study the effects of uncoated and coated tools, and the influence of rake angles on the residual stresses. They found that, for both uncoated and coated tools, higher temperature levels are reached in the cutting zone, which in turn is responsible for higher tensile residual stresses. They found no clear connection between the influence of rake angle and the thickness of residual stress layer.

Outeiro et al. [46] worked on machining induced residual stresses in AISI 1045 steel using coated and uncoated carbide cutting tools. They found that when cutting with coated cutting tools, with an increase in cutting speed, residual stresses also increased. The inverse trend is followed when machining with uncoated cutting tools. Outeiro et al. [47] worked on the turning of AISI 316L and AISI 1045 steel with coated and uncoated tools having finite edge radii. They found that machining with coated cutting tools produces higher residual stresses, larger tensile layer thickness and higher work hardening as compared to machining with uncoated cutting tools. Although, they focused on other materials other than titanium alloys, Outeiro et al. [48] are some of the very few researchers to have tackled the kinds of problem discussed in this thesis. They worked on the effects of tool geometry, tool coating and other cutting parameters on the residual stress distribution in orthogonally machined AISI 316L steel. Their investigation included experimental and numerical modeling. They found that the residual stresses increases with most of the cutting parameters such as cutting speed, uncut chip thickness and tool cutting edge radius. Among all of them, uncut chip thickness (or feed) has the greatest effect on the residual stress distribution. They also found that when the uncoated cutting tool is replaced by the coated one, the superficial residual stress increases

considerably at a higher cutting speed.

2.9.3 Effects of Cutting Fluid Application

Cutting fluid application also plays important role in the manufacturing industry. The two main functions of cutting fluid application are lubrication at relatively low cutting speed and cooling at relatively higher cutting speed [1]. The work of some of the researchers who studied the effects of different types of cutting fluid applications on the surface integrity of the machined workpieces is mentioned in this subsection.

Elkhabeery and Bailey [40, 41] showed that the depth of affected zone increases with the increase in cutting speed and chip-tool contact length, but remain unaffected by the method of tool preparation. They also worked on the effect of lubrication conditions on the surface integrity and concluded that at low cutting speeds, application of lubricant produces a reduction in tool forces, power consumption, surface roughness, surface defects and subsurface deformation, whereas at high cutting speeds, application of a lubricant has a very little influence on the cutting process.

2.9.4 Machining of Titanium Alloys

Machining of titanium alloys has always been a challenge [1]. Titanium alloy has a strong tendency to react with oxygen, nitrogen, carbon, etc. at higher temperatures, which makes it susceptible while machining because of the abundance of these gases in the air. Moreover, titanium surfaces are very difficult to lubricate while machining due to the formation of titanium oxide [1]. Titanium alloys also have relatively low thermal conductivity. Very high temperatures are reached while machining titanium alloys under higher cutting speeds which are normal for other metals. Hence, comparatively lower

cutting speeds are recommended while machining titanium alloys. There is the presence of adiabatic shear banding while machining titanium alloys. This is due to the fact that the energy associated with the deformation while machining is converted into thermal energy. Due to the low thermal conductivity of titanium alloys, the titanium alloys retain most of the temperature during machining due to which large temperature rise occurs. This in turn causes the effect of thermal softening locally and the strain instead of moving to the new plane continues to move in the same plane. As the deformation proceeds, the deforming shear plane rotates and becomes larger until it breaks due to force from rotation of the plane [1]. Due to the adiabatic shear banding, the chips generated while machining titanium alloys are serrated chips. Other previous work done in the area of machining titanium alloys is described in this section.

Sun and Guo [49] worked on an experimental study of surface integrity of Ti-6Al-4V and reported the influence of cutting speed and feed in an end milling operation on the surface residual stresses. Hughes et al. [50, 51] worked on the effects of tool edge preparation on the surface integrity and tool life of Ti-6Al-4V work pieces. They found some microstructural damage consisting of grain boundaries in the cutting direction. They also conducted an experimental analysis to study the effect of worn tools. They found that the tool wear under all conditions was due to attrition. They also observed the presence of built-up edge welded to the tool surface on both the flank and the crater faces due to the high temperatures and pressures generated during machining.

Puerta-Velasquez et al. [52] worked on the analysis of the surface and subsurface due to high speed orthogonal machining of Ti-6Al-4V alloy. They found out that there is no phase transformation in the near-surface region. Also, the composition of α and β

phase does not change with the cutting speed, which means that no chemical reaction or phase transformation occurs in the vicinity of the sample. Their results provided better understanding of the cutting process along with the microstructures in high speed machining of titanium alloy.

Thomas et al. [53] also worked on the microstructural damage of titanium alloys during high-speed milling. Their work focused on indentifying the microstructural sub-surface damage in the form of intense slip bands after high-speed milling of Ti-6Al-4V and Ti-834 alloys. Such microstructural features were undetected with the current surface integrity techniques. Ginting and Nouari [54] worked on the dry machining of titanium alloys. Apart from surface roughness, their research also focused on the microstructural alterations in the titanium alloy due to the milling process. Che-Haron and Jawaid [55] worked on the effect of machining on the surface integrity and microstructural alteration of Ti-6Al-4V alloy. They found slightly higher surface roughness values at lower cutting speeds. They also found severe tearing and plastic deformation of the machined surface, when machining Ti-64 titanium alloy for prolonged period under dry cutting condition.

Ibrahim et al. [56] worked on the effect of dry machining on the surface integrity of Ti-6Al-4V alloy. In their work, the focus was on the surface roughness, hardness, and microstructural analysis. However, they ignored the study on residual stress aspect. Colafemina et al. [57] worked on the effects of ultra-precision diamond turning on the surface integrity of titanium and its alloys. Even though they claimed to have worked on surface integrity, they ignored residual stress as a factor that influences surface integrity. Palanisamy et al. [58] investigated the effect of coolant application pressure on tool life and chip morphology while turning Ti6Al4V alloy. They found out that the application of

highly pressurized coolant increases the life of the cutting tool by three times and also results in the generation of smaller chips. Barry et al. [59] investigated the chip formation phenomenon in machining Ti6Al4V alloy. They showed that within the range of selected conditions, saw-tooth chips were produced. With the increase in speed and/or feed, a transition from nonperiodic to periodic saw tooth chip formation was observed.

Bayoumi and Xie [60] worked on the metallurgical aspects of chip formation in the machining of Ti-6Al-4V alloy. In their work, they discussed the adiabatic shear banding phenomenon while machining titanium alloys. Komanduri and Von Turkovich [61] worked on the mechanism of segmented chip formation due to adiabatic shear banding while machining titanium alloys. They found out that the adiabatic shear band formation is caused by the localized shear deformation.

It can be seen from this section that a relatively small amount of work has been performed on the effects (both individual as well as combined) of cutting fluid applications and cutting tool coatings on the machining induced residual stress in titanium alloys, which are some of the most important alloys used in the aerospace industry. A detailed work is still essential in this area. Hence, the issue of addressing the effects of cutting tool coatings and cutting fluid application on the machining induced residual stresses in Ti6Al4V alloy has been studied as a part of this thesis.

Chapter 3 provides information about the experimental setup, methodology and other experimental conditions used in this thesis.

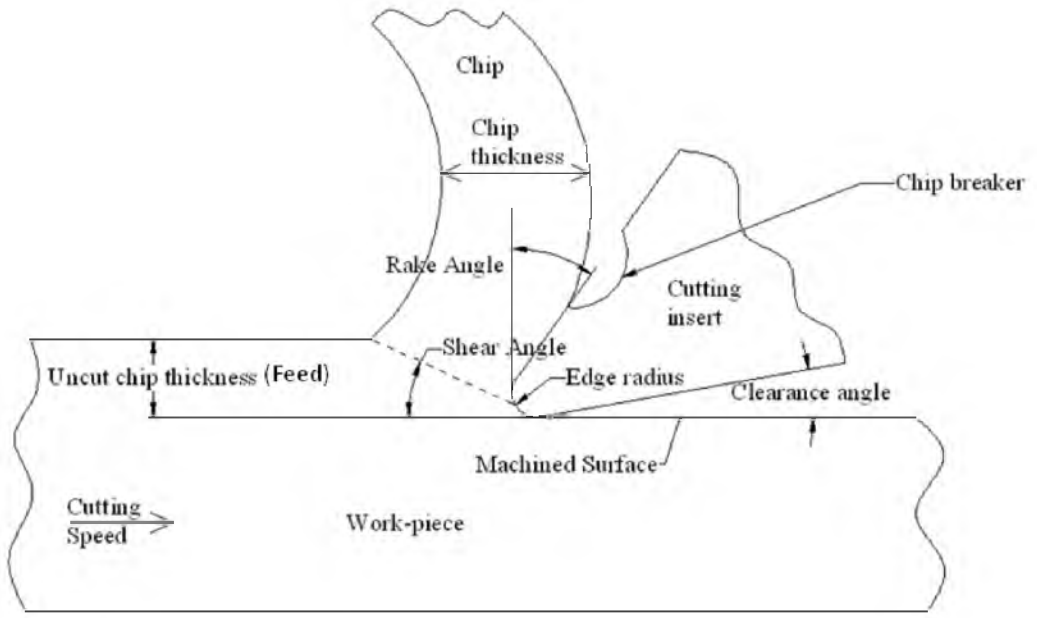

Figure 2.1: Basic terminology used in metal cutting.
(Adapted from [3])

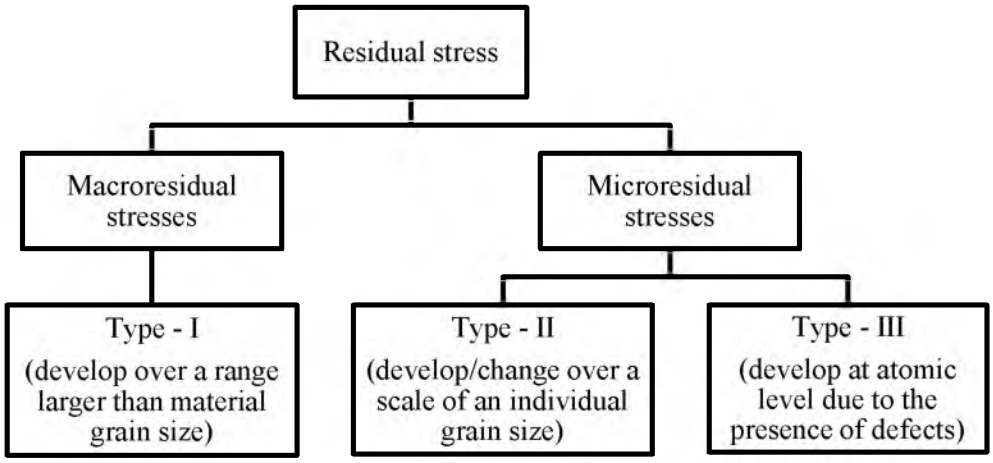

Figure 2.2: Classification of stresses based on the above discussion.
(Modified from [12])

Figure 2.3: Flat faced cutting insert.

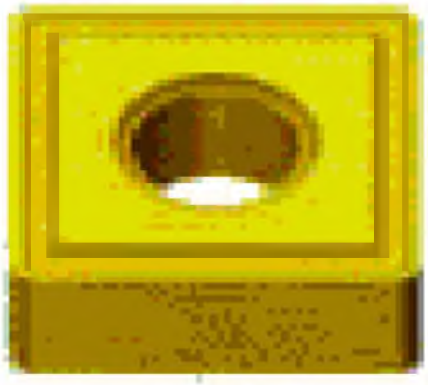

Figure 2.4: Grooved cutting insert.

Table 2.1: Physical characteristics of different residual stress measurement methods (Data from [19])

Method	Penetration	Spatial Resolution	Accuracy
Hole Drilling	~1.2 X hole dia.	50μm depth	±50MPa-Varies
Curvature	0.1-0.5 thickness	0.05 of thickness	Limited
X-ray Diffraction	<50μm for Al <5μm for Ti	1mm laterally 20μm depth	±20MPa- Varies
Hard X-Rays	150-50mm for Al	20μm lateral 1mm parallel	$\pm 10X10^{-6}$ strain
Neutrons (atomic strain gauge)	200mm for Al 4mm for Ti	500μm	$\pm 50X10^{-6}$ strain
Ultrasonic	>10cm	5mm	10%
Magnetic	10mm	1mm	10%

CHAPTER 3

RESEARCH METHODOLOGY

This chapter describes the experimental procedure and methodology for the machining experiments, surface roughness measurements, microstructure analysis procedure, and the hole-drilling strain gage method for measuring the residual stresses in the machined surfaces.

3.1 Description of Machining Experiments

The titanium alloy used for experimentation was annealed Ti6Al4V (grade 5). Titanium machining involved facing a cylindrical surface to produce a new flat machined surface that was investigated for surface integrity. Dimensions of work-pieces used for experiments were 4" (101.6mm) in diameter and 2" (50.8mm) in length as shown in Figure 3.1. A 24" (609.6mm) long and 4" (101.6mm) diameter bar was cut into small bars of 2" (50.8mm) length with a band saw. Later, facing and turning operations were performed at relatively low feed rate, speed and depth of cut, respectively, to eliminate rough band saw cuts and to prepare the workpiece for the machining (facing) experiments. Due to these machining operations residual stress might have been induced into the work-piece. In order to remove such induced residual stresses from the work-pieces, the work-pieces were stress relieved by heat treating them. Annealing is a process of heating the material to above its critical temperature, maintaining it at that temperature

for a suitable time and then cooling it to the room temperature. It is used as a stress relieving process [7]. Time-temperature transformation (TTT) charts were used in order to decide the conditions for stress relieving the Ti6Al4V titanium alloy work-pieces to remove any induced residual stresses due to machining operations. The machined workpieces are shown schematically in Figure 3.2.

A HAAS SL-20 CNC turning center, with a travel of 20" and maximum cutting diameter of 10.3", was used in all the machining experiments. The cutting forces were measured using a Kistler® three component force dynamometer (type: 9121) and charge amplifier (type: 5010) coupled with National Instruments Lab View based data acquisition system. This three-component force dynamometer is connected and installed on the tool holder system of the HAAS SL-20 CNC machining center. The assembly is schematically depicted in Figure 3.3.

The three-component force dynamometer measures the forces as F_f, F_r, and F_c. F_f is the feed force acting on the tool in the feed direction; F_r is the radial force acting on the tool in the radial direction; while F_c is the main cutting force acting on the tool in the direction as shown in Figure 3.3.

The material element component properties and the thermal and mechanical data are given in Tables 3.1 and 3.2.

3.1.1 Experimental Plan

All the experiments were facing experiments. The detailed experimental plan is depicted in Table 3.3. Four different types of cutting inserts were used – uncoated flat faced carbide, uncoated grooved carbide, multilayered CVD coated carbide and single-layered PVD coated carbide. Three different types of cutting fluid applications were used

– dry, minimal quantity lubrication (MQL), and flood. Total number of experiments = 4 X 3 X 1 X 1 X 1 = 12.

3.1.2 Cutting Tools

The cutting tools used for the experimentation were manufactured and supplied by Ceratip-Kyocera. Hence, the Kyocera designation is used to list the tools. Figure 3.4 shows the general cutting tool terminology. In the present research, the tool used has a rake and inclination angle of -5° and major cutting edge angle of 90°.

The following is the list of tools used in the experimentation.

- CNMA 432 KW10 – Flat faced uncoated tungsten carbide cutting insert
- CNMG 432 AH KW10 – Grooved (AH) uncoated tungsten carbide cutting insert
- CNMG 432 TK CA6515 – Grooved (TK) multi-layered CVD (TiCN/Al_2O_3/TiN) coated tungsten carbide insert
- CNMG 432 TK PR1125 – Grooved (TK) single-layered PVD (TiAlN) coated tungsten carbide insert

Each of the letters has its own significance and is mentioned below:

- First letter/digit – It represents the shape of the insert. In this case C indicates diamond (rhombus) shape with 80° included angle.
- Second letter/digit – It represents the relief angle. In this case N indicates 0° relief angle.
- Third letter/digit – It represents the tolerances that are applied to the tool prior to the edge preparation and coating.
- Fourth letter/digit – It represents the insert type. In this case A indicates that the shape of the internal hole is cylindrical, and the tool is without chip breaker and G

indicates that the shape of the internal hole is cylindrical, and the tool has a chip breaker groove on both sides.

- Fifth letter/digit – It represents the size of the cutting tool insert. In this case, 4 indicates that the diameter of the inscribed circle that defines the insert is 0.5 inch.
- Sixth letter/digit – It represents the thickness of the cutting tool insert. In this case, 3 indicates the insert thickness is 3/16 inch.
- Seventh letter/digit – It represents the corner radius of the insert. In this case, 2 indicates 1/32 inch (or 0.8 mm) corner radius.
- Eighth and Ninth letter/digit – It represents the chip-breaker geometry of the cutting insert. In this case, AH and TK are Kyocera designed chip-breaker geometries.

The cutting insert tool holder used for the experimentation was manufactured by Kennametal. The ISO designation of this tool holder is given by MCFNR 124B. The ISO tool holder identification system can be found in any major cutting tool manufacturer's catalogue.

3.1.3 Cutting Fluid Applications

In this work, three different cutting fluid conditions were used, which are as follows:

- Dry machining: In this condition, no cutting fluid was used.
- Minimal quantity lubrication (MQL): This is a form of mist lubrication, in which very small droplets of a liquid are distributed in a large volume of air. In this condition, Coolube 2210, a highly refined vegetable based metal lubricant from UNIST was applied on the rake face zone at a flow rate of 30 ml/hr. This

lubricant has very good lubricating properties.

- Flood machining: This is a form of lubrication in which a high volume stream of fluid is applied on the rake face zone at a predefined flow rate. In this condition, Cimtech 310, which is a synthetic cutting fluid with good coolant properties, was applied on the rake face zone during machining at a flow rate of 9 liters/min.

3.2 Surface Roughness Measurement

Surface roughness is one of the important ingredients of surface integrity and is defined as the geometric deviation of the final surface from the desired surface [1]. A Zygo® NewView 5000 series optical interferometry-based surface profilometer was used to measure the surface roughness values of the machined workpieces. The surface roughness values were measured at three different locations on the machined surface of each workpiece and an average of all the three values was obtained as the surface roughness value of that work-piece. From the Zygo profilometer, we get R_a and RMS (root mean square) values of surface roughness. R_a values were considered for comparison in this present research as it is a very commonly used surface roughness measurement reported in the literature.

3.3 Residual Stress Measurement

The hole drilling strain gage method was used for the measurement of the residual stresses induced due to machining of Ti6Al4V alloy. The strain gages used in the residual stress measurements were manufactured and supplied by Vishay Micromeasurements Inc.

3.3.1 Strain Gauge Selection

A CEA-06-062UL-120 type of strain gauge was used in the experiments (which is shown in Figure 3.5). The strain gauge designation system used for this company is described below:

- First two letters/digits – It denotes the carrier matrix (Backing). In this case, CE indicates thin, flexible gages with a cast polyimide backing and encapsulation featuring large, rugged, copper-coated solder tabs. This construction provides optimum capability for direct lead wire attachment.
- Third letter/digit – It represents the type of foil alloy used. In this case, A indicates Constantan alloy in self-temperature-compensated form is used.
- Fourth and Fifth letters/digits – It represents the self-temperature-compensation number which is the appropriate thermal expansion coefficient in ppm/°F of the structural material on which the gage is used.
- Sixth, Seventh, and Eighth letters/digits – They represent the active gage length in inches. Hence, in this case, 062 indicated that the gage length of the selected gage is 0.062 inches.
- Ninth and Tenth letters/digits – They represent the grid and tab geometry. In this case UL indicates the grid and tab geometry of the strain gage as shown in the figure.
- Eleventh, twelfth, and thirteenth letters/digits – They represents the resistance of the strain gage in Ohms. In this case, 120 indicates that the resistance of the selected gage is 120 Ohms.

3.3.2 Strain Gage Installation

After the selection of the required strain gage, the next step followed was to install the strain gage on the machined work-piece. The strain gage installation procedure is mentioned in the next section.

3.3.3 Surface Preparation

The strain gage installation area was cleaned properly with the help of a degreaser and a neutralizer. Degreasing was performed to remove oils, greases, organic contaminants, and soluble chemical residues from the surface. It was performed using a CSM-1A degreaser. The next step was to clean the surface of the work-piece using M-prep conditioner A and then to wipe the surface dry with the help of clean gage sponge. After that, the desired location and orientation of the strain gage on the test surface was marked with a pair of crossed, perpendicular reference lines with the help of a medium-hard drafting pencil. The strain gages to be placed on the workpieces were oriented in such a way that strain gage 1 was in the direction of the cutting speed for the machining (facing) operation and strain gage 3 was in the direction of the feed. Moreover, all the strain gages were placed on the workpieces in such a way that the hole was drilled at the same radial distance from the center of the workpiece in order to ensure consistency of measurement. Figure 3.6 shows the workpiece with the strain gages mounted on it. After the layout lines were marked, conditioner A was applied repeatedly, and the surface was scrubbed with cotton-tipped applicators until a clean tip was no longer discolored by scrubbing. To provide optimum alkalinity for the strain gage adhesives, the cleaned surfaces were neutralized by applying M-prep neutralizer 5A to the cleaned surface.

3.3.4 Strain Gage Bonding

The performance of the strain gage is dependent on the bond between itself and the tested part. The strain gage was removed from the pack and was oriented in the required direction. Then a small layer of catalyst C was applied on the strain gage. Then, the M-Bond 200 adhesive was applied and the strain gage was also applied on the desired location. Once the strain gage was bonded to the work-piece, the next step was to solder the lead wires to the strain gage tabs.

3.4 Hole Drilling Method

Tungsten carbide endmills were used to drill/machine the hole in the end milling experiments for measuring the machining induced residual stress in the Ti6Al4V alloy work material. The experiments were performed on a Haas CNC-VFE (Vertical Machining Center) with 765/408/508mm X/Y/Z Axis Travel and 20 HP Spindle motor. The dimensions and the other cutting conditions of the endmills used in this research were:

- Mill diameter = 1/16 inches or 0.0625" (1.5875 mm)
- Length of the shank = 3/16 inches (4.76 mm)
- Length of Cut (LOC) = 0.1875 inches (4.7625 mm)
- Spindle speed = 2000 rpm
- Feed rate = 1 inch/min (25.4 mm/min)

As per ASTM standards [21], the center of the drilled hole should be concentric with the center of the strain gage circle within ± 0.004D or ± 0.001" tolerance limit, whichever is greater. In this research, D is 0.202", 0.004D is 0.0008", and hence 0.001" is the greater tolerance limit as mentioned above. For centering the end-mill with respect

to the strain gage circle within the ±0.004D tolerance limit, a centering microscope with a 25X magnification was used. The centering microscope attached to the spindle of the CNC-VFE machining center is shown in Figure 3.7. It has two crosswire axes perpendicular to each other. Each division on the crosswire axes is equal to 0.001" length. The center of the hole to be drilled can be aligned with the strain gage circle center by adjusting the *y* and *z* axis movements on the CNC, thereby adjusting the crosswire on the centering microscope.

After adjusting the center of the drill in line with the center of the strain gage circle, the location was recorded as the "part zero" on the machine coordinate system. Before starting the drilling tests, the strain gage wires (3 wires) were connected to three different channels of the switch and balance unit. Then, using another set of wires, the switch and balance unit was connected to the strain gage indicator. Once the wires were connected, the whole circuit was balanced by selecting one channel at a time, and setting the value on the strain gage indicator to zero. Figure 3.8 shows the general CNC-VFE machine setup of the digital strain indicator and switch and balance unit connected to the strain gage rosette for measuring the relieved strains. Before the start of the hole drilling experiments, it was verified that the circuit was balanced. Each time the hole was drilled to the desired location, the machine was stopped and the end-mill was allowed to cool for around 2-3 minutes. The strain gage indicator readings indicating the relieved strains were read by selecting one of the three different channels. After the 2-3 minutes of cooling time was over, the next hole depth was drilled and the same procedure was repeated for the rest of the depths.

3.5 Residual Stress Calculations

The relieved strain readings measured from the strain gage indicators were used to calculate the residual stresses induced in the work-piece due to machining. The diameter of the work-piece is 4", while the length is 2". The ASTM standard [21] states that if the thickness of the work-piece is less than 0.4D, it is considered a "thin work-piece," else if the thickness of the work-piece is greater than or equal to 1.2D, then the work-piece is considered a "thick work-piece." In this study, the value of D (diameter of center circle of the strain gage) is 0.202"; hence the length of the work-piece is greater than 1.2D. Therefore, in this study, the work-piece can be considered a "thick work-piece." Before calculating the residual stresses, the measured strain readings were checked for uniform/nonuniform stress cases. In this study, the residual stress profile was assumed to be nonuniform due to the fact that the residual stress varies with respect to depth [5]. The procedure for the residual stress calculations was strictly based on the ASTM standards [21] and Tech note TN503 [18] from Vishay Micro Measurements. There are three basic methods for calculating the residual stresses using the measured relieved strains. They are equivalent uniform stress method (or average strain method), power series method and integral method [12]. All these methods are described in this section.

3.5.1 Equivalent Uniform Stress (EUS) Method

This method assumes that the residual stresses are uniform within the depth from the surface of the workpiece [22]. The method has no spatial resolution. The machining induced residual stresses are not uniform along the depth. Hence this method was not used for obtaining the results in this thesis.

3.5.2 Power Series Method

This method provides a limited amount of spatial resolution by assuming that the residual stresses vary linearly with depth from the surface of work-piece [22]. This method cannot resolve the fine details of a nonuniform stress field. This method also requires the calibration functions to be obtained from numerical methods. Since machining induced residual stresses do not vary linearly (uniformly) along the depth [5], as per the previous literature available on this topic [21, 22], this method is not suitable for calculating the nonuniform residual stresses induced due to machining.

3.5.3 Integral Method

This method provides a separate evaluation of residual stresses within each increment of depth used during the hole-drilling measurements [22]. Moreover, the spatial resolution is the highest among the three methods. This is the method of choice when measuring rapidly varying residual stresses which are generally observed in machining induced residual stresses. This method is able to find relaxed strains that relate to highly nonuniform residual stress distribution. A great degree of precision is required while measuring the strains, as the calculations in this method are highly sensitive to strain measurement errors. "This method recognizes that the strains measured during hole drilling are the cumulative result of relieving the residual stresses that were originally present at all depth steps within the total hole depth [12]." This method was used for the residual stress calculations done in this research.

As we know, one of the leading causes of a component failure is due to the maximum principal stresses [62], hence, the maximum principal stress profile induced due to machining is considered henceforth. In this research, the integral method is used

using the H-Drill software [22] for calculating the residual stresses.

3.6 Sample Preparation for Microstructure Analysis

Once the machining experiments were completed, and the surface roughness and residual stress measurement stages were completed, the final study in this present thesis was microstructure observation of the machined workpiece subsurface. The current work-piece was too big to fit in the optical microscope base. Small samples of 0.3" X 0.3" X 0.2" sizes were cut out (using a band-saw) of the work-pieces. The cut work pieces were polished enough to remove the band-saw effected zones. Each sample was mounted in an epoxy mold with the help of Buehler Simplimet 3000 series automatic mounting press. Figure 3.9 shows a sample mounted in an epoxy mould. Once the epoxy mold was ready, the next step was to polish the samples with a series of silicon carbide abrasive papers ranging from 320 grit size to 1200 grit size, followed by final polishing on a velvet cloth by alumina slurry of particle sizes 1, 0.3 and 0.05 microns sequentially. Once all the samples were polished in this manner, they were dried completely. Then, the polished surface of the samples was etched with Kroll's reagent for about 15 seconds. Kroll's reagent was prepared by mixing 92 ml of distilled water with 6 ml of HNO_3 (Nitric acid) and 2 ml of HF (Hydrofluoric acid) for each 100ml of Kroll's reagent preparation. Once all these steps were completed, the samples were examined under an optical microscope. Figure 3.10 shows the epoxy mould on top of an optical microscope. The microscope used was an Olympus GX51 optical microscope capable of imaging up to 1000X magnification. The photographed micrographs were then used for further analysis with the results being reported in the next chapter.

This concludes Chapter 3 of this thesis. Chapter 4 discusses the results and summarizes the present research endeavor in detail.

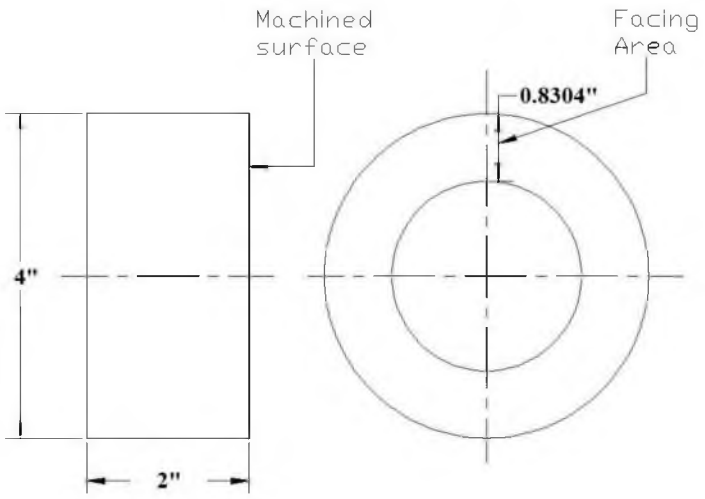

Figure 3.1: Ti6Al4V alloy work-piece dimensions before machining.

Figure 3.2: Machined Ti6Al4V alloy work-piece, ready for residual stress measurement.

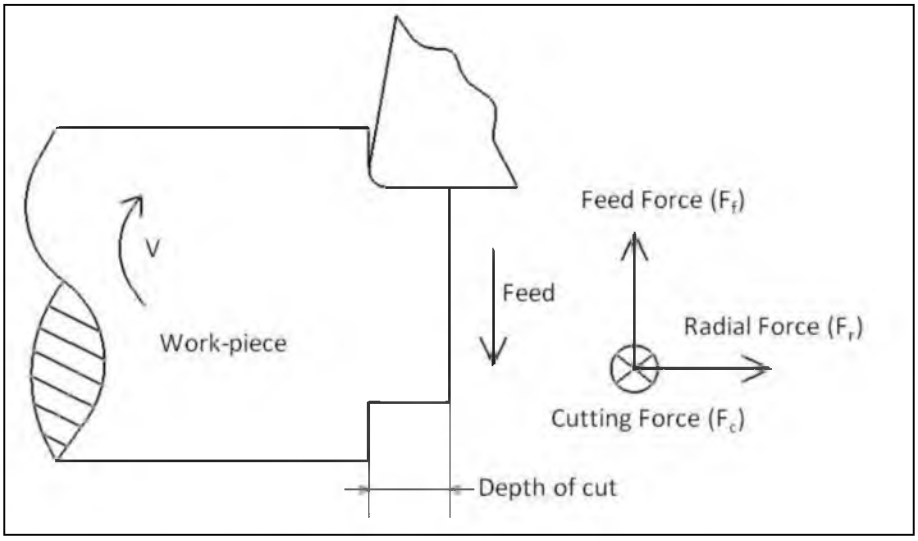

Figure 3.3: Schematic of the experimental setup.

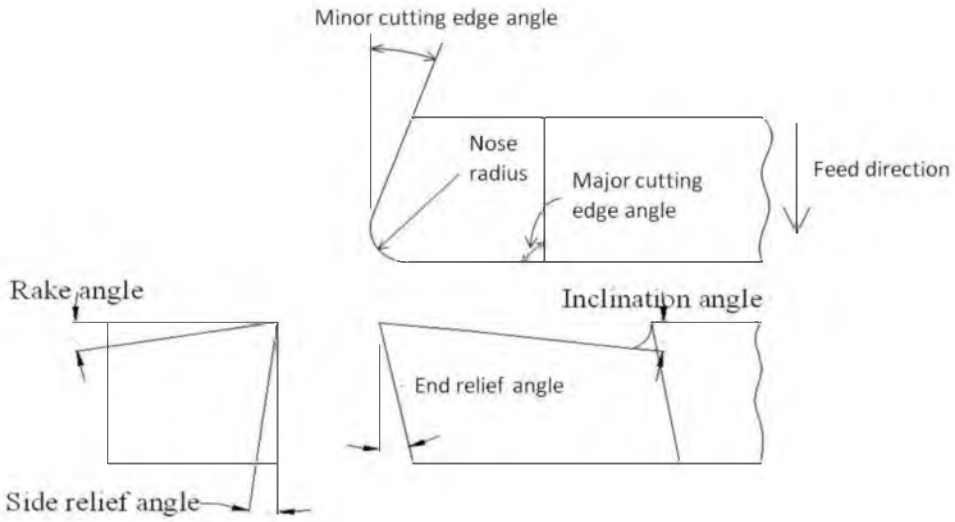

Figure 3.4: Cutting tool terminology.
(Adapted from [1])

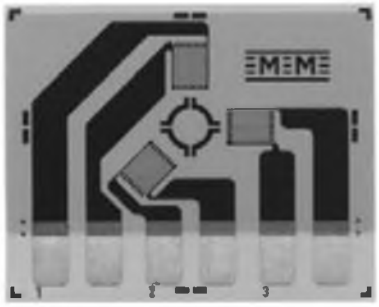

Figure 3.5: CEA-06-062UL-120 type of strain gage.
(Modified from [18])

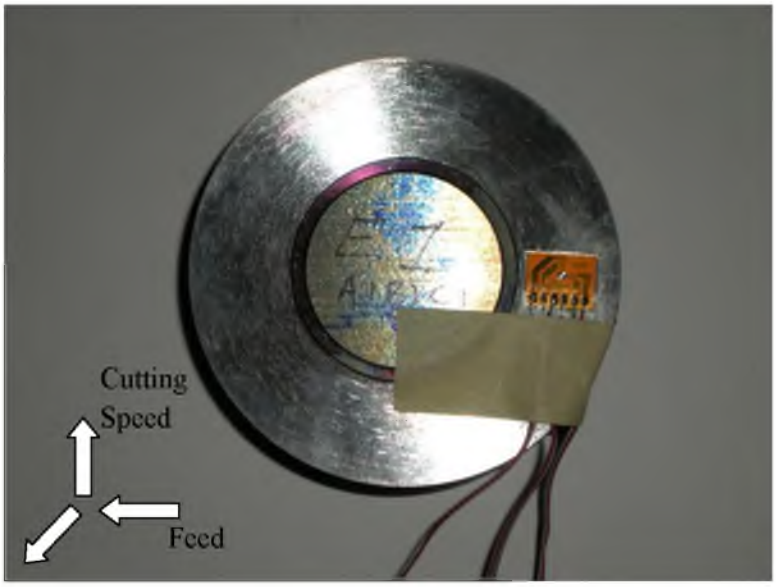

Figure 3.6: Location and direction of the strain gage mounted on the workpiece.

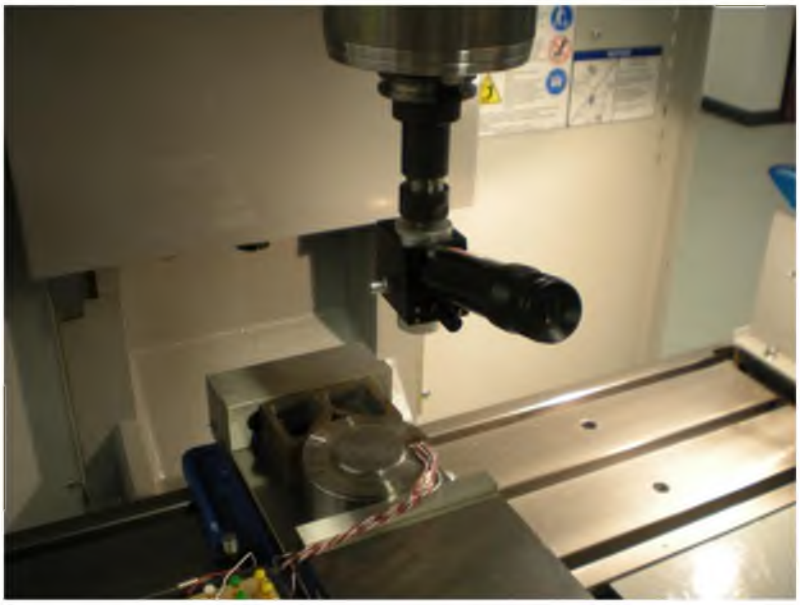

Figure 3.7: Centering microscope attached to the machine spindle.

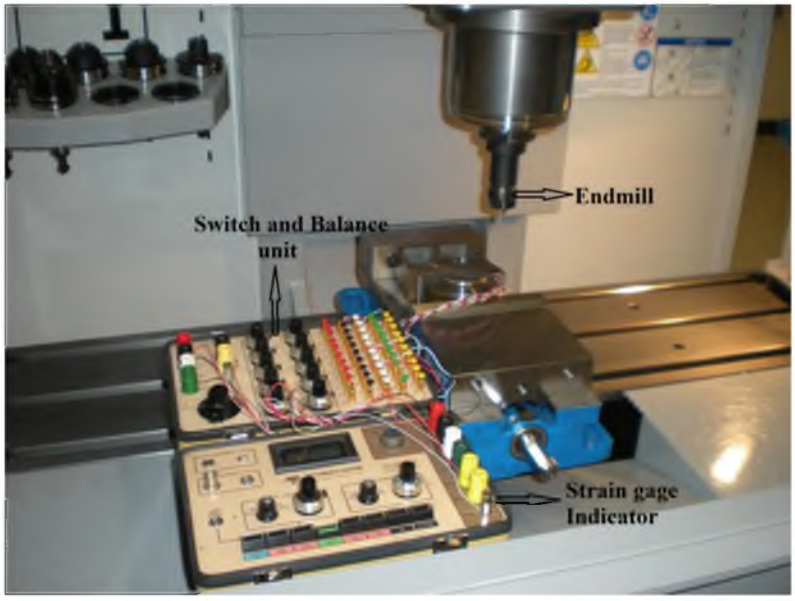

Figure 3.8: The general CNC-VFE machine setup showing the digital strain indicator and switch and balance unit connected to the strain gage rosette for measuring the relieved strains.

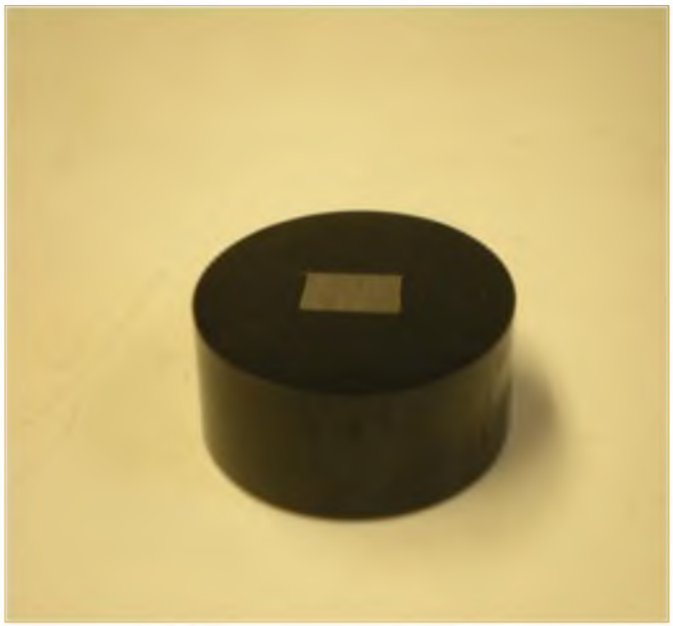

Figure 3.9: Sample mounted in an epoxy mould.

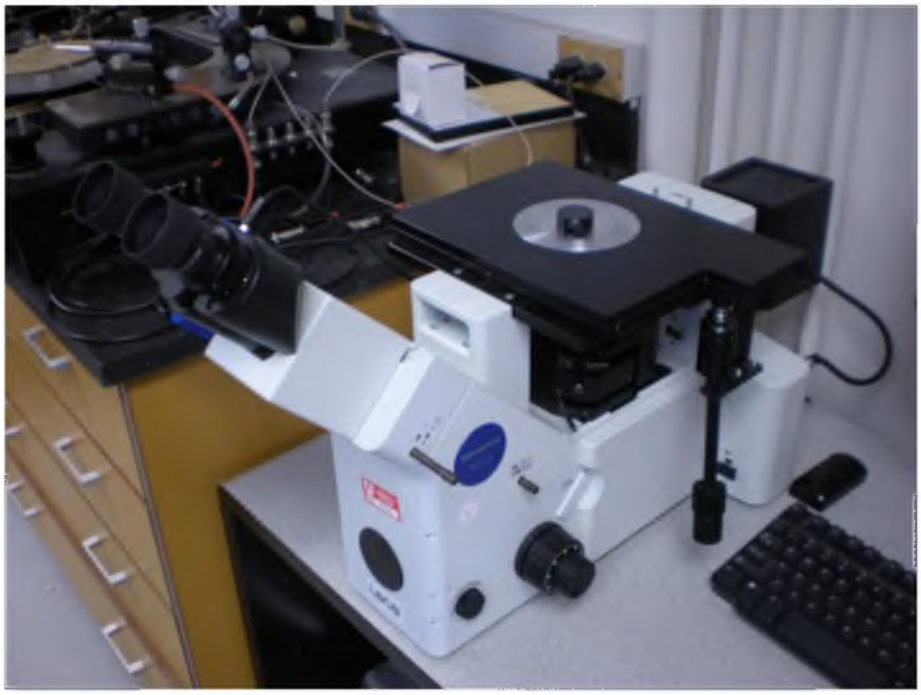

Figure 3.10: Epoxy mould mounted at the base of the optical microscope.

Table 3.1: Material component constituents for Ti-6Al-4V alloy (Data source [7])

Constituents	**Ti-6Al-4V (unit)**
Aluminum, Al	6.00%
Oxygen, O	<=0.25%
Iron, Fe	<=0.20%
Titanium, Ti	90.00%
Vanadium, V	4.00%

Table 3.2: Mechanical properties data of the Ti-6Al-4V alloy (Data source [7])

Mechanical Properties	**Ti-6Al-4V (unit)**
Ultimate tensile strength	950 MPa
Tensile yield strength	880 MPa
Modulus of elasticity	113.8 GPa
Poisson's ratio	0.342
Machinability	22%
Shear modulus	44 GPa
Shear strength	550 MPa
Brinell Hardness	334
Density	4.42 g/cc
Thermal Conductivity	6.70 W/m-K
Melting Point	1604 – 1660 °C

Table 3.3: Detailed experimental plan

Variable	No. of variables	Description
Tool Materials	4	– Uncoated flat-faced carbide, KW10 – Uncoated grooved carbide, KW10 – Multilayered CVD coated carbide [TiCN/Al_2O_3/TiN], CA6515 – Single-layered PVD coated carbide [TiAlN], PR1125
CF application	3	– Dry; – MQL (30 ml/hr); – Flood (9 l/min);
Cutting Speed	1	75 m/min
Feed Rate	1	0.2 mm/rev
Width (depth) of Cut	1	1.2 mm
Rake Angle	-	-5°
Inclination Angle	-	-5°
Major Cutting edge angle	-	90°

CHAPTER 4

RESULTS AND DISCUSSION

This chapter describes the results and provides a detailed discussion of results for all the experiments conducted as a part of this thesis. As mentioned in the previous chapters, machining experiments were conducted on Ti-6Al-4V titanium alloy using four different tools; namely: uncoated flat-faced tungsten carbide, uncoated grooved tungsten carbide, grooved multilayered ($TiCN/Al_2O_3/TiN$) CVD coated tungsten carbide, and grooved single-layered (TiAlN) PVD coated tungsten carbide, under three different cutting fluid application conditions, namely dry, MQL, and flood.

4.1 Outline of Chapter 4

Section 4.2 gives a detailed comparison of the feed, radial and main cutting forces, respectively, generated while machining Ti-6Al-4V titanium alloys with the four different tools under the influence of three different cutting fluid application conditions.

Section 4.3 gives a detailed comparison of surface roughness generated on the machined surface of Ti-6Al-4V titanium alloys. This section also compares the chips formed during the machining process.

Section 4.4 explains the different subsurface microstructures of the machined Ti-6Al-4V workpieces.

Section 4.5 explains the effect of tool insert coatings on residual stresses while machining Ti-6Al-4V titanium alloys.

Section 4.6 explains the effect of cutting fluid application on the residual stresses while machining Ti-6Al-4V titanium alloy.

Section 4.7 explains the effect of different cutting tool parameters on machining induced residual stresses in Ti-6Al-4V titanium alloy.

Section 4.8 summarizes the entire chapter.

4.2 Cutting Forces

The cutting forces were measured using a Kistler® three component force dynamometer (type: 9121) and charge amplifier (type: 5010) coupled with a National Instruments® Lab View based data acquisition system. This three component force dynamometer is connected and installed on the tool holder system of the HAAS SL20 CNC turning center. Detailed information about the assembly and its working was provided in Chapter 3.

As mentioned in the previous chapters, the Ti-6Al-4V titanium alloy work-piece was machined with four different tools: namely, uncoated flat-faced, uncoated grooved, multilayered ($TiCN/Al_2O_3/TiN$) CVD coated grooved and single-layered (TiAlN) PVD coated grooved tools. Three different cutting fluids condition were used, namely: dry, minimal quantity lubrication (MQL) and flood. The comparison between the feed, radial and main cutting forces obtained while machining Ti-6Al-4V alloy with respect to different cutting tool and cutting fluid conditions can be seen in Figures 4.1, 4.2, and 4.3 respectively.

Figure 4.1 shows the bar graph of feed forces obtained while machining Ti-6Al-4V titanium alloy using four cutting inserts under the influence of three cutting fluid applications. It can be seen that the highest feed force was obtained while machining using the uncoated grooved cutting insert under dry machining conditions. The lowest feed force was obtained while machining using the multilayered ($TiCN/Al_2O_3/TiN$) CVD coated grooved cutting insert under the application of flood cutting fluid condition.

Figure 4.2 shows the bar graph of the radial forces obtained while machining Ti-6Al-4V titanium alloys using different cutting inserts under the influence of different cutting fluid conditions. It was observed that the highest radial force was obtained while machining using the single-layered PVD coated grooved cutting insert under dry machining conditions. The lowest radial force was obtained while machining using uncoated flat-faced cutting insert under the application of flood cutting fluid condition.

Figure 4.3 shows the bar graph of the main cutting forces obtained while machining Ti-6Al-4V titanium alloys using four cutting inserts under the influence of three cutting fluid application conditions. From Figure 4.3, it can be seen that the highest main cutting forces were obtained while machining with the uncoated flat-faced cutting insert under MQL condition. The lowest forces were obtained when machining with the single-layered (TiAlN) PVD coated grooved cutting insert under MQL condition.

It can also be seen that MQL condition behaves differently for uncoated (grooved or flat-faced) and coated (CVD or PVD) cutting inserts. The main cutting forces for coated tools (CVD and PVD) under MQL conditions were the least for all the three conditions, which was not the case for uncoated tools (flat-faced or grooved). A different trend was observed when machining under dry condition. The variation in the main

cutting forces under dry condition was quite less irrespective of the type of cutting tool used. When the performance of flood condition was compared, it was observed that for uncoated (flat-faced and grooved) cutting inserts under flood condition, the main cutting forces were the least. This was not the case in coated (CVD and PVD) tools, for which MQL condition showed the least main cutting forces. Hence, MQL and flood cutting fluid application trends are almost opposite of each other.

4.3 Surface Roughness

The surface roughness values were measured using a Zygo® NewView 5000 series optical interferometry-based surface profilometer. Figure 4.4 shows the surface roughness values on machined Ti-6Al-4V alloys with four cutting tools under three cutting fluid application conditions. A relatively smoother surface was produced when Ti-6Al-4V titanium alloy was machined with single-layered (TiAlN) PVD coated grooved cutting insert under flood cutting condition. Incidentally, surface roughness was highest for the work-piece that was machined with single-layered (TiAlN) PVD coated grooved cutting insert under the dry cutting condition.

A general trend was observed when the surface roughness values of all the work-pieces were compared. For all the cutting inserts, a relatively smoother surface finish was obtained when machined under flood cutting fluid condition, followed by MQL condition, while relatively rougher surface finish was obtained when machined under dry cutting condition. However, the overall variations were not very significant. It is interesting to note that the surface roughness variation using grooved uncoated cutting insert under all the three cutting conditions was minimal as compared to other cutting inserts in which the variation was comparatively higher.

4.4 Chip Formation

The chips that were produced after machining Ti-6Al-4V alloy with four cutting tool inserts under three cutting fluid application conditions are shown in Figure 4.5. Flat faced uncoated tools were the tools with unrestricted tool-chip contact length and hence should comparatively produce more continuous chips. At lower cutting speeds the chip is often discontinuous, while the chip becomes serrated as the cutting speed is increased [1]. Serrated chips with accompanying adiabatic shear bands are commonly observed in machining materials that exhibit poor thermal properties with either low thermal conductivity or low specific heat [63]. The chips produced by machining with grooved cutting tool inserts were of comparatively shorter length, as shown in Figure 4.5. The flat-faced tool insert exhibits extremely poor chip control. The grooved tools were marginally better in the sense that the chip forms were a little better recognized in terms of their geometry.

4.5 Machined Subsurface Microstructures

The microstructural changes in the machined subsurface with respect to different cutting tool inserts and under different cutting fluid application conditions are discussed in this section. The mechanical properties of titanium alloys strongly depend on the processing history and heat treatment [84]. For example, when an alloy is hot worked and heat treated in the $\alpha+\beta$ phase field, below the β transus, it develops a duplex microstructure consisting of primary α and transformed β structures. The primary α forms through nucleation and growth and its morphology can vary from elongated plates in lightly worked material to equiaxed globular morphology in heavily worked materials [6].

Ti-6Al-4V is a α+β alloy, with 6 wt% aluminum stabilizing the α phase and 4 wt% vanadium stabilizing the β phase. At room temperature, prior to machining, the microstructure at equilibrium consists mainly of the hexagonal closed packed (HCP) α phase with some retained body centered cubic (BCC) β phase. Depending on the cooling rate and prior heat treatment, the microconstituents and microstructure is divided into several types: namely, grain boundary allotriomorph α, globular or primary α, widmanstatten basket weave, and martensitic types. For very slow cooling rates from high up in the α+β region or above the β transus temperature (995°C ± 20°C), the β phase mainly transforms into globular type of α structures. Increasing the cooling rate enhances the formation and growth of α platelets into the prior β grains [65]. The length and width of these α platelets are determined by the cooling rate. An increased cooling rate enhances the nucleation rate of these α platelets and slows the diffusion process or the growth rate. According to Pelcastre [65], the most important microstructural parameter determining the mechanical properties of α+β titanium alloys is α colony size. With decreasing α colony size, the yield strength, ductility, and crack propagation resistance is improved, whereas the fracture toughness is improved by larger or coarser α colony size.

All the processes that are necessary to manufacture a given part are responsible for inducing residual stresses in the part. The main criteria that were under consideration in this research are cutting tool coatings and cutting fluid application. As discussed in the previous section, Ti-6Al-4V titanium alloy has a widmanstatten basket-weave microstructure at room temperature. The microstructure of the Ti-6Al-4V titanium alloy before machining was well organized, with no traces of "coarsened α" structure in the microstructure. As the machining experiments were performed, the high heat and

pressure generated during machining changes the microstructure of the Ti-6Al-4V titanium alloy. Hence, after machining, the HCP structured alpha phase was coarsened more thereby compressing the BCC structured beta phase. Hence, conversely it can be claimed that high temperature and pressure levels were reached at the place where coarsened α structure was present. Higher temperature and temperature gradients generate thermal stresses. It is a well known fact that thermal stresses are responsible for tensile residual stresses [24].

Figures 4.6 – 4.17 shows the microstructures of the Ti-6Al-4V workpiece subsurfaces obtained after machining them with four cutting tools and three cutting fluid application conditions.

4.6 Residual Stresses: Effects of Cutting Tools (Material/Coatings and Geometry)

4.6.1 Machining with Uncoated Flat-Faced Cutting Tool Insert

The residual stress profiles of the machined Ti-6Al-4V titanium alloy using the uncoated flat-faced (KW-10) tungsten carbide cutting insert under different cutting fluid conditions is shown in Figure 4.18. MQL and flood conditions resulted in a comparatively better residual stress profile in this case. The dry condition induced the highest initial tensile residual stresses just below the machined surface followed by the MQL condition. The least initial tensile residual stress just below the machined surface was induced by the flood condition. However, this trend changes after a certain subsurface depth.

There is a presence of an unrestricted tool-chip contact length between the cutting tool and the chip when machining with the flat-faced cutting tool. Hence, the chip flow is

also unrestricted. In this case, the dry condition provided higher tensile residual stresses initially. Tensile residual stresses are typically unwanted as they invite failure complications. The thermal conductivity of tungsten carbide is also relatively higher than the coatings. As it is an uncoated cutting insert, while machining, the tungsten carbide tool comes in direct contact with the work-piece. As Ti-6Al-4V titanium alloy has a very low thermal conductivity of 6.7 W/m-K [6], most of the heat produced while machining is absorbed by the tool. However, as the machining progresses, the already hot tool tries to channel the heat back to the work-piece. Residual stress also includes the stresses due to temperature effect. Thermal stresses induce tensile residual stresses. Hence, it appears that more tensile residual stresses are induced in the work-piece. However, when the cutting fluid is applied, the cooling is much faster and the tool cools down, thereby not thermally impacting the subsurface. Hence, due to the application of either MQL or flood conditions, it is hypothesized that we get lower residual stresses as compared to the dry condition.

The comparison of Figures 4.6, 4.9, 4.14 and 4.18 shows the microstructures and the residual stress profile obtained by machining the Ti-6Al-4V titanium alloy using the flat-faced uncoated cutting insert under the influence of three different cutting fluid conditions. It can be seen from the microstructures that the coarsened α structure is obtained in the microstructure when machined under the dry condition. Hence, with reference to the explanation given in the previous section, it can be stated that due to high temperatures induced into the work-piece, the residual stresses are relatively higher and on the tensile side due to the thermal stresses. If all three microstructures are observed carefully, it can be seen that the quantity of coarsened α structure is highest in dry

machining, it is relatively less when machined under the flood cutting fluid condition, and the least in the MQL cutting fluid condition. The residual stress profile was relatively worse when the work-piece was machined under the dry machining condition as compared to when the work-piece was machined under the MQL cutting fluid condition. Hence, from the theory discussed here, it is clear that microstructural changes are in some way responsible for the residual stress profiles. The thermal gradients appear to be the prime factors responsible for the produced residual stresses.

4.6.2 Machining with Uncoated Grooved Cutting Tool Insert

The residual stress profiles of the machined Ti-6Al-4V titanium alloy using the uncoated grooved (KW-10) tungsten carbide cutting insert under different cutting fluid conditions is shown in Figure 4.19. Again, MQL and flood conditions comparatively provided the better residual stress profiles in this case. It can be seen that the dry condition produced higher initial near the surface tensile residual stresses and produces an oscillating pattern with reduced amplitude along the subsurface depth. The MQL and flood residual stress profiles are much better as they both start with compressive residual stresses near the surface. Compressive residual stresses are always preferred at the surface, when compared to tensile residual stresses.

Machining with grooved cutting inserts typically restricts the tool-chip contact length when appropriate feed rates are used. Moreover it acts as a chip-breaker. Hence, discontinuous chips are generally obtained while machining with grooved cutting tools.

Due to the presence of grooves, in this case, it was observed that the tensile stresses got reduced comparatively, moving the profile towards the compressive side. Although the chips were not broken into very small forms, relatively better control of

chips was obtained when compared to a flat-faced tool.

The comparison of Figures 4.7, 4.11, 4.15, and 4.19 shows the microstructures and the residual stress profile obtained by machining Ti-6Al-4V titanium alloy using the grooved uncoated cutting insert under the influence of three different cutting fluid conditions. It can be seen from the figures that higher quantity of coarsened α structure was obtained in the microstructure when machined under the dry machining condition. Hence with reference to the explanation given in the previous section, it can be stated that due to high temperature reached in the work-piece while machining, the residual stresses are relatively higher and on the tensile side due to the contribution of thermal stresses. The residual stress profile was relatively worse when the work-piece was machined under the dry machining condition. Relatively better profile was obtained when the work-piece was machined under flood cutting fluid condition. Moreover, by observing the microstructures, it can be verified that the dry cutting condition microstructure contains the highest quantity of coarsened α structure, MQL cutting condition is next and then the least quantity is observed in the flood cutting condition. The highest tensile residual stresses were also observed in the same order confirming the results.

4.6.3 Machining with Multilayered ($TiCN/Al_2O_3/TiN$) CVD Coated Grooved Cutting Insert

The residual stress profile of the machined Ti-6Al-4V titanium alloy using the multilayered ($TiCN/Al_2O_3/TiN$) CVD coated grooved tungsten carbide cutting insert under different cutting fluid conditions is shown in Figure 4.20. Machining under the flood and dry conditions comparatively gave better residual stress profiles that were on the compressive side. Machining under the MQL condition induced comparatively higher

initial tensile residual stresses near the surface.

On the other hand, it was observed that, the residual stress profile for the dry and flood conditions start on the compressive side and follow hook like profiles. The thermal conductivities of TiCN, TiN and Al_2O_3 are 12.3 W/m-deg. K, 17.2 W/m-deg. K and 22 W/m-deg. K, respectively, which are low [6]. As these coatings were applied one after another, they can be assumed to be in series and hence we can treat the whole as a heat circuit as assumed by Balaji and Mohan [13].

Hence, the combined thermal conductivity of the multilayered CVD coating can be assumed to be low. The thermal conductivity of Ti-6Al-4V titanium alloy is also small. Hence, while machining under dry condition, the cutting tool insert and the work-piece both theoretically absorb less heat. Hence, while dry machining using the multilayered CVD coated grooved cutting insert, the residual stress due to temperature gets reduced considerably. Hence, the values for residual stress while machining under the dry conditions are less as compared to uncoated cutting inserts. Todinov [66, 67] showed in his study that oil quenched steel work-pieces generate tensile residual stresses while water quenched work-pieces generate compressive residual stresses. In this work, MQL uses an oil based lubricant, while flood uses a water based coolant. The results in this research show that the residual stresses are tensile when MQL cutting fluid is used while machining using multilayered grooved CVD coated cutting insert. Correspondingly, the residual stresses are on the compressive side when flood cutting fluid condition is used.

The comparison of Figures 4.8, 4.12, 4.16 and 4.20 shows the microstructures and the residual stress profile obtained by machining the Ti-6Al-4V titanium alloy using

grooved multilayered CVD coated cutting insert under the influence of three different cutting fluid conditions. It can be seen from the figures that more quantity of coarsened α structure is observed in the microstructure when machined the under MQL machining condition. Hence with reference to the explanation given in the previous section, it can be stated that due to the high temperature reached in that work-piece, the residual stresses are relatively higher due to the thermal stress contribution. The residual stress profile was comparatively the worst when the work-piece was machined under the MQL cutting fluid condition. The "best" profile was obtained when the work-piece was machined under the dry machining condition. Moreover, by observing the microstructures, it can be verified that the MQL cutting condition microstructure contains the highest quantity of coarsened α structure, flood cutting condition is next, and then the least quantity is observed in the dry cutting condition. Thus, the residual stress pattern is correlated and verified with the microstructure.

4.6.4 Machining with PVD Coated Grooved Cutting Insert

The residual stress profiles of the machined Ti-6Al-4V titanium alloy using the single-layered (TiAlN) PVD coated grooved tungsten carbide cutting insert under different cutting fluid conditions are shown in Figure 4.21. Machining under the dry cutting condition comparatively produced the better residual stress profile with less initial surface tensile residual stresses. MQL condition comparatively induced higher initial surface tensile residual stresses. It is interesting to note that, all the profiles for all the three conditions i.e., dry, MQL and flood, behave in a similar manner. All start on the tensile side and follow the hook-like curve to move towards the compressive side before stabilizing these stress profiles.

The comparison of Figures 4.10, 4.13, 4.17 and 4.21 shows the microstructures and the residual stress profile obtained by machining the Ti-6Al-4V titanium alloy using the grooved single-layered PVD coated (TiAlN) cutting tool insert under the influence of three different cutting fluid conditions. It can be seen from these figures that the coarsened alpha structure was obtained in the microstructure when machined under the MQL cutting fluid condition. Hence, with reference to the explanation given in the previous section, it can be followed that due to high temperature reached in that work-piece, the residual stresses are relatively higher due to the thermal stress contribution.

The residual stress profile was comparatively the worst when the work-piece was machined under the MQL cutting fluid condition. A relatively better profile was obtained when the work-piece was machined under the dry machining condition. Moreover, by observing the microstructures, it can be verified that the MQL cutting condition microstructure contains the highest quantity of coarsened α structure, flood cutting condition is next and then the least quantity of coarsened α structure was observed under the dry cutting condition. The residual stress pattern matches the microstructural observations.

It is interesting to note that the residual stresses for machining of Ti-6Al-4V titanium alloy under the MQL condition using grooved coated tools (multilayered CVD and single-layered PVD) were observed to be highest. As indicated in the previous section, Todinov [66, 67] showed in his work that the oil quenched component produces higher tensile residual stresses while, water quenched component produced lower initial residual stresses.

In this case, MQL is an oil based lubricant, while flood coolant is a water based coolant. Hence, for grooved coated tools (multilayered CVD and single-layered PVD) using MQL condition, higher initial tensile residual stresses were observed. Under flood condition, lower initial tensile residual stresses were observed.

4.7 Role of Different Cutting Fluid Applications on Residual Stresses

In this section, the effects of cutting fluids on the residual stress profiles are elaborated.

4.7.1 Machining of Ti-6Al-4V Titanium Alloy under Dry Condition

Figure 4.22 shows the residual stress profiles produced by all four tools used in this thesis when machining under dry machining condition. When comparing the performance of all four cutting tool inserts under dry machining conditions, it was observed that the coated cutting tool inserts (single-layered PVD and multilayered CVD) comparatively produced lower initial near-the-surface tensile residual stresses as compared to the uncoated (flat-faced and grooved) cutting inserts. Of the four cutting inserts, the multilayered CVD coated cutting insert comparatively produces better residual stress profile, while the worst residual stress profile was obtained when machining with the uncoated flat-faced and uncoated grooved cutting tool inserts.

4.7.2 Machining of Ti-6Al-4V Titanium Alloy under MQL Cutting Fluid Condition

Figure 4.23 shows the residual stress profiles produced by all four tools used in this thesis when machining under MQL cutting fluid application condition. When

comparing the performance of all four cutting inserts under MQL cutting fluid condition, the exact opposite trend was observed to the one under dry machining condition. The uncoated (flat-faced and grooved) cutting tool inserts produced comparatively lower tensile residual stresses as compared to the coated cutting tool inserts (single-layered PVD and multilayered CVD). Of the four cutting inserts, uncoated grooved cutting tool insert produced a comparatively better residual stress profile while the comparatively worst residual stress profile was produced by the single-layered PVD coated cutting tool insert.

4.7.3 Machining of Ti-6Al-4V Titanium Alloy under Flood Cutting Fluid Condition

Figure 4.24 shows the residual stress profiles produced by all four tools used in this thesis when machining under flood cutting fluid application condition. When comparing the performance of all four cutting tool inserts under flood cutting fluid condition, it was observed that uncoated grooved and multilayered CVD coated cutting inserts produced comparatively lower near-the-surface tensile residual stresses, while comparatively higher near-the-surface tensile residual stresses were produced by the uncoated flat-faced and single-layered PVD coated cutting inserts. This trend is quite different when compared to dry and MQL cutting fluid conditions.

4.8 Effects of Cutting Tool Parameters on Residual Stresses

This section discusses the effect of cutting tool parameters such as tool coating, chip breaker geometry, etc., under the influence of three different cutting fluid applications on the machining induced residual stresses in Ti-6Al-4V alloy.

4.8.1 Effects of Chip Breaker Geometry

Figures 4.25, 4.26 and 4.27 compare the residual stress profiles generated by machining with flat-faced and grooved chip breaker geometry under the influence of dry, MQL and flood cutting fluid application conditions, respectively. The coated tools are not considered here since we want to isolate and explain the effects of tool surface geometry alone. When the residual stresses induced by the uncoated flat-faced cutting insert were compared with the uncoated grooved cutting insert under the influence of dry machining condition, it was found that the uncoated flat-faced cutting insert produced comparatively better residual stress profile. However, with the addition of cutting fluid, the picture changes completely. In both cases (under the application of MQL and flood), the uncoated grooved cutting tool insert gave a better residual stress profile. This may be due to the effect of the groove acting as a pocket for storing extra coolant/lubricant, which in turn aids in reducing the tensile residual stresses. Jayal and Balaji [68] found that the chip-breaking grooves on the tool surface allowed the applied cutting fluid to influence the machining process more significantly due to the presence of a groove which can act as a retaining pocket. This may be the reason that the grooved tools perform better under the influence of the cutting fluid application. Moreover, the microstructures in Figures 4.19 and 4.21 show that an increase in coarsened α structure indicates generation of comparatively higher tensile residual stresses in that work-piece, which further explains these results. Thus, we see that, the generated microstructures are linked to the residual stress profiles.

Table 4.1 provides a summary of the effect of the chip breaker geometry on machining induced residual stresses. “Preferred” in Table 4.1 indicates that the stated tool

produces comparatively better residual stress profile.

4.8.2 Effect of the Type of Tool Coating

Figures 4.28, 4.29 and 4.30 compare the residual stress profile generated by machining with grooved multilayered CVD coated cutting tool and grooved single-layered PVD coated cutting tool under the influence of dry, MQL and flood cutting fluid application conditions, respectively. These tools have different coatings on the same tool geometry and hence they are used to assess the isolated effect of coatings alone.

With the consideration of coatings, the scenario changes completely. When the residual stresses induced by coated cutting tools (multilayered CVD coated and single-layered PVD coated) were compared, surprisingly, under all the cutting fluid application conditions, the multilayered CVD coated cutting insert gave a comparatively better residual stress profile.

Mohan and Balaji's [13] work introduced the term "effective thermal conductivity." The "effective thermal conductivity" of the whole multilayered coating depends on the thermal conductivity of each coating and the thickness of each coating. Using that work as a basis, we can treat the multilayered coating as a heat circuit. Hence, the combined thermal conductivity of the multilayered CVD coating can be assumed to be low due to the presence of aluminum oxide. The multilayered CVD coating has higher thermal resistance compared to single-layered PVD coating.

One more reason is that, single-layered PVD coated tools are sharper as compared to multilayered CVD coated tools. This is due to the presence of three different coatings applied one after another, ultimately increasing the hone radius of the cutting tool. It has been already shown that sharper tools move the residual stress profile towards the tensile

side [28, 50]. Moreover, the microstructures shown in Figures 4.23 and 4.25 also show an increase in the coarsened α structure, which indicates generation of higher tensile residual stresses in that work-piece, thereby correlating with the plotted residual stress results.

Table 4.2 provides a summary of the effect of the type of tool coating on machining induced residual stresses. "Preferred" in Table 4.2 indicates that the stated tool produces a comparatively better residual stress profile.

4.8.3 Comparison of the Uncoated and Coated Tools

Figures 4.31, 4.32 and 4.33 compare the residual stress profiles generated by machining with an uncoated cutting tool (the best of the flat-faced and grooved) and CVD coated cutting tool (as CVD coated tool produced better residual stress profile than PVD coated tool under all conditions) under the influence of dry, MQL, and flood cutting fluid application conditions, respectively.

When the residual stresses induced by the uncoated (the best of the flat-faced and grooved) cutting tools are compared with coated (multilayered CVD) cutting tools, under dry machining condition the multilayered CVD coated cutting tool insert gives a comparatively better residual stress profile. However, with the application of cutting fluids (MQL and Flood conditions), the uncoated grooved cutting tool inserts provide a better residual stress profile. This may be due to the work hardening phenomenon caused by the multilayered CVD coated cutting tools under the influence of cutting fluid application.

Similar results were obtained by Outeiro et al. [47] when machining 1045 steel. Hence, the uncoated grooved tool is better if used under MQL/flood condition. For machining under dry condition, the CVD coated cutting tool insert is better. Moreover,

the microstructures shown in Figures 4.19, 4.21, 4.23 and 4.25 show the increase in coarsened α structure which indicates generation of higher tensile residual stresses in that work-piece; this finding also verifies these results.

Table 4.3 provides a summary of the effect of coated and uncoated cutting tools on machining induced residual stresses. "Preferred" in Table 4.3 indicates that the stated tool produces a comparatively better residual stress profile.

Table 4.4 summarizes the results discussed in this section.

All the comparisons in this section are based upon comparing the highest tensile point in the measured residual stress profile. "Preferred" indicates that the stated tool produced a comparatively better (compressive) residual stress profile. The uncoated grooved tools are better if used under MQL/flood condition. For machining under dry condition, CVD coated cutting tools are seen to be better.

4.9 Discussion and Summary

This section discusses the results described in the previous sections in detail and also provides a brief summary of the entire chapter.

It is well known that high temperatures are generated while machining titanium alloys [35]. About 80% of the heat generated while machining Ti-6Al-4V titanium alloy is conducted into the tool as it cannot be removed with the fast flowing chip in the workpiece due to the low thermal conductivity of the titanium alloy [32]. The thermal conductivity of tungsten carbide (62W/m-k [6]) is greater than the thermal conductivity of the Ti-6Al-4V titanium alloy. When the tools are more conductive than the work-piece, and are used for machining under the flood cutting fluid condition, they reduce the thermal effects on the residual stress distribution of the work material. Hence, this

combination is expected to produce comparatively less tensile residual stresses. In this work, the effective thermal conductivity of uncoated tungsten carbide tools is much higher than the coated (multilayered CVD and single-layered PVD) tungsten carbide tools. Correspondingly, the results show that the coated tungsten carbide tool induced more tensile residual stresses as compared to the uncoated tungsten carbide tool under flood cutting fluid condition.

Liu and Guo [69, 70] worked on the relation between the residual stress distribution and the friction condition of the tool-chip interface and concluded that as the friction increases while machining (304 stainless steel), tensile residual stresses are reduced. In this thesis, when residual stresses were compared while machining was performed using coated tools (CVD and PVD) under dry, MQL and flood cutting fluid condition, it was observed that the machining under the MQL cutting fluid condition gave the highest tensile residual stress values. The best profile was obtained when machined under the dry machining condition. MQL is an oil based lubricant, which has a very low friction coefficient. On the other hand, machining with the dry condition has a comparatively higher coefficient of friction. The findings of Liu and Guo [69, 70] support the findings in this thesis.

Todinov [66, 67] showed in his work on steels that the oil quenched component produces higher tensile residual stresses while the water quenched component produces lower initial tensile residual stresses. In this work, MQL is an oil-based lubricant, while flood is a water-based coolant. For grooved coated tools (multilayered CVD and single-layered PVD) using the MQL condition, higher initial tensile residual stresses was observed. Under the flood condition, lower initial tensile residual stresses were observed.

Although, titanium is a different material, it appears that similar mechanisms may be at work. Especially, the observation of subsurface microstructures supports these conclusions.

Outeiro et al. [47], in their work on steels, compared the residual stresses induced by the CVD coated cutting tool and by the uncoated tungsten carbide cutting tool. They concluded that the CVD coated tool induces larger tensile residual stresses when compared to those produced by an uncoated carbide cutting tool when a cutting fluid is applied. This is due to the local work hardening phenomenon caused by the coating. Their results match with the results in this present work. In this work also, the residual stresses induced by the multilayered CVD coated cutting insert are more than the residual stresses induced by the uncoated carbide cutting insert when a cutting fluid is applied, even though a different material is machined.

When the microstructures of the machined work-pieces are compared, it can be seen that there is a lot of variation in the size of the "α" microstructures. The "α" structure has become more coarsened at the places where more thermal stresses are present. A large amount of heat is generated when machining. This heat is responsible for the thermal stresses in the work-piece. It can be concluded from the results of this research that higher tensile residual stresses are present in the work-piece in which the coarsened α microstructure is present. It can be seen that greater quantities of coarsened α structure were present when the work-piece was machined under dry cutting condition, which is also the same condition inducing more tensile stresses.

When the work-pieces for the grooved uncoated cutting insert were compared, the same dry machining gave the highest tensile residual stress values along with larger

quantities of coarsened α structures present in the microstructure. For the multilayered CVD coated cutting insert, the MQL condition gave the highest values for tensile residual stresses along with a greater quantity of coarsened α structure present in the microstructure.

Finally, when the single-layered cutting insert results were compared, the MQL cutting fluid condition gave the highest values of the tensile residual stresses along with greater quantities of coarsened α structures present in the subsurface.

The final surface integrity of the component is generated due to the effects of numerous different factors and constraints, all of which are difficult to track. Some of the important factors responsible for the generation of surface integrity are discussed in this section. The combination of different factors such as cutting tools and coatings, cutting fluid application, etc., ideally need to be adjusted at their optimum level to attain the desired surface integrity. This thesis is a beginning attempt towards such a goal.

This concludes the discussion of the results and summary of all the experiments that were conducted as a part of this research. The next chapter summarizes the thesis and provides some recommendations for future work that can answer other questions related to the topics investigated in this thesis.

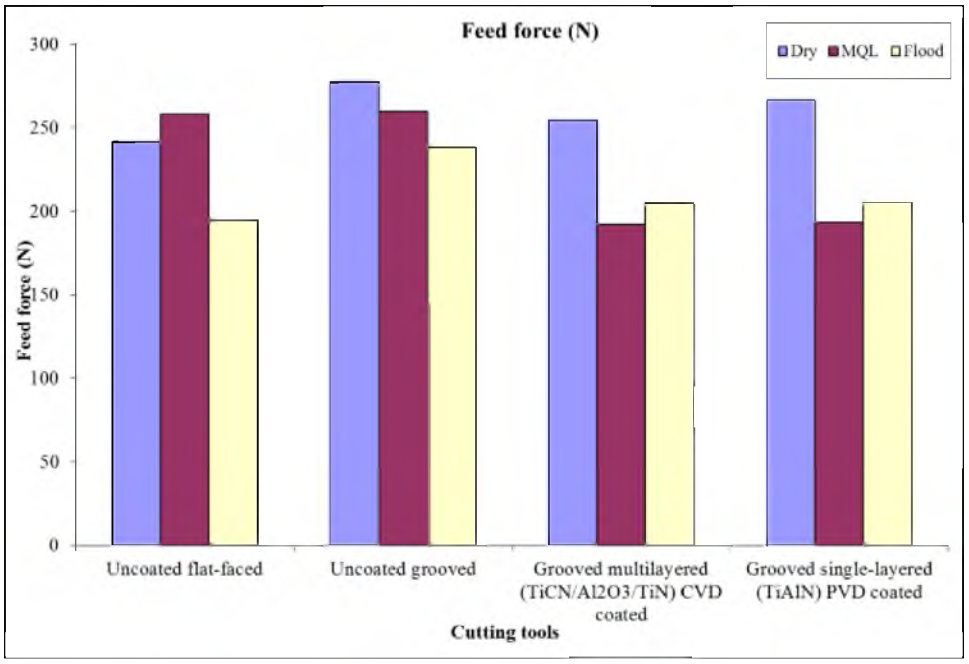

Figure 4.1: Feed forces obtained during machining Ti-6Al-4V alloys.

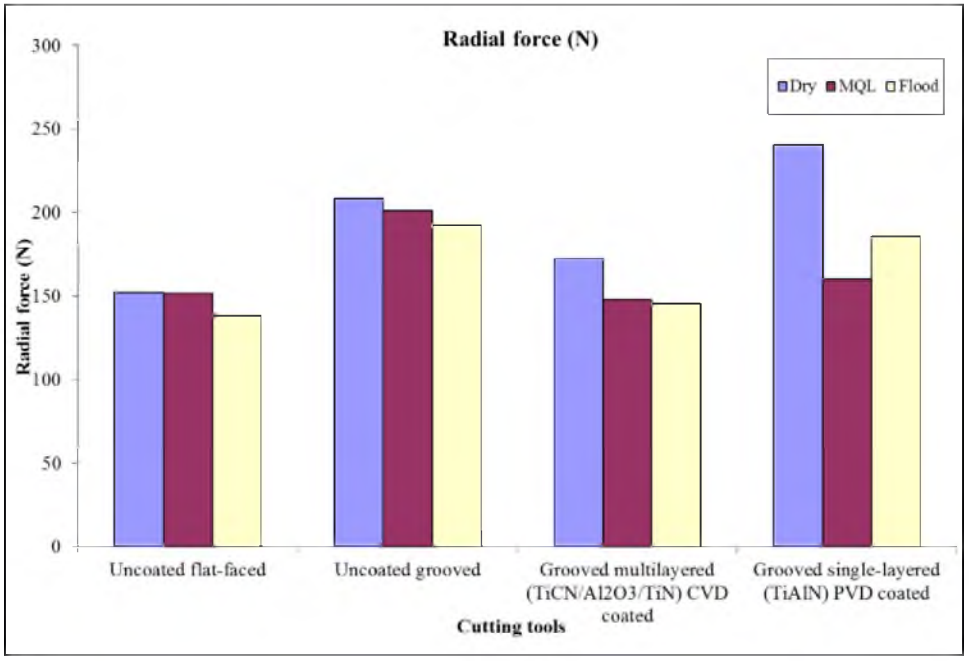

Figure 4.2: Radial forces obtained during machining Ti-6Al-4V alloys.

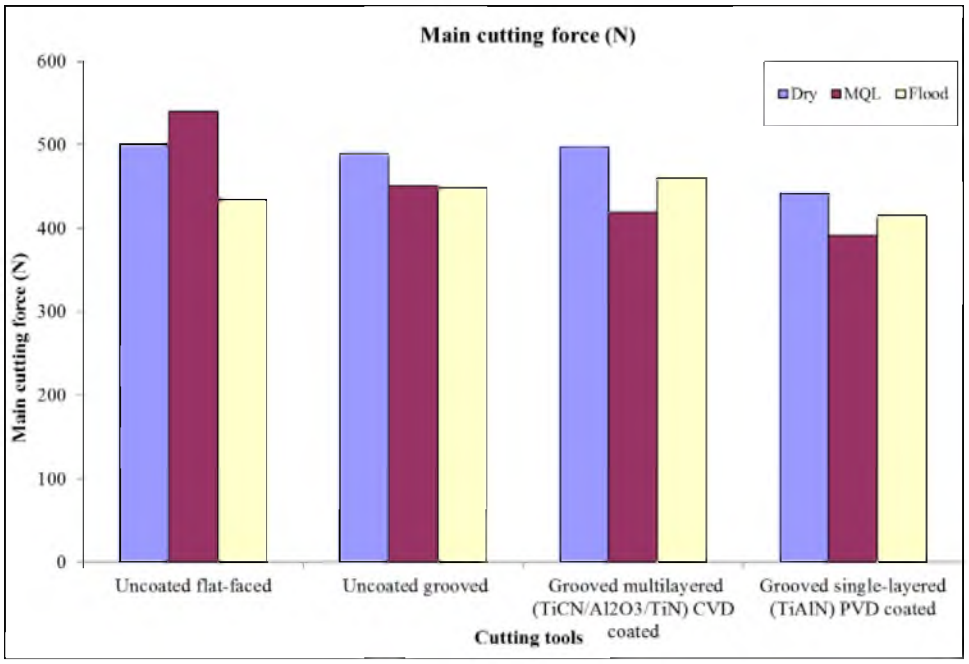

Figure 4.3: Cutting forces obtained during machining Ti-6Al-4V alloys.

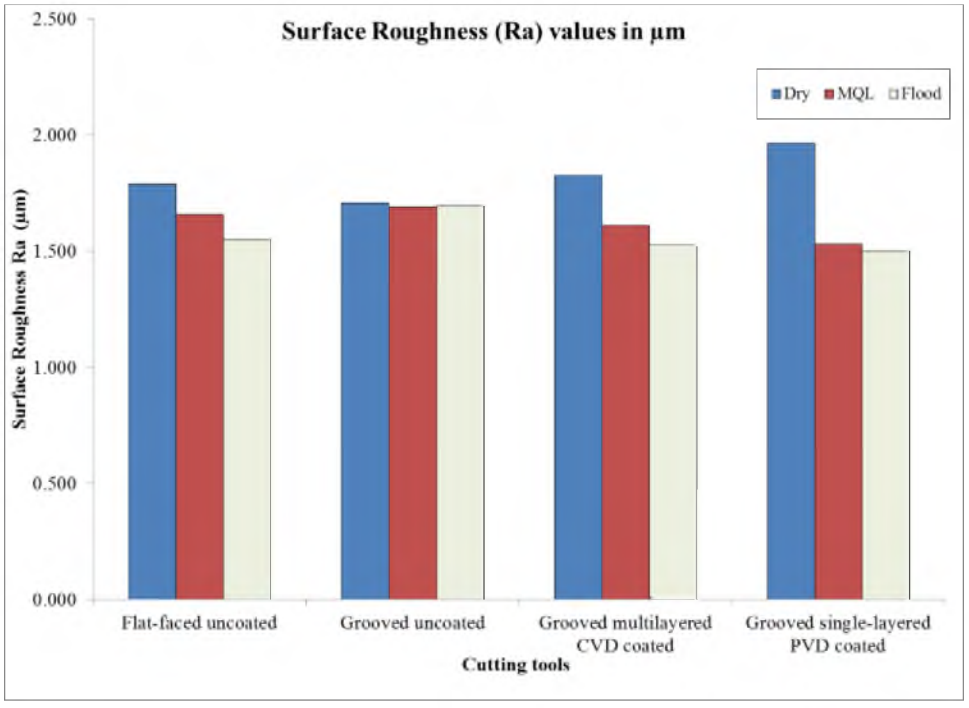

Figure 4.4: Surface roughness of Ti-6Al-4V alloy machined with four tools and three cutting fluid application conditions.

	DRY	MQL	FLOOD
Uncoated flat-faced KW-10			
Uncoated grooved KW-10			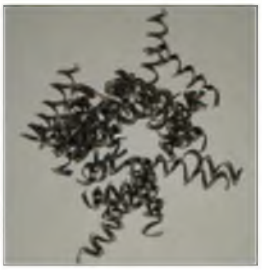
Multilayered CVD coated CA-6515		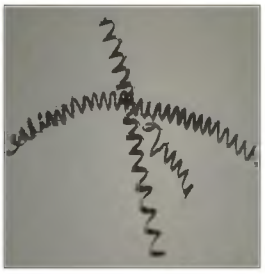	
Single-layered PVD coated PR-1125	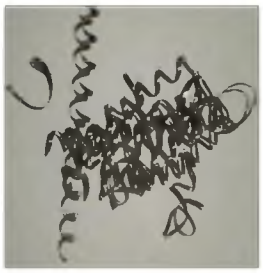		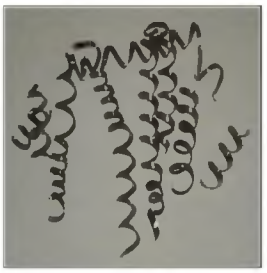

Figure 4.5: Chips produced during machining Ti-6Al-4V alloy with four cutting tools when using three cutting fluid application conditions.

Figure 4.6: Ti-6Al-4V subsurface microstructure developed when machined using flat-faced uncoated cutting tool insert and dry machining condition.

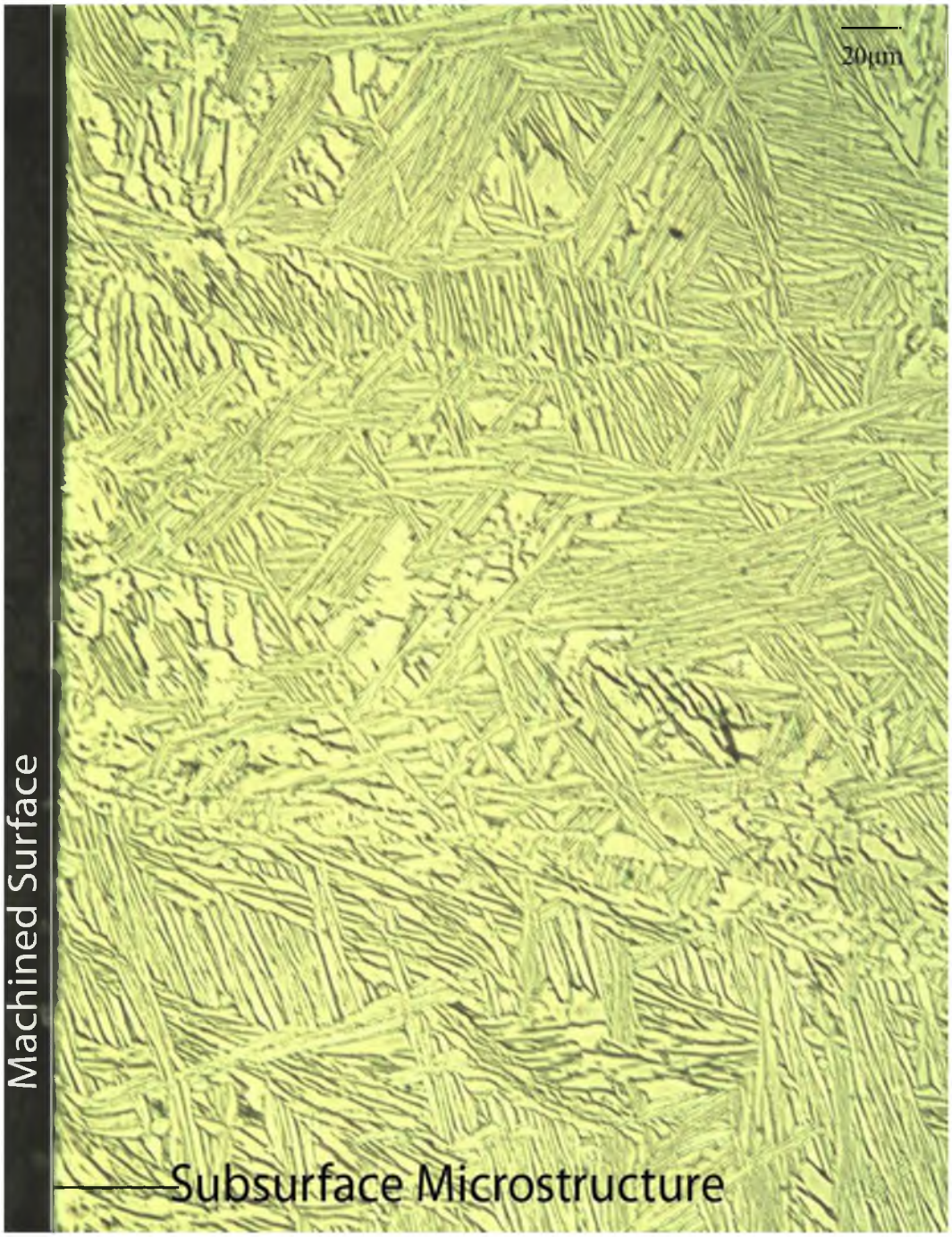

Figure 4.7: Ti-6Al-4V alloy subsurface microstructure developed when machined using grooved uncoated cutting tool insert and dry machining condition.

Figure 4.8: Ti-6Al-4V alloy subsurface microstructure developed when machined using grooved multilayered CVD coated cutting tool insert and dry machining condition.

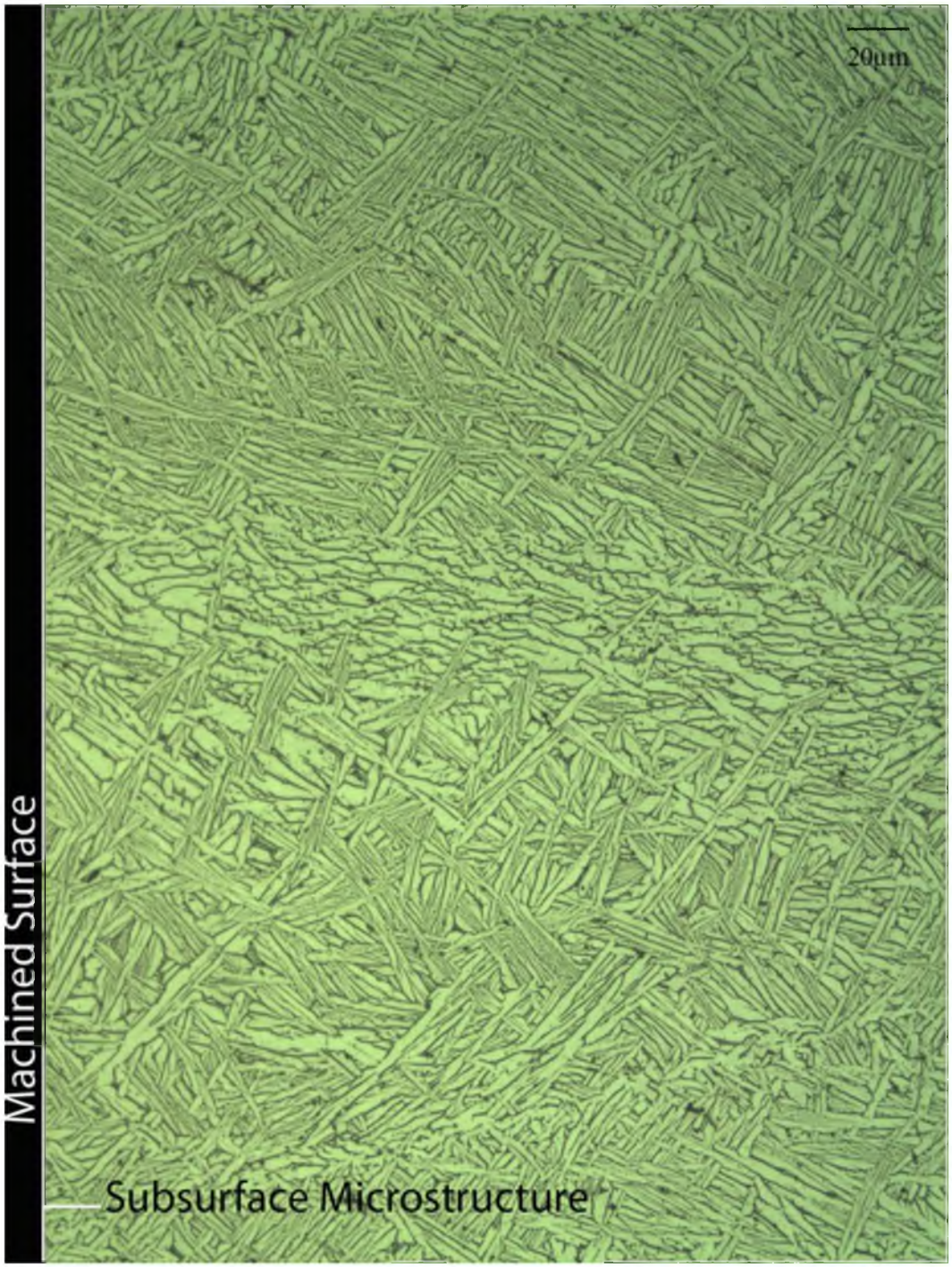

Figure 4.9: Ti-6Al-4V alloy subsurface microstructure developed when machined using flat-faced uncoated cutting tool insert and flood cutting fluid application condition.

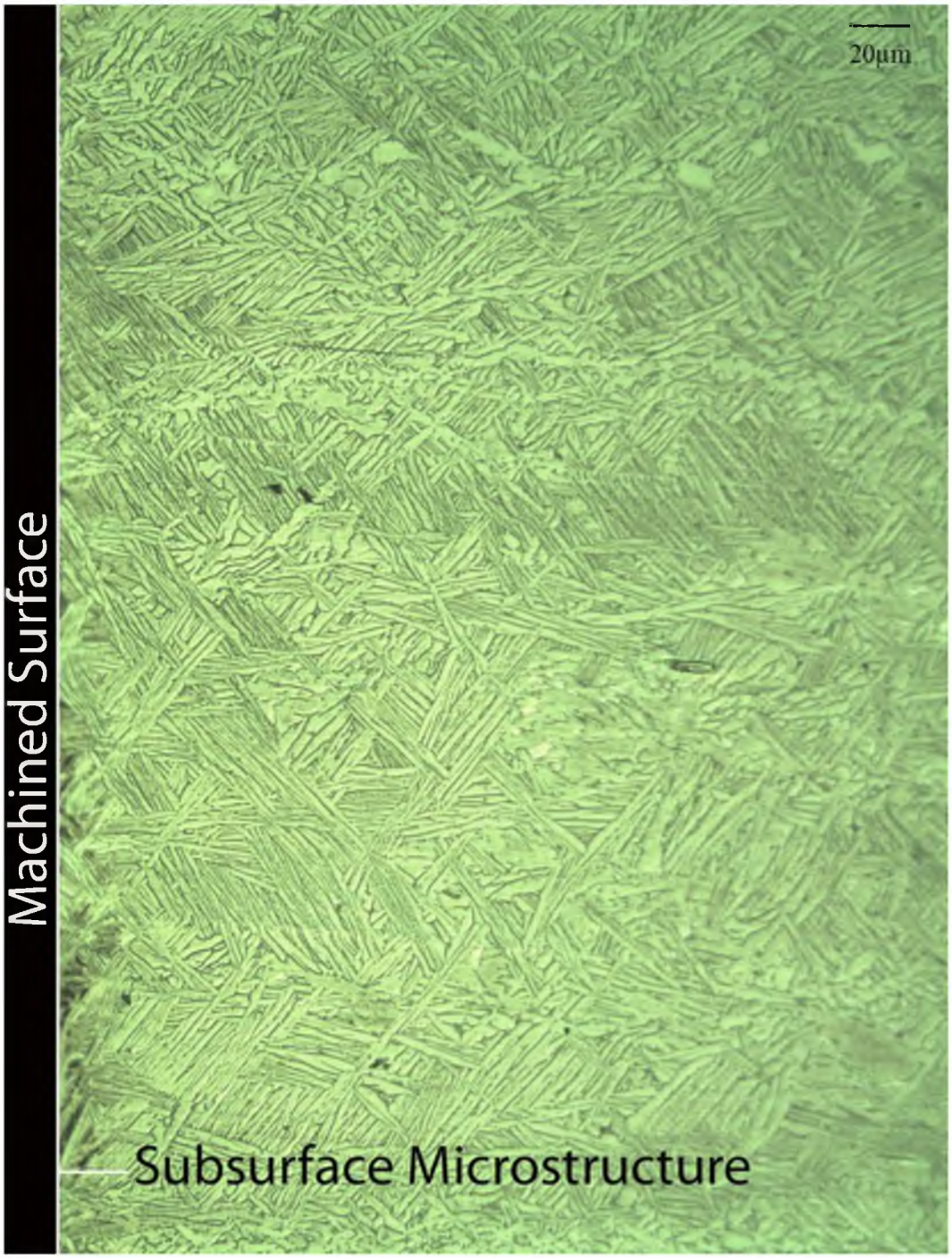

Figure 4.10: Ti-6Al-4V alloy subsurface microstructure developed when machined using grooved single-layered (TiAlN) PVD coated cutting tool insert and dry machining condition.

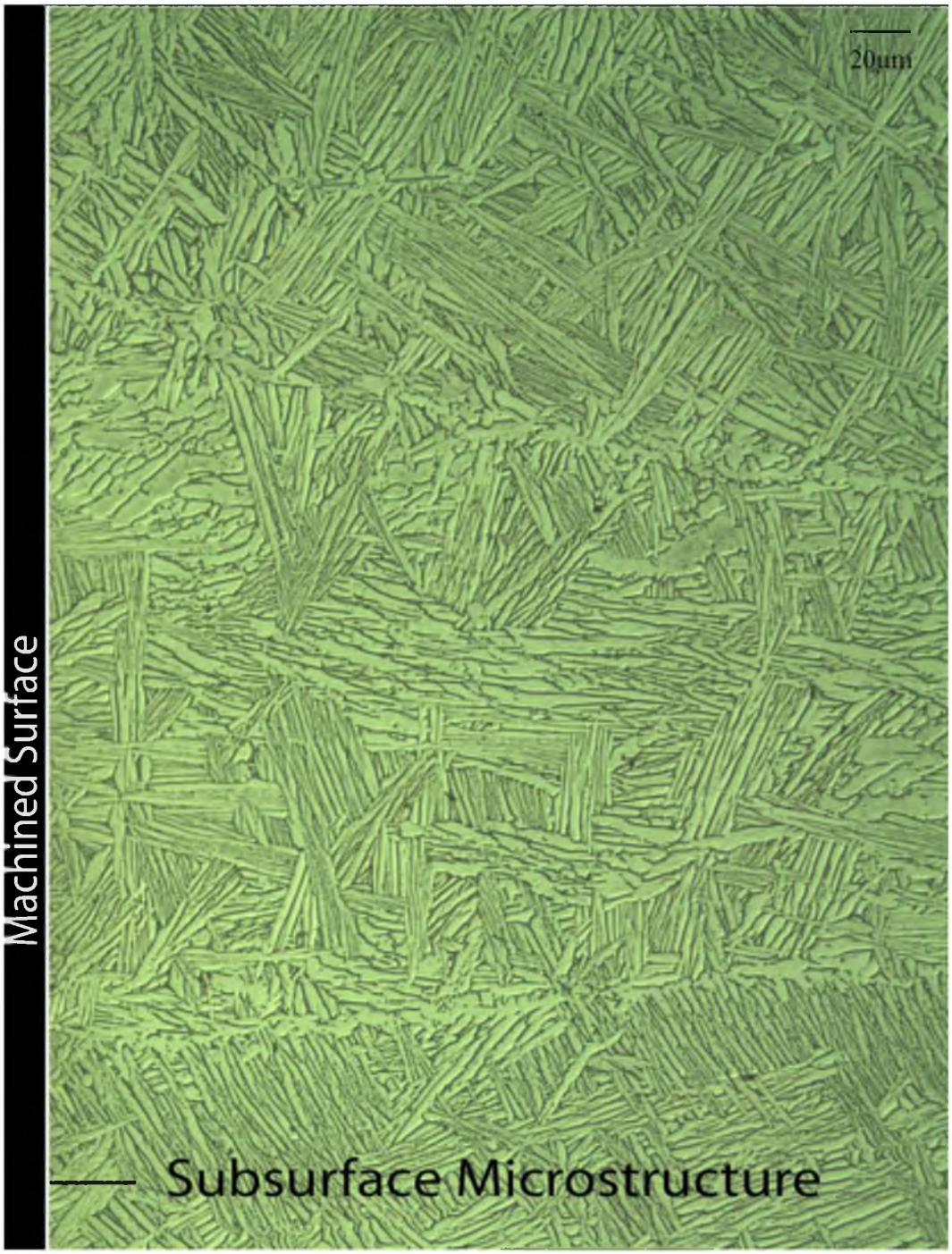

Figure 4.11: Ti-6Al-4V alloy subsurface microstructure developed when machined using grooved uncoated cutting tool insert and flood cutting fluid application condition.

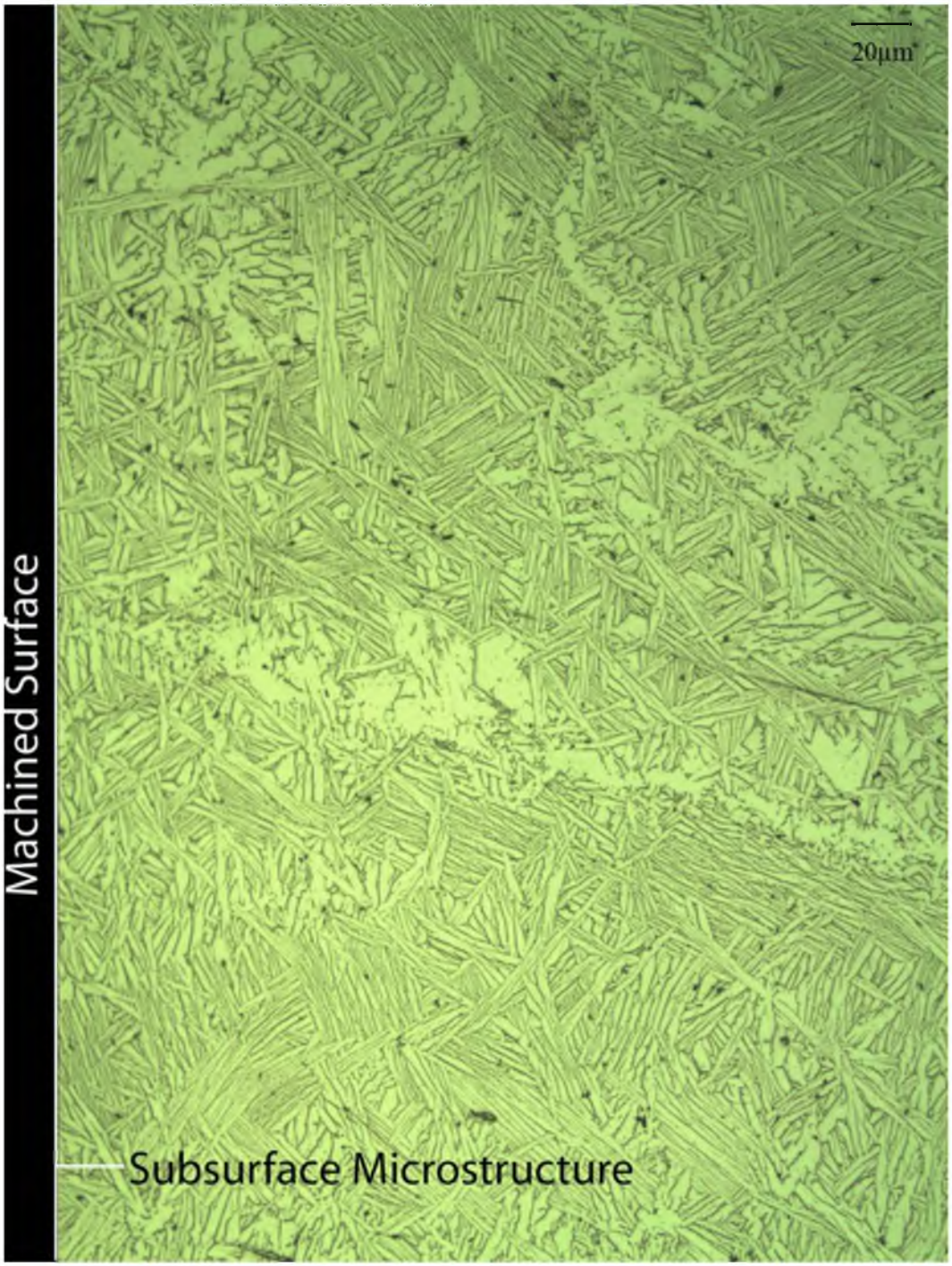

Figure 4.12: Ti-6Al-4V alloy subsurface microstructure developed when machined using grooved multilayered CVD coated cutting tool insert and flood cutting fluid application condition.

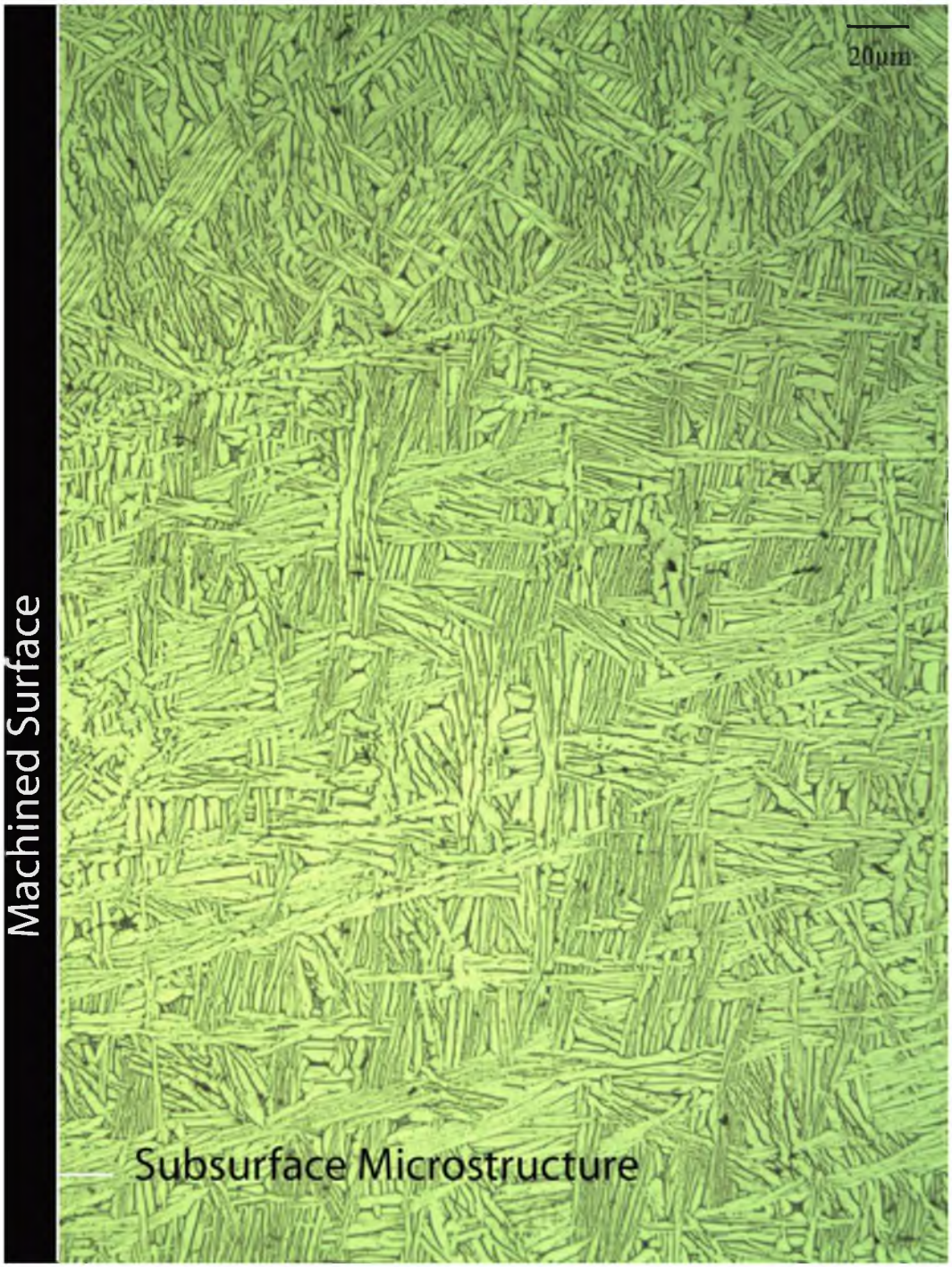

Figure 4.13: Ti-6Al-4V alloy subsurface microstructure developed when machined using grooved single-layered (TiAlN) PVD coated cutting tool insert and flood cutting fluid application condition.

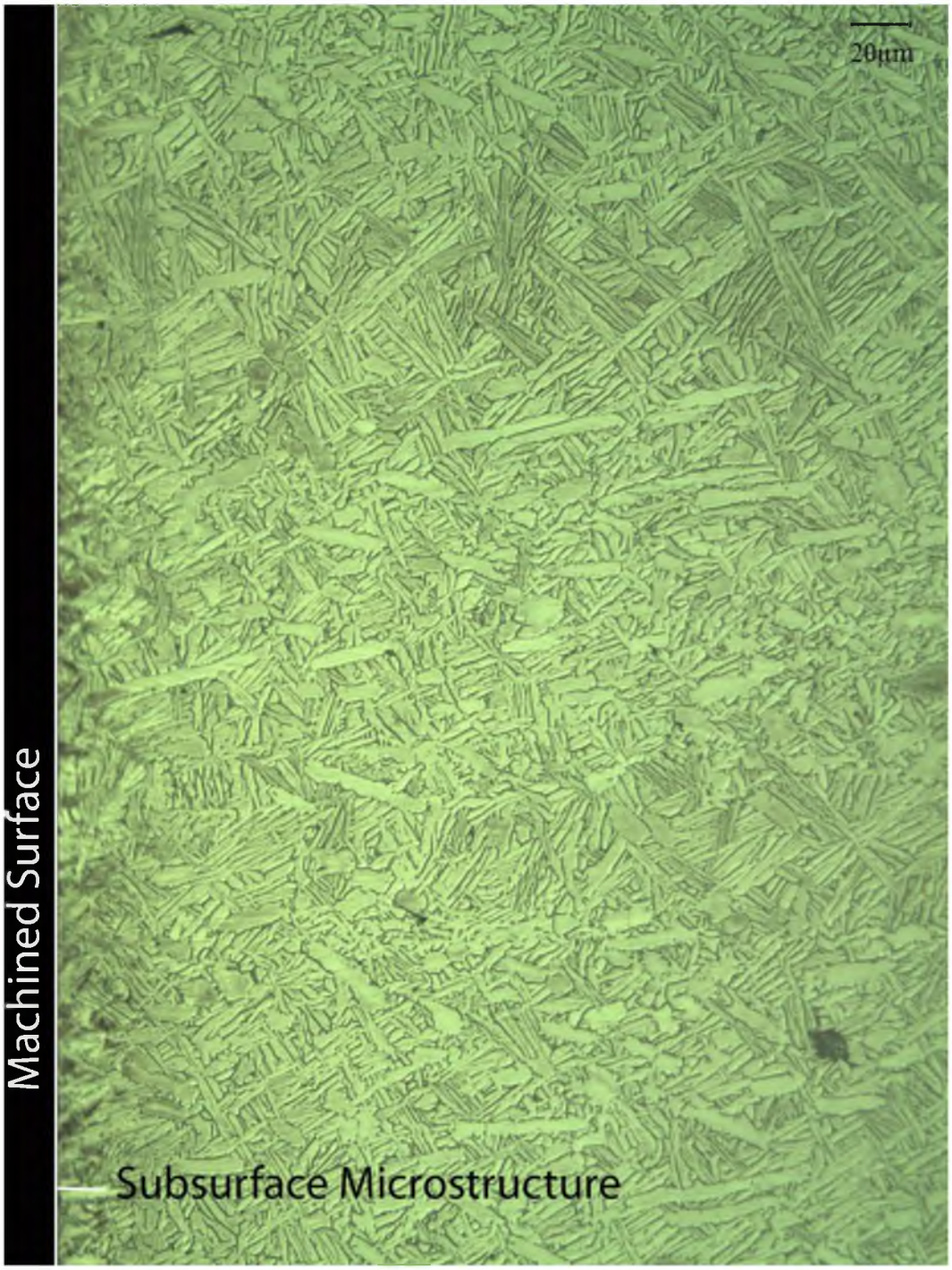

Figure 4.14: Ti-6Al-4V alloy subsurface microstructure developed when machined using flat-faced uncoated cutting tool insert and MQL cutting fluid application condition.

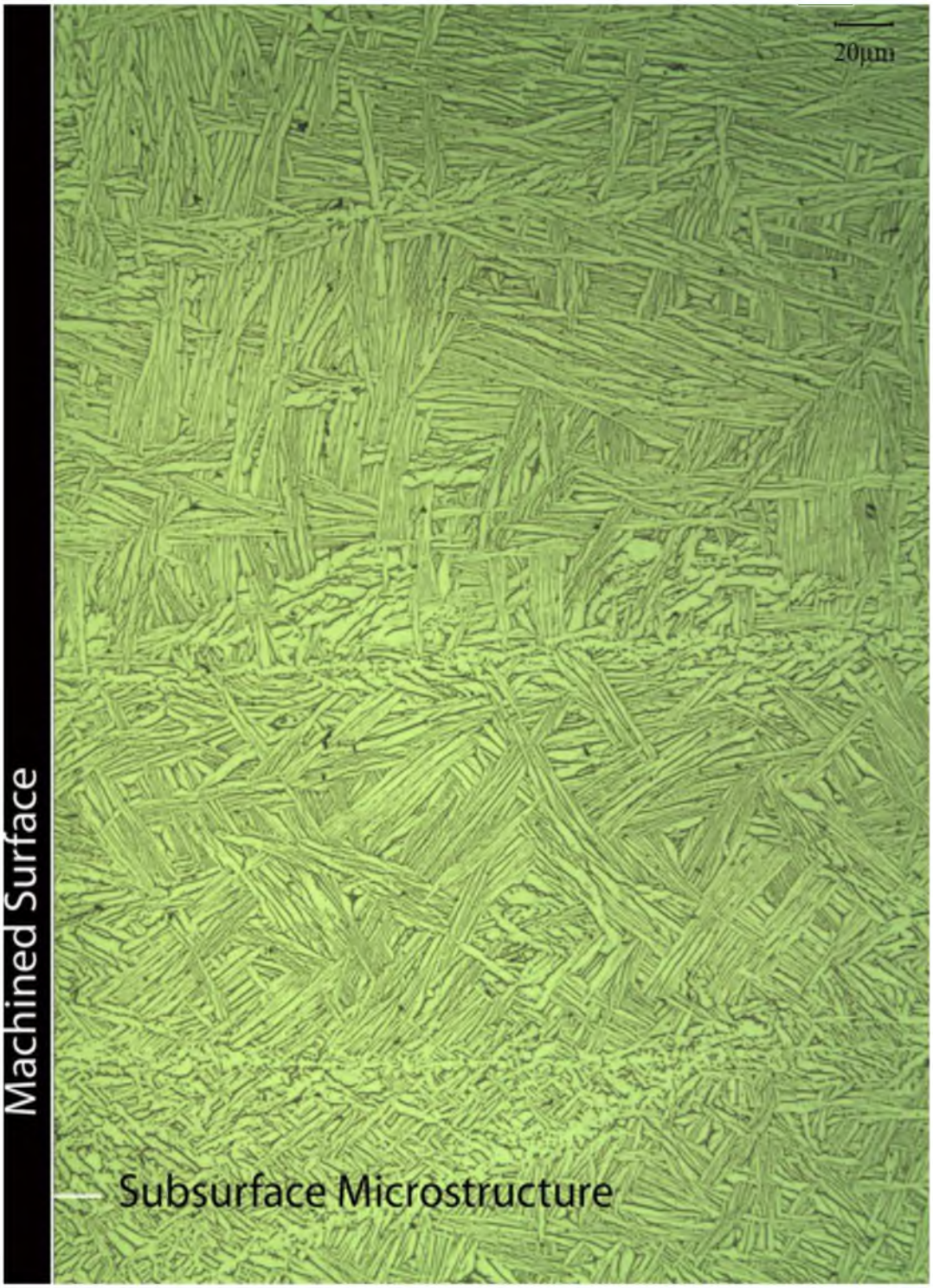

Figure 4.15: Ti-6Al-4V alloy subsurface microstructure developed when machined using grooved uncoated cutting tool insert and MQL cutting fluid condition.

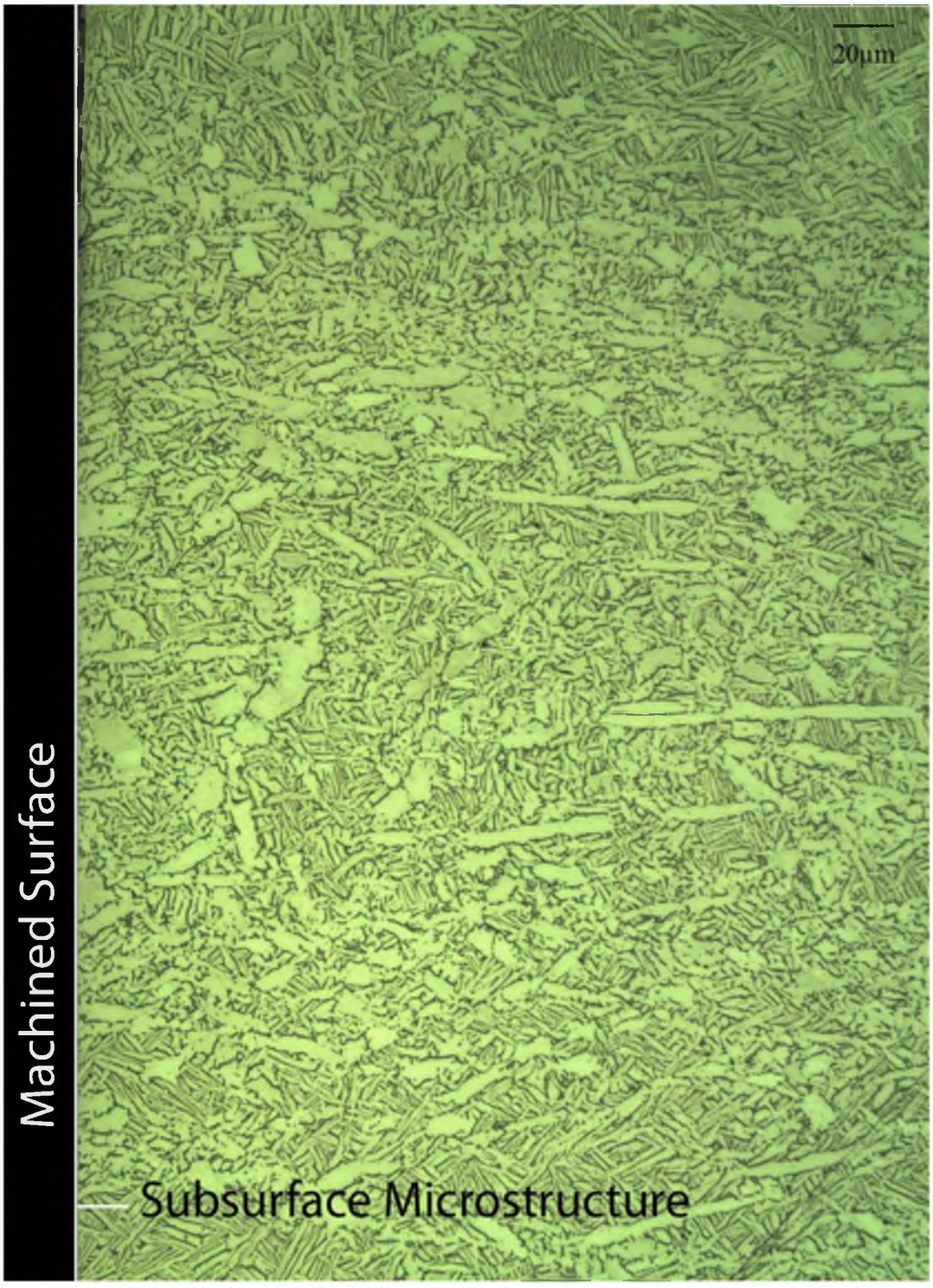

Figure 4.16: Ti-6Al-4V alloy subsurface microstructure developed when machined using grooved multilayered CVD coated cutting tool insert and MQL cutting fluid application condition.

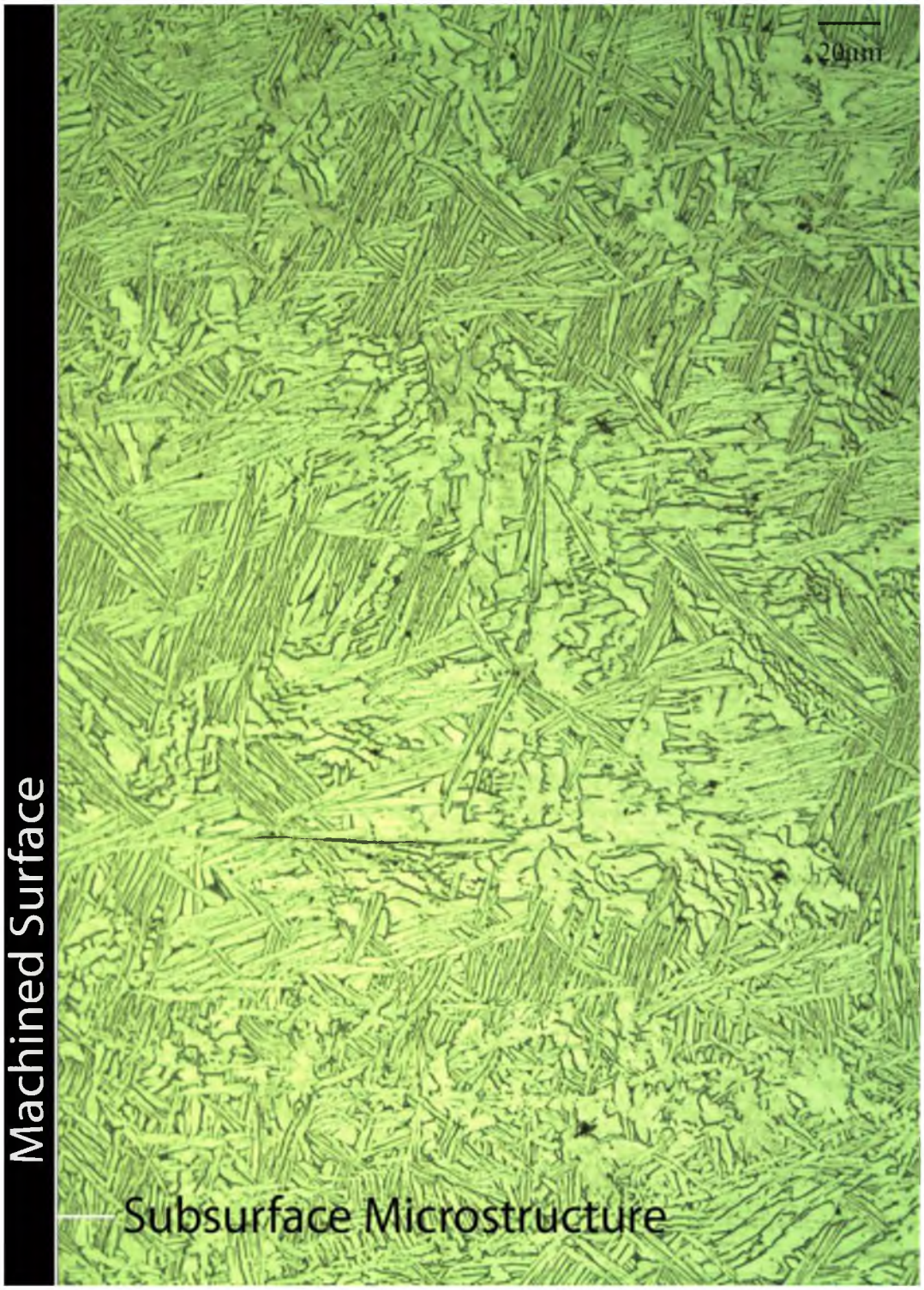

Figure 4.17: Ti-6Al-4V alloy subsurface microstructure developed when machined using grooved single-layered (TiAlN) PVD coated cutting tool insert and MQL cutting fluid application condition.

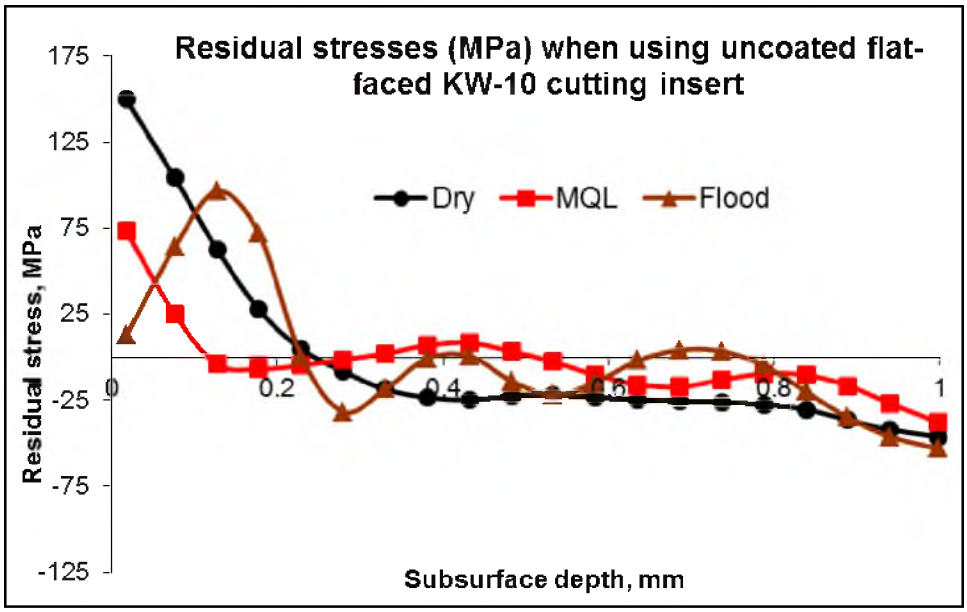

Figure 4.18: Residual stresses induced by flat faced uncoated cutting insert in machined Ti-6Al-4V alloy.

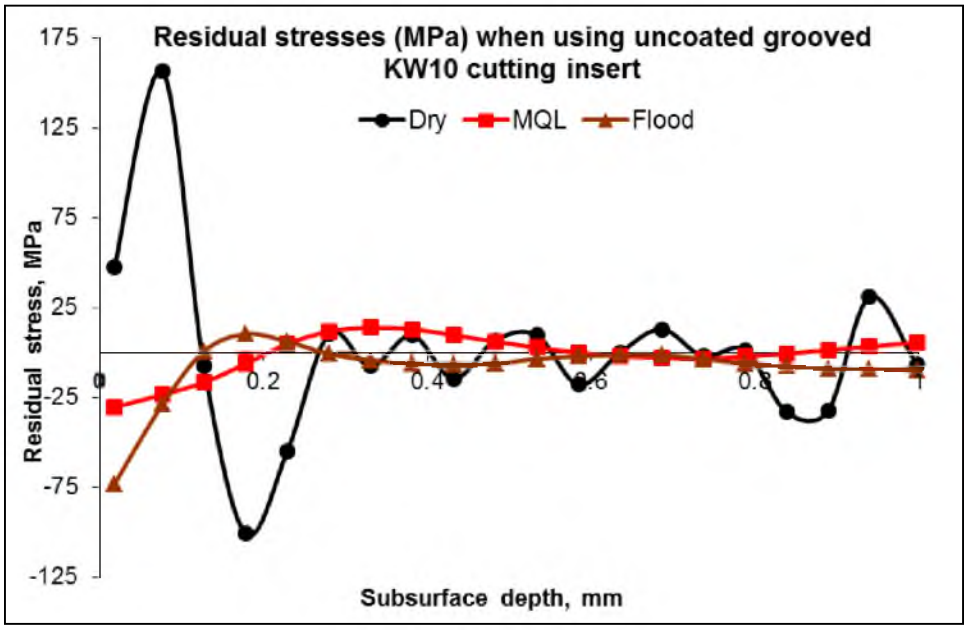

Figure 4.19: Residual stresses induced by grooved uncoated cutting insert in machined Ti-6Al-4V alloy.

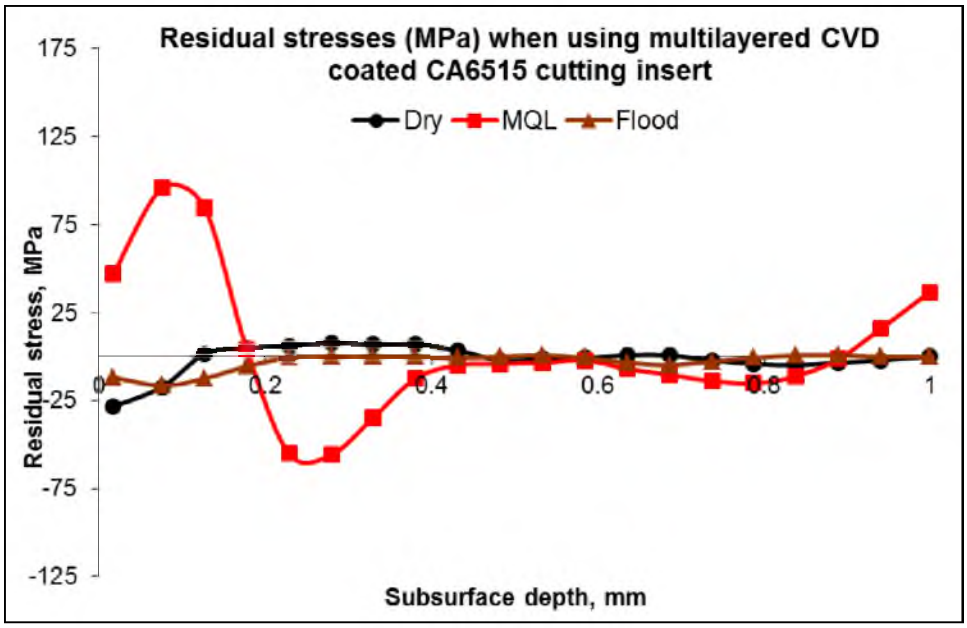

Figure 4.20: Residual stresses induced by multilayered ($TiCN/Al_2O_3/TiN$) CVD coated grooved cutting insert in machined Ti-6Al-4V alloy.

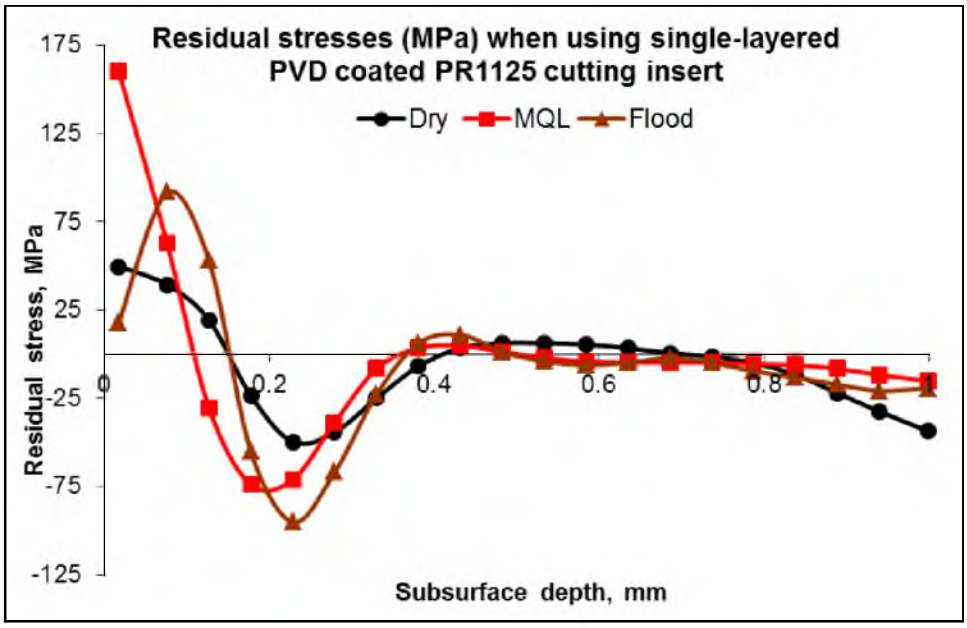

Figure 4.21: Residual stresses induced by single-layered (TiAlN) PVD coated grooved cutting insert in machined Ti-6Al-4V alloy.

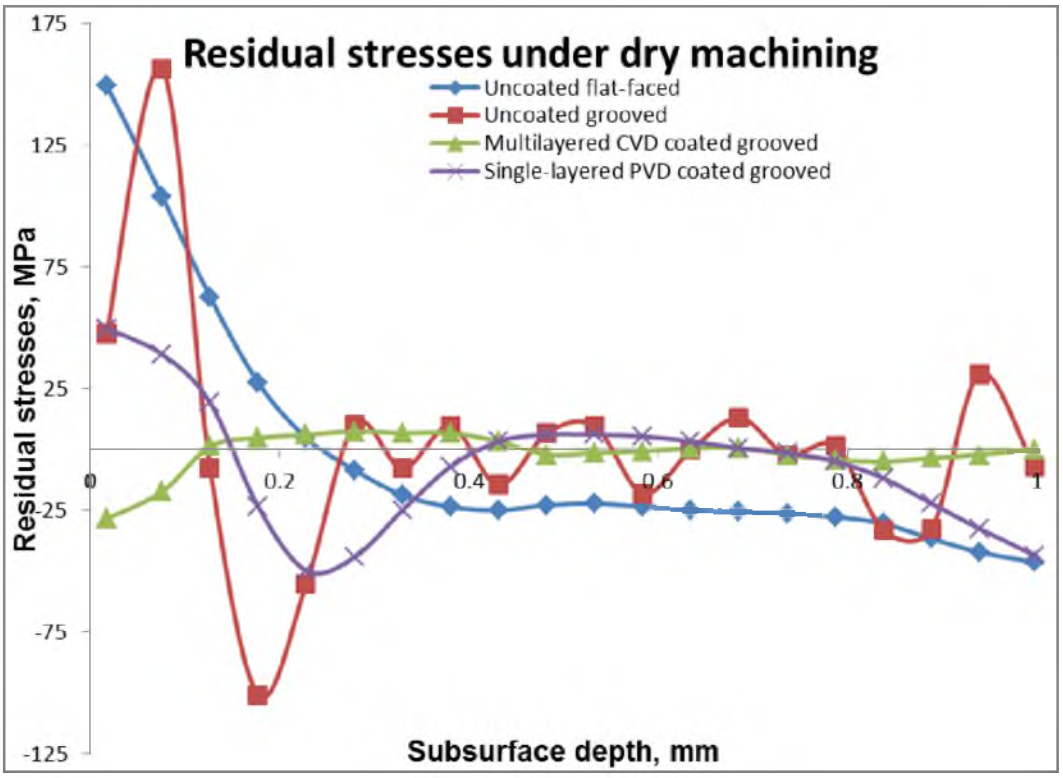

Figure 4.22: Residual stresses induced by different cutting inserts when using dry machining condition in Ti-6Al-4V alloy.

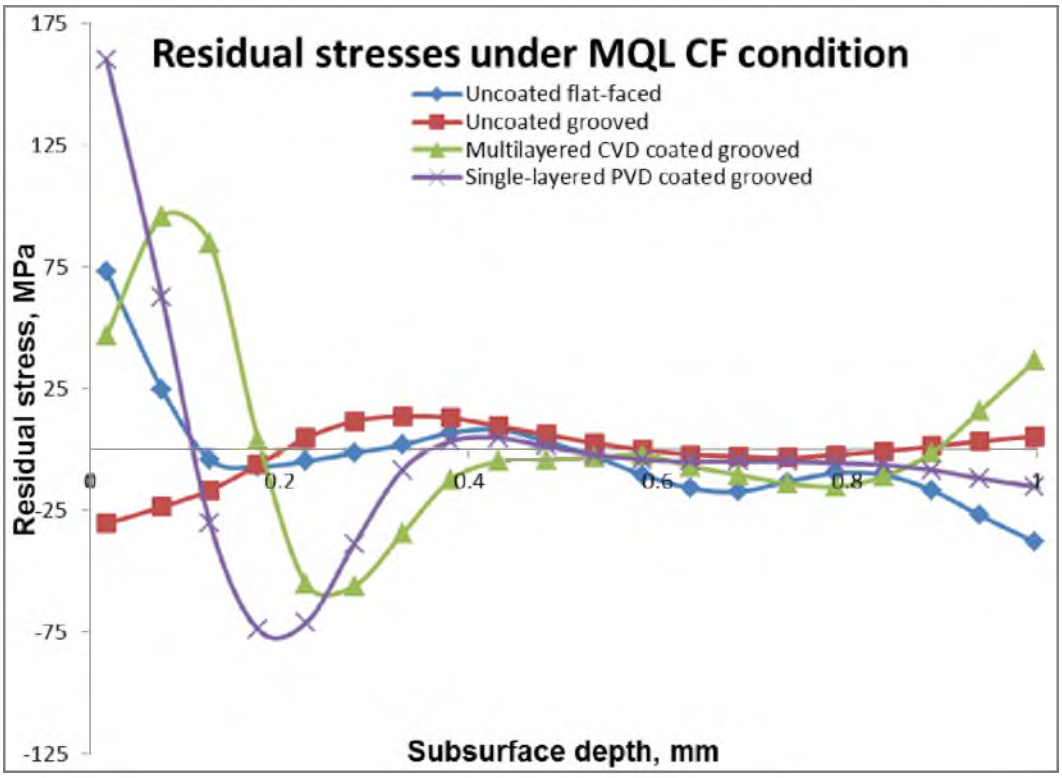

Figure 4.23: Residual stresses induced by different cutting inserts when using MQL cutting fluid application condition in Ti-6Al-4V alloy.

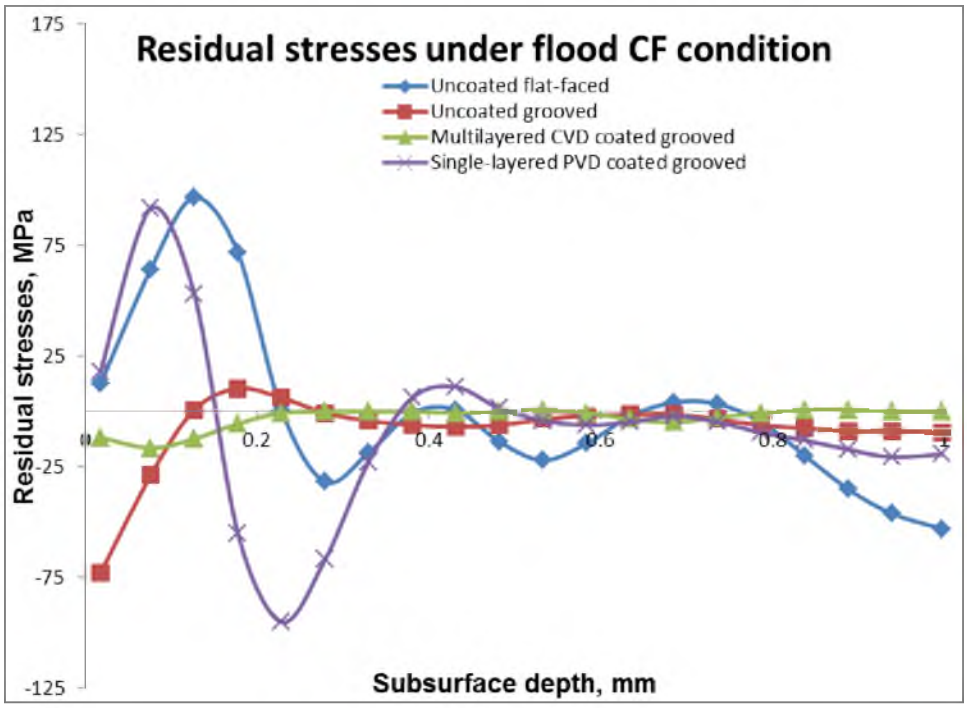

Figure 4.24: Residual stresses induced by different cutting tool inserts when using flood cutting fluid application condition in Ti-6Al-4V alloy.

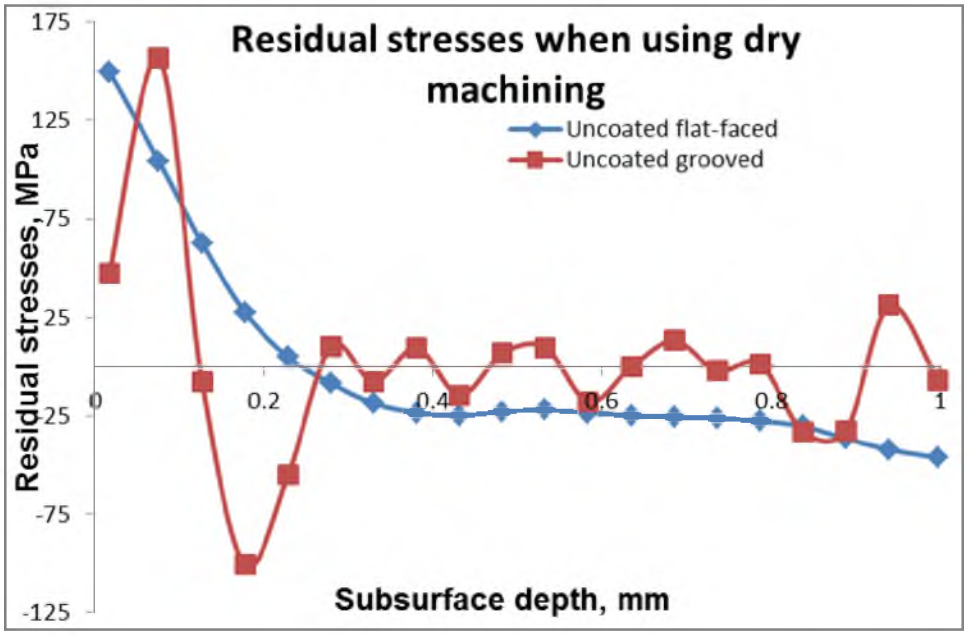

Figure 4.25: Residual stresses induced by uncoated flat-faced and uncoated grooved cutting inserts when using dry machining condition in machined Ti-6Al-4V alloy.

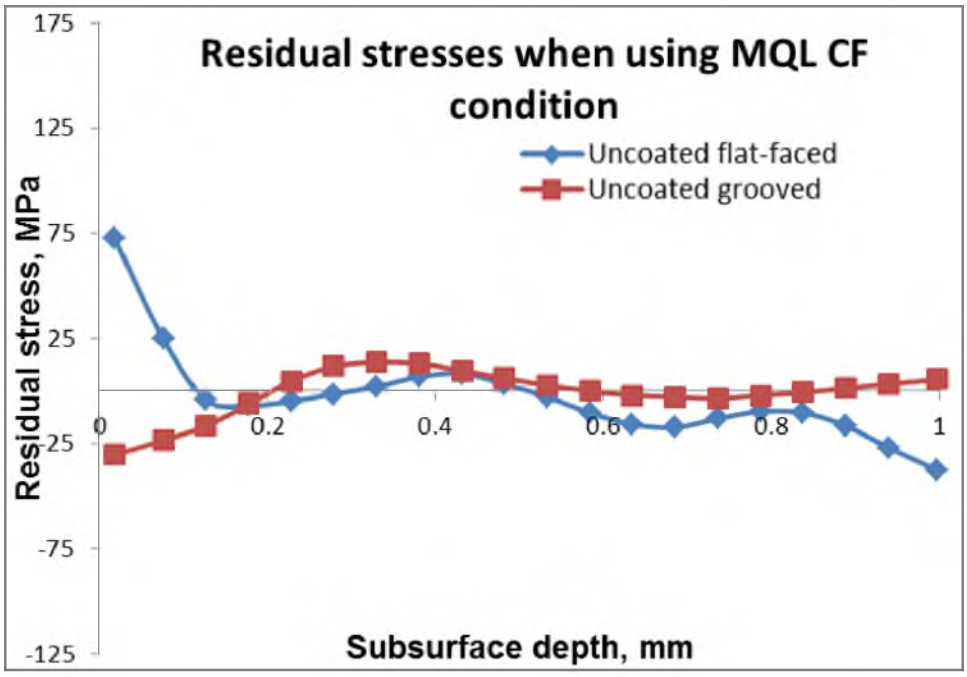

Figure 4.26: Residual stresses induced by uncoated flat-faced and uncoated grooved cutting inserts when using MQL cutting fluid application condition in Ti-6Al-4V alloy.

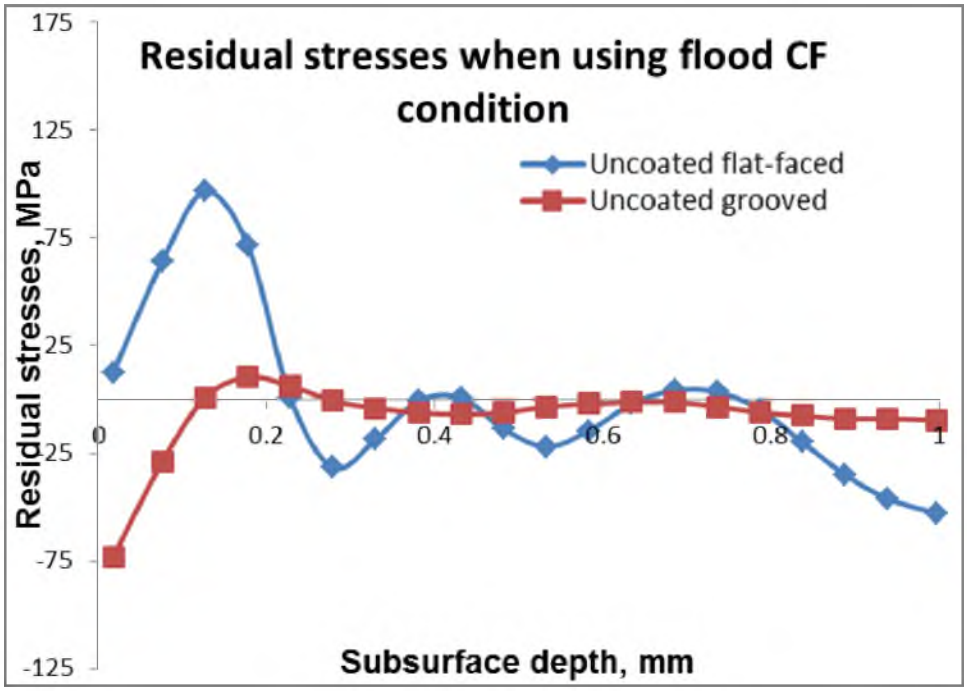

Figure 4.27: Residual stresses induced by uncoated flat-faced and uncoated grooved cutting inserts when using flood cutting fluid application condition in Ti-6Al-4V alloy.

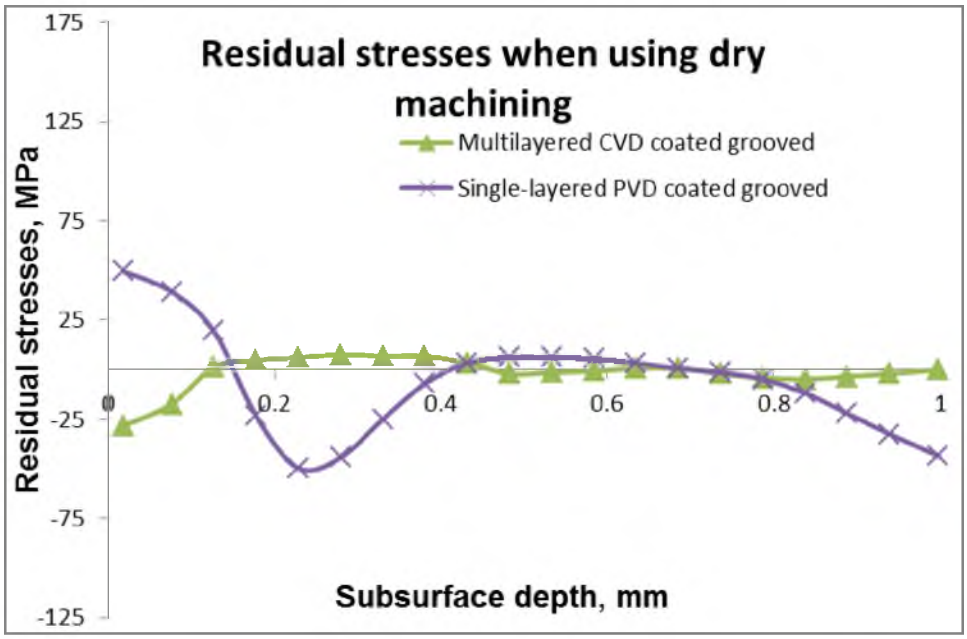

Figure 4.28: Residual stresses induced by multilayered CVD coated and single-layered PVD coated cutting inserts when using dry machining condition in Ti-6Al-4V alloy.

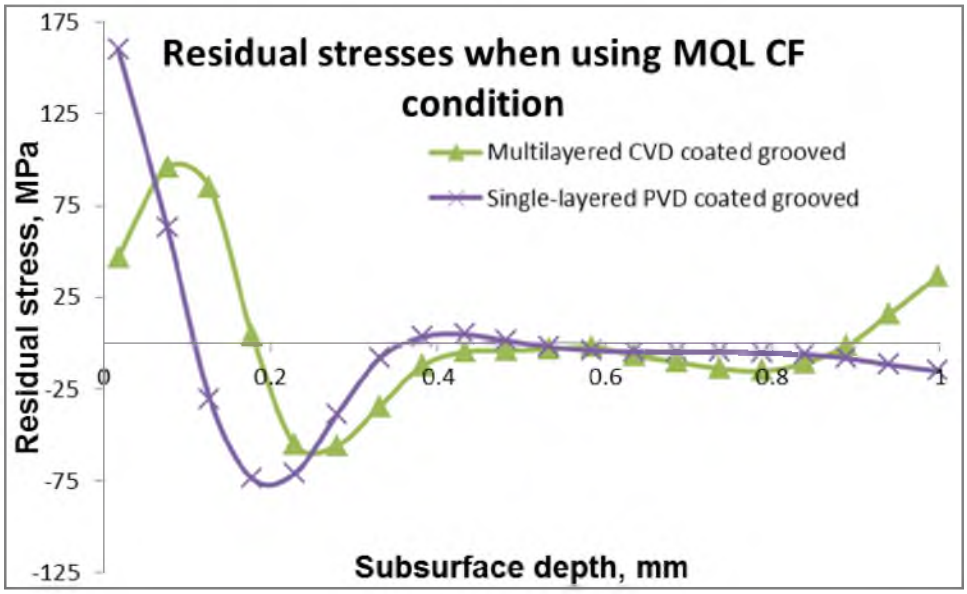

Figure 4.29: Residual stresses induced by multilayered CVD coated and single-layered PVD coated cutting inserts when using MQL cutting fluid application in Ti-6Al-4V alloy.

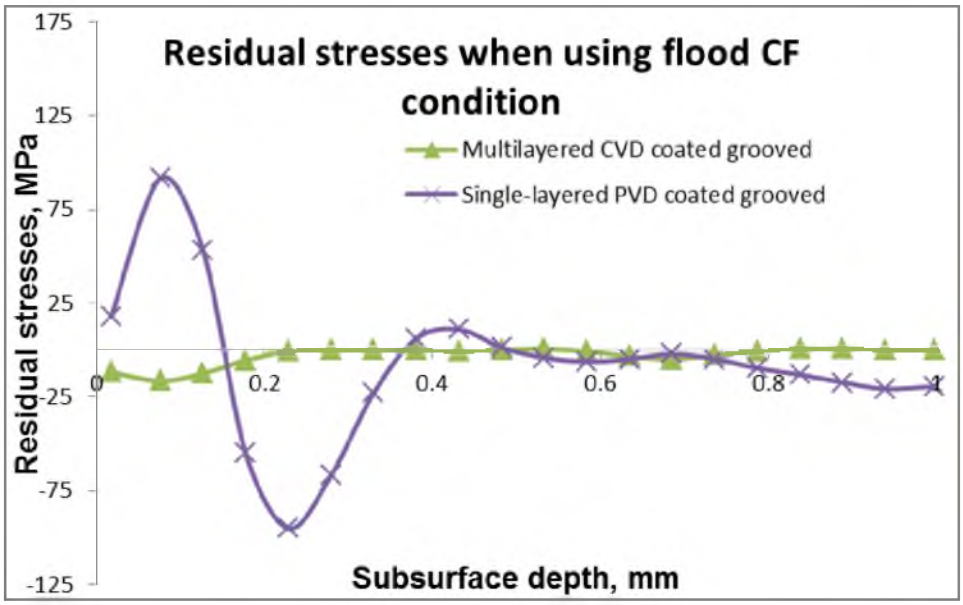

Figure 4.30: Residual stresses induced by multilayered CVD coated and single-layered PVD coated cutting inserts when using flood cutting fluid application in Ti-6Al-4V alloy.

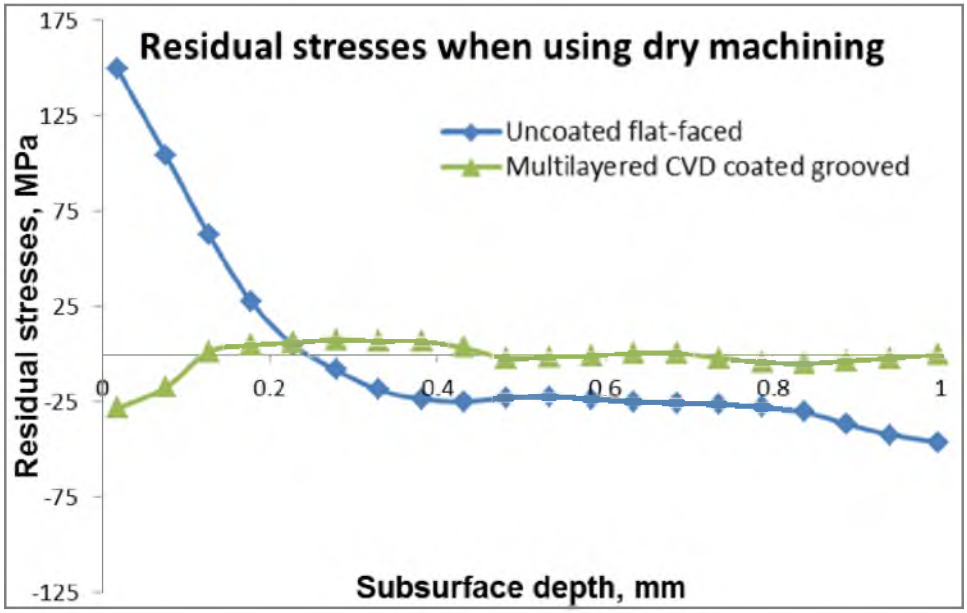

Figure 4.31: Residual stresses induced by uncoated flat-faced and multilayered CVD coated cutting inserts when using dry machining condition in Ti-6Al-4V alloy.

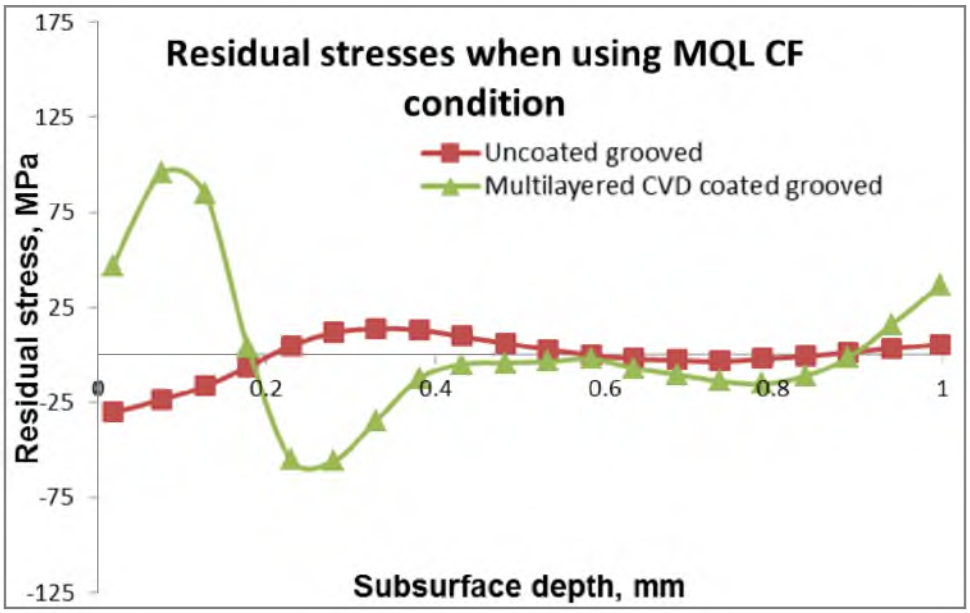

Figure 4.32: Residual stresses induced by uncoated grooved and multilayered CVD coated cutting inserts when using MQL cutting fluid application condition in Ti-6Al-4V alloy.

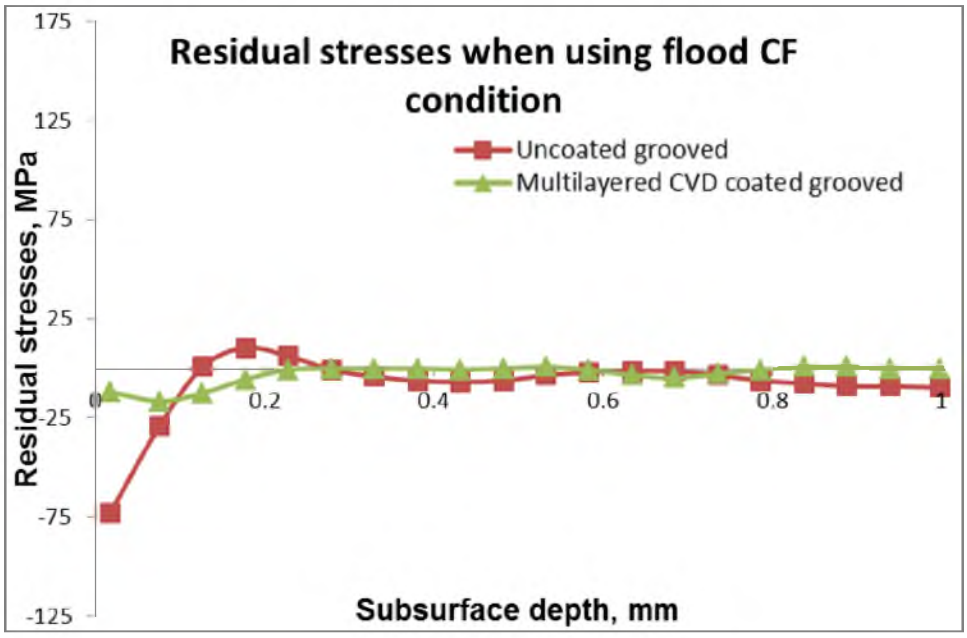

Figure 4.33: Residual stresses induced by uncoated grooved and multilayered CVD coated cutting inserts when using flood cutting fluid application condition in Ti-6Al-4V alloy.

Table 4.1: Summary of the effect of the chip breaker geometry on machining induced residual stresses in Ti-6Al-4V alloy

	Uncoated flat-faced	**Uncoated grooved**
Dry	Preferred	-
MQL	-	Preferred
Flood	-	Preferred

Table 4.2: Summary of the effect of the type of tool coating on machining induced residual stresses in Ti-6Al-4V alloy

	Multilayered CVD coated	**Single-layered PVD coated**
Dry	Preferred	-
MQL	Preferred	-
Flood	Preferred	-

Table 4.3: Summary of the effect of coated and uncoated cutting tool on machining induced residual stresses in Ti-6Al-4V alloy

	Uncoated grooved/Flat-faced	**Multilayered CVD coated**
Dry	-	Preferred
MQL	Preferred	-
Flood	Preferred	-

Table 4.4: Summary of the results

	Uncoated flat-faced	**Uncoated grooved**	**Multilayered CVD coated**	**Single-layered PVD coated**
Dry	-	-	Preferred	-
MQL	-	Preferred	-	-
Flood	-	Preferred	-	-

CHAPTER 5

SUMMARY AND CONCLUSIONS

The previous chapters provided information about the introduction to the thesis, experiments that were conducted as a part of this research and discussed the results obtained from these experiments in detail. This chapter concludes the thesis and also provides recommendations for future work.

5.1 Summary

The main aim of this thesis was to study the effects of cutting tool coatings and cutting fluid application conditions on the surface integrity (as characterized by surface roughness, residual stresses, and microstructural changes) in machined Ti-6Al-4V titanium alloy. As mentioned in Chapter 2, much of the previous research available in the literature focused on the effects of cutting speed, feed rate, rake angle, depth of cut, type of machining, etc. on the cutting forces, surface roughness, residual stresses, etc. Very limited work is available on the study of the effects of cutting tool coatings and cutting fluid application conditions (especially, the combined effects of these two factors) on surface roughness, residual stresses, and microstructural changes in machined work-pieces. Most of the work material investigation has been performed on several steels, aluminum alloys, or Inconel 718. Very few researchers investigated surface integrity in machined titanium alloys, which are one of the most widely used alloys in the aerospace

industry.

In this present research, machining experiments were performed on Ti-6Al-4V titanium alloys with an objective to focus on the surface integrity in the machined surfaces. The measured parameters in the experiments were cutting forces, type of chips obtained, surface roughness, residual stresses, and microstructural analysis. The hole drilling method was used to measure the relieved strains and to then calculate the residual stress in the work-piece thereafter. Microstructural analysis was performed by metallographically processing the specimens and observing the machined subsurface under an optical microscope.

When the feed forces were compared, the highest feed force was obtained when machining using the single-layered (TiAlN) PVD coated grooved cutting insert under the dry machining condition, while the lowest feed force was obtained while machining using the uncoated flat-faced cutting insert under the application of the flood cutting fluid condition. There was no specific trend observed in the feed forces data. When the radial forces were compared, the highest radial force was obtained while machining using uncoated grooved cutting insert under the dry machining condition, while the lowest radial force was obtained while machining using the multilayered ($TiCN/Al_2O_3/TiN$) CVD coated grooved cutting insert under the application of MQL cutting fluid condition. There was no specific trend observed in radial force data. Finally, when the main cutting forces were compared, the highest cutting forces were obtained with uncoated flat-faced cutting insert under MQL condition, while the lowest cutting forces were obtained with single-layered (TiAlN) PVD coated grooved cutting insert under MQL condition. When all the cutting force values are considered with respect to the cutting fluid application

conditions used, it can be seen that dry machining gave the highest cutting forces in general, while the lowest cutting forces were seen when machining under flood cutting fluid application condition.

When the surface roughness values are compared, for all the cutting inserts, among all the cutting fluid application conditions, the best surface finish was obtained when machining under flood cutting fluid application condition, while the worst surface finish was obtained when machined under dry cutting condition. It was also noticed that the type of coating used on the cutting insert did not have much impact on the surface roughness values.

Most of the cutting tools used in the experimentation under three different cutting fluid application conditions produced tensile residual stresses very near the surface, with the exception of a few work-pieces. However, the depths up to which the residual stresses are tensile are different for all the work-pieces.

When the residual stress profiles are compared for machining using the flat-faced uncoated tool, under the influence of three different cutting fluid application conditions, the worst profile among the three cutting fluid application conditions was observed when the work-piece was machined under dry machining condition, while the best profile was obtained when the work-piece was machined under MQL cutting fluid condition. Moreover, when all the microstructures of the work-pieces which were machined using the flat-faced uncoated cutting insert under dry, MQL and flood cutting fluid application conditions were compared, it was found that more quantity of coarsened α structure was present when the work-piece was machined under dry cutting condition. This is also the same condition which induces larger tensile stresses. Relatively less quantity of

coarsened α structure was observed when machined under flood cutting condition, while the least quantity of coarsened α structure was obtained when machined under MQL cutting fluid condition, which validates the residual stress profile trend reported herein.

When the residual stress profiles are compared for machining using the grooved uncoated tool, under the influence of three different cutting fluid application conditions, the worst profile among the three cutting fluid application conditions was observed when the work-piece was machined under dry machining condition while, once again, the best profile was obtained when the work-piece was machined under MQL cutting fluid condition. This trend is exactly similar to the one obtained by machining with flat-faced uncoated cutting insert. Moreover, when all the microstructures of the work-pieces which were machined using grooved uncoated cutting insert under dry, MQL and flood cutting fluid application conditions were compared, it was found that more quantity of coarsened α structure was present when the work-piece was machined under dry cutting condition. This is also the same condition which induces more tensile stresses. Relatively less quantity of coarsened α structure was observed when machined under flood cutting condition, while the least quantity of coarsened α structure was obtained when machined under MQL cutting fluid condition, which, again, validates the residual stress profile trend reported above.

When the residual stress profiles were compared for machining with multilayered CVD coated cutting insert under dry, MQL and Flood cutting fluid application condition, it was observed that the worst profile was observed when the work-piece was machined under MQL cutting fluid application condition, among the three conditions, while the best profile was obtained when the work-piece was machined under dry machining

condition. Moreover, when all the microstructures of the work-pieces which were machined using grooved multilayered CVD coated cutting insert under dry, MQL and flood cutting fluid application conditions were compared, it was found that more quantity of coarsened α structure was present when the work-piece was machined under MQL cutting fluid application condition, which is also the same condition inducing more tensile stresses. Relatively less quantity of coarsened α structure was observed, when machined under flood cutting condition, while the least quantity of coarsened α structure was obtained when machined under dry machining condition, which validates the residual stress profile trend reported above. Thus, we see a direct correlation between the observed subsurface microstructure and the nature of residual stresses. Moreover, we see that using a coating completely changed the effective surface integrity results as a function of cutting fluid application.

When the residual stress profiles were compared for machining with the single-layered PVD coated cutting insert under dry, MQL and flood cutting fluid application condition, the worst profile among the three conditions was observed when the work-piece was machined under MQL cutting fluid application condition, while the best profile was obtained when the work-piece was machined under dry machining condition. Moreover, when all the microstructures of the work-pieces which were machined using grooved single-layered PVD coated cutting insert under dry, MQL and flood cutting fluid application conditions were compared, it was found that more quantity of coarsened α structure was present when the work-piece was machined under MQL cutting fluid application condition. This is also the same condition which induces more tensile stresses. Relatively less quantity of coarsened α structure was observed when machined

under flood cutting condition, while the least quantity of coarsened α structure was obtained when machined under dry machining condition, which validates the residual stress profile trend reported above. Once again, this trend is similar to the one obtained while machining using multilayered CVD coated cutting insert.

When comparing the performance of all four cutting inserts under dry cutting fluid condition, it was observed that the coated cutting inserts (single-layered PVD and multilayered CVD) perform much better as compared to the uncoated (flat-faced and grooved) cutting inserts. Of the four cutting inserts under dry condition, multilayered CVD coated cutting insert produces, comparatively, the best residual stress profile. The worst residual stress profile was obtained when using the uncoated flat-faced cutting insert. When comparing the performance of all four cutting inserts under MQL cutting fluid condition, the exactly opposite trend was observed to the one under dry cutting fluid condition. The uncoated (flat-faced and grooved) cutting inserts perform much better as compared to the coated cutting inserts (single-layered PVD and multilayered CVD). Of the four cutting inserts under MQL condition, uncoated grooved cutting insert produces the best optimal residual stress profile. The worst residual stress profile was obtained by single-layered PVD coated cutting insert. When comparing the performance of all four cutting inserts under flood cutting fluid condition, it was observed that uncoated grooved cutting insert produces the best optimal residual stress profile. In contrast, the worst residual stress profile was obtained by uncoated flat-faced cutting insert. The multilayered CVD coated cutting insert's performance is slightly better, while the single-layered PVD cutting insert's performance is on the worse side. This trend is quite different when compared to dry and MQL cutting fluid conditions.

5.2 Recommendations for Future Work

The following are the recommendations for the future work in the related areas of this present thesis.

Experiments similar to this present study should be conducted on several other titanium alloys using a greater number of different cutting tools having different types of coatings so that the variation trends in residual stress distributions for each material can be understood, which will aid in obtaining a clearer picture.

The effects of different tool coating thickness and types, taking their thermal conductivities into account, on the surface integrity of the machined surfaces should be studied in detail.

The effects of machining on the microstructural changes in the material should be studied in detail and the microstructure analysis then obtained should be linked with the surface integrity in the machined surface to get a broader view of the area.

Considerably less work has been performed on the combined effect of cutting tool coatings and cutting fluid application on residual stress distribution. Most of the studies are investigating the residual stress profiles in different types of steels, aluminum and some in difficult-to-machine materials such as Inconel 718. Very little work has been done on the surface integrity aspect in machining titanium alloys that are mainly used for aircraft industry. Though a few studies including the present one tried to investigate some of these aspects, a very detailed study in these aspects is still essential.

Based on the understanding of the surface integrity in machined surfaces, a theoretical machining induced residual stress model could be developed which can be used to incorporate the required surface integrity profile in the final product after

manufacturing as a design input criterion to manufacturing process planning which will help in designing a machining process such that it directly gives the desired surface integrity profile in the final product.

REFERENCES

1. Shaw, M.C., 1984, *Metal Cutting Principles*, Oxford University Press, New York.

2. Griffiths, B., 2001, *Manufacturing Surface Technology – Surface Integrity and Functional Performance*, Taylor and Francis Books, Inc., NY, USA, pp. 1-67.

3. Groover, M.P., 2006, *Fundamentals of Modern Manufacturing: Materials, Processes and Systems*, John Wiley and Sons, Inc., pp. 481-642.

4. Balaji, A. K., Juturu, R., Paranjpe, A. R., "On surface texture and integrity in machined surfaces," *Eighth International Conference on Residual Stresses*, August 2008 (presentation).

5. Almen, J.O. and Black, P.H., 1963, *Residual Stresses and Fatigue in Metals*, Mcgraw-Hill Book Company, Inc., USA, pp. 1-90.

6. Matthew, J.D. Jr., 1988, *Titanium – a Technical Guide*, ASM International, Metals Park, OH.

7. ASM handbook, 1990, *Properties and Selection: Non-ferrous Alloys and Special-Purpose Materials,* ASM International, Volume 2, pp. 500-630.

8. Field, M. and Kahles, J.F., 1964, *The Surface Integrity of Machined and Ground High Strength Steels*, DMIC Report, Vol. 210, pp. 54–77.

9. Field, M. and Kahles, J.F., 1971, "Review of surface integrity of machined components," *Annals of the CIRP*, Vol. 20, No. 2, pp. 153–162.

10. Field, M., Kahles, J.F. and Cammett, J.T., 1972, "Review of measuring methods for surface integrity," *Annals of the CIRP*, Vol. 21, pp. 219–238.

11. El-Kaberry, M. M., and Fattouh, M., 1989, "Residual stress distribution caused by milling," *International Journal of Machine Tools and Manufacture,* Vol. 29, pp. 391-401.

12. Kandil, F.A., Lord, J.D., Fry, A.T. and Grant, P.V., 2001, "A review of residual stress measurement methods – A guide to technique selection," *National Physical Laboratory Report MATC(A)04,* NPL Materials Centre, UK.

13. Mohan, V. S., Balaji, A. K., 2002, "An effective cutting tool thermal conductivity based model for tool-chip contact in machining with multi-layer coated cutting tools," *Machining Science and Technology*, Vol. 6, Issue 3, pp. 415-436.

14. Mattox, D. M, 2010, *Handbook of Physical Vapor Deposition (PVD) Processing*, Elsevier Inc., USA.

15. Sreejith, P.S. and Ngoi, B.K.A., 2000, "Dry machining: Machining of the future," *Journal of Materials Processing Technology,* Vol. 101, pp. 287-291.

16. Lu, J., 1996, *Handbook of Measurement of Residual Stresses*, Society for Experimental Mechanics, Inc., The Fairmont Press, Inc., USA.

17. Bulletin 309E, "Student manual for strain gage technology," *Vishay Measurements Group, Inc.*, <www.vishay.com>

18. Measurements Group Tech Note TN-503, "Measurement of residual stresses by the hole-drilling strain-gage method," *Vishay Measurements Group, Inc.*, <www.vishay.com>

19. Withers, P. J. and Bhadeshia, H. K. D. H., 2001, "Residual stress. Part 1 - Measurement techniques and Part 2 – Nature and origins," *Materials Science and Technology,* Vol. 17(4), pp. 355-375.

20. Guo, Y. B., Li, W., Jawahir, I. S., 2009, "Surface integrity characterization and prediction in machining of hardened and difficult-to-machine alloys: A state-of-art research review and analysis," *Machining Science and Technology,* Vol. 13, pp. 437-470.

21. ASTM E 837-08, 2008, "Standard test method for determining residual stresses by the hole-drilling strain-gage method," *American Society for Testing and Materials.*

22. Schajer, G .S., 2001, "Hole drilling residual stress calculation program," Version 2.20.

23. Henriksen, E.K. (1951) "Residual stresses in machined surfaces," *Transactions of the ASME*, Vol. 73, pp. 69–74.

24. Colwell, L.V., Sinnot, M.J. and Tobin, J.C., 1955, "The determination of residual stresses in hardened, ground steel," *Trans. ASME*, Vol. 77, pp. 1099–1105.

25. Field, M. and Kahles, J.F., 1964, *The Surface Integrity of Machined and Ground High Strength Steels*, DMIC Report, Vol. 210, pp. 54–77.

26. Field, M. and Kahles, J.F., 1971, "Review of surface integrity of machined components," *Annals of the CIRP*, Vol. 20, No. 2, pp. 153–162.

27. Field, M., Kahles, J.F. and Cammett, J.T., 1972, "Review of measuring methods for surface integrity," *Annals of the CIRP*, Vol. 21, pp. 219–238.

28. Matsumoto, Y., Barash, M. M. and Liu, C.R., 1984, "Residual stress in the machined surface of hardened steel," *High Speed Machining*, pp. 193-204.

29. Leskovar, P. and Peklenik, J., 1982, "Influences affecting surface integrity in the cutting process," *Annals of CIRP*, Vol. 31 (1), pp. 441-450.

30. Sadat, A. B. and Bailey, J. A., 1987, "Residual stresses in turned AISI 4340 steel," *Experimental Mechanics*, Vol. 27, No. 1, pp. 80-85.

31. Sadat, A. B., 1990, "Effect of high cutting speed on surface integrity of AISI 4340 steel during turning," *Material Science Technology,* Vol. 6, pp. 371-375.

32. Ezugwu, E. O., Wang, Z .M., 1997, "Titanium alloys and their machinability – A review," *Journal of Materials Processing Technology*, Vol. 68, pp. 262-274.

33. Guo, Y. B., Li, W., Jawahir, I. S., 2009, "Surface integrity characterization and prediction in machining of hardened and difficult-to-machine alloys: A state-of-art research review and analysis," *Machining Science and technology,* Vol. 13, pp. 437-470.

34. M'Saoubi, R., Outeiro, J. C., Chandrasekaran, H., Dillon Jr., O. W., Jawahir, I. S., 2008, "A review of surface integrity in machining and its impact on functional performance and life of machined products," *International Journal of Sustainable Manufacturing,* Vol. 1, Nos. 1/2, pp. 203-236.

35. Rahman, M., Wang, Z., Wong, Y., 2006, "A review on high-speed machining of titanium alloys," *JSME International Journal Series C,* Vol. 49 (1), pp. 11-20.

36. Nabhani, F., 2001, "Machining of aerospace titanium alloys," *Robotics and Computer Integrated Manufacturing,* Vol. 17, pp. 99-106.

37. Ezugwu, E. O., 2005, "Key improvements in the machining of difficult-to-cut aerospace superalloys," *International Journal of Machine Tools and Manufacture,* Vol. 45, pp. 1353-1367.

38. Liu, C. R. and Barash, M. M., 1976, "The mechanical state of the sublayer of a surface generated by chip-removal process - Part-1," *Transactions of the ASME, Journal of Engineering for Industry*, pp.1192-1201 and *Wear* 194 (1996) 168173(2).

39. Liu, C. R. and Barash, M. M., 1976, "The mechanical state of the sublayer of a surface generated by chip-removal process – Part-2," *Transactions of the ASME, Journal of Engineering for Industry*, pp.1192-1201 and *Wear* 194 (1996) 168173(2).

40. Elkhabeery, M. M. and Bailey, J. A., 1984, "Surface integrity in machining solution - Treated and aged 2024 – Aluminium alloy, using natural and controlled contact length tools. Part I – Unlubricated conditions," *Transactions of the ASME*, Vol. 106, pp. 152-160.

41. Elkhabeery, M. M. and Bailey, J. A., 1984, "Surface integrity in machining solution - Treated and aged 2024 – Aluminium alloy, using natural and controlled contact length tools. Part II – Lubricated conditions," *Transactions of the ASME*, Vol. 106, pp. 161-166.

42. Okushima, K. and Kakino, Y., 1971, "The residual stress produced by metal cutting," *Annals of CIRP*, Vol. 20 (1), pp. 13-14.

43. Sadat, A. B. and Bailey, J. A., 1985, "Residual stress distribution in machining an annealed bearing bronze," *International Journal of Mechanical Science*, Vol. 27, No. 11/12, pp. 717-724.

44. Jeelani, S., 1986, "Effect of cutting speed and tool rake angle on residual stress distribution in machining 2024 – T351 Aluminum alloy – Unlubricated conditions," *Journal of Material Science*, Vol. 21 (8), pp. 2705 – 2710.

45. M'Saoubi, R., Outeiro, J. C., Changeux, B., Lebrun, J. L. and Dias, A. M., 1998, "Residual stress analysis in orthogonal machining of standard and resulfurized AISI 316L steels," *Journal of Materials Processing Technology* (1999), Vol. 96, pp. 225-233.

46. Outeiro, J.C., Dias, A.M., Lebrun, J.L. and Astakhov, V.P., 2002, "Residual stresses induced by machining of a plain carbon steel using coated and uncoated commercial tungsten carbide tools," *Key Engineering Materials,* Vol. 230-232, pp. 118-121.

47. Outeiro, J.C., Dias, A.M. and Jawahir, I.S., 2006, "On the effects of residual stresses induced by coated and uncoated cutting tools with finite edge radii in turning operations," *Annals of the CIRP,* Vol. 55(1), pp. 111-116.

48. Outeiro, J.C., Umbrello, D. and M'Saoubi, R., 2006, "Experimental and numerical modeling of the residual stresses induced in orthogonal cutting of AISI 316L steel," *International Journal of Machine Tools and Manufacture,* Vol. 46(14), pp. 1786-1794.

49. Sun, J., Guo, Y. B., 2009, "A comprehensive experimental study on surface integrity by end milling Ti-6Al-4V," *Journal of Materials Processing Technology,* Vol. 209, pp. 4036-4042.

50. Hughes, J. I., Sharman, A. R. C., Ridgway, K., 2004, "The effect of tool edge preparation on tool life and work-piece surface integrity," *Proceedings of the Institution of Mechanical Engineers,* Vol. 218, pp. 1113-1123.

51. Hughes, J. I., Sharman, A. R. C., Ridgway, K., 2006, "The effect of cutting tool material and edge geometry on tool life and workpiece surface integrity," *Proceedings of the Institution of Mechanical Engineers,* Vol. 220, pp. 93-107.

52. Puerta Velasquez, J. D., Tidu, A., Bolle, B., Chevrier, P., Fundenberger, J. J., 2010, "Sub-surface and surface analysis of high speed machined Ti-6Al-4V alloy," *Materials Science and Engineering A,* Vol. 527, pp. 2572-2578.

53. Thomas, M., Turner, S., Jackson, M., 2010, "Microstructural damage during high-speed milling of titanium alloys," *Scripta Materialia,* Vol. 62, pp. 250-253.

54. Ginting, A., and Nouari, M., 2009, "Surface integrity of dry machined titanium alloys," *International Journal of Machine Tools and Manufacture,* Vol. 49, pp. 325-332.

55. Che-Haron, C. H., and Jawaid, A., 2005, "The effect of machining on surface integrity of titanium alloy Ti-6% Al-4% V," *Journal of Materials Processing Technology,* Vol. 166, pp. 188-192.

56. Ibrahim, G A., Che-Haron, C. H., Ghani, J. A., 2009, "The effect of dry machining on surface integrity of titanium Alloy Ti-6Al-4V ELI," *Journal of Applied Sciences,* Vol. 9(1), pp. 121-127.

57. Colafemina, J. P., Jasinevicius, R. G., Duduch, J. G., 2007, "Surface integrity of ultra-precision diamond turned Ti (commercially pure) and Ti alloy (Ti-6Al-4V)," *Journal of Engineering Manufacture,* Vol. 221, pp. 999-1006.

58. Palanisamy, S., McDonald, S. D., and Dargusch, M. S., 2009, "Effects of coolant pressure on chip formation while turning Ti6Al4V alloy," *International Journal of Machine Tools and Manufacture,* Vol. 49, pp. 739-743.

59. Barry, J., Byrne, G., and Lennon, D., 2001, "Observations on chip formation and acoustic emission in machining Ti-6Al-4V alloy," *International Journal of Machine Tools and Manufacture,* Vol. 41, pp. 1055-1070.

60. Bayoumi, A. E., and Xie, J. Q., 1995, "Some metallurgical aspects of chip formation in cutting Ti-6wt.% Al-4wt.% V alloy," *Materials Science and Engineering A,* Vol. 190, pp. 173-180.

61. Komanduri, R., and Von Turkovich, B. F., 1981, "New observations on the mechanism of chip formation when machining a titanium alloy," *Wear,* Vol. 69, pp. 179-188.

62. Cook, R., and Young, W., 1999, *Advanced Mechanics of Materials*, Prentice Hall, Michigan.

63. Shih, A. J., Luo, J., Lewis, M. A., Strenkowski, J. S., 2004, "Chip morphology and forces in end milling of elastomers," *Journal of Manufacturing Science and Engineering*, Vol. 126, pp. 124-130.

64. Pederson, R., 2002, *Microstructure and Phase Transformation of Ti6Al4V*, Lulea University of Technology, Sweden, pp. 3-12.

65. Pelcastre, L., 2008, *Microstructural Evolution of Ti6Al4V Alloy*, Lulea University of Technology, Sweden, pp. 40-78.

66. Todinov, M. T., 1998, "Mechanism for formation of the residual stresses from quenching," *Modeling Simulations Material Science Engineering*, Vol. 6, pp. 273-291.

67. Todinov, M. T., 1999, "Influence of some parameters on the residual stresses from quenching," *Modeling Simulations Material Science Engineering*, Vol. 7, pp. 25-41.

68. Jayal, A. D., Balaji, A. K., 2009, "Effects of cutting fluid application on tool wear in machining: Interactions with tool-coatings and tool surface features," *Wear*, Vol. 267, pp. 1723-1730.

69. Liu, C.R. and Guo, Y.B., 2000, "Finite element analysis of the effect of sequential cuts and tool-chip friction on residual stresses in a machined layer," *International Journal of Mechanical Sciences,* Vol. 42, pp. 1069-1086.

70. Guo, Y. B. and Liu, C. R., 2002, "FEM analysis of mechanical state on sequentially machined surfaces," *Machining Science and Technology*, Vol. 6 (1), pp. 21-41.